# Click Chemistry as A Versatile Reaction for Construction and Modification of Metal-Organic Frameworks

Pei-Zhou Li[a,b], Xiao-Jun Wang[c], Yanli Zhao[a,*]

[a] *Division of Chemistry and Biological Chemistry, School of Physical and Mathematical Sciences, Nanyang Technological University, 21 Nanyang Link 637371, Singapore*

[b] *School of Chemistry and Chemical Engineering, Shandong University, No.27 South Shanda Road, Jinan 250100, P. R. China*

[c] *Jiangsu Key Laboratory of Green Synthetic Chemistry for Functional Materials, School of Chemistry and Materials Science, Jiangsu Normal University, Xuzhou 221116, P. R. China*

**ABSTRACT:**

Intriguing porous architectures, fascinating physical and chemical properties, and wide application potentials have made metal–organic frameworks (MOFs) a class of highly promising functional materials. The inherent feature of incorporating decorative organic components as building blocks has facilitated MOF constructions by ingenious pre-design and post-synthetic modifications of the organic moieties through appropriate reactions. Meanwhile, the click chemistry has become an effective and robust tool in the fabrication and modification of various functional materials. The azide-alkyne 1,3-dipolar cycloaddition is usually conducted in mild conditions using diversely available substrates to generate 1,4-regioisomers of 1,2,3-triazoles as sole products in high yields, which meets the characteristics of the conceptual click chemistry and has been referred as the premier example of a click reaction. In 2007, the azide-alkyne 1,3-dipolar cycloaddition as a representative reaction of the click chemistry was introduced into the field of MOFs. In the past decade, utilizing the azide-alkyne 1,3-dipolar cycloaddition, not only lots of organic ligands have been designed and synthesized for MOF constructions, but also diverse functional groups have been grafted into/onto MOF networks for targeted applications. Although other click reactions,

* Corresponding author
E-mail address: zhaoyanli@ntu.edu.sg

such as Diels-Alder click reaction and thiol-ene click reaction, have also been introduced into the MOF field, more and more successful examples have undoubtedly demonstrated that the azide-alkyne 1,3-dipolar cycloaddition is a highly efficient click reaction in the MOF construction and modification toward purposed applications. Herein, we highlight representative research progresses on MOFs derived from the azide-alkyne 1,3-dipolar cycloaddition along with their attractive applications.

***Keywords:*** click chemistry • 1,3-dipolar cycloaddition • metal-organic frameworks • porous materials • post-synthetic modification

## Contents

## 1. Introduction

Metal–organic frameworks (MOFs) are a class of highly promising functional materials owing to their intriguing porous architectures, fascinating physical and chemical properties, and wide application potentials [1-5], especially in the adsorption and separation of gases or small molecules including $H_2$ [6,7], $CO_2$ [8,9], $CH_4$ or other hydrocarbons [10,11] and toxic chemicals [12,13], heterogeneous catalysis [14,15] or catalyst supports [16,17], drug delivery and bioimaging [18,19], and electronic and photophysical aspects [20,21]. Distinct from other inorganic porous materials such as zeolites and activated porous carbons, crystallographically infinite lattices and perspicuous topologies of MOFs are typically derived from the modular combination of polytopic organic bridging ligands and metal ions or *in situ* generated metal clusters [22,23]. Although a large library of porous MOF architectures has been developed so

far by judicious coordination of diverse organic linkers [24-29] and abundant inorganic nodes [30-37] under various synthetic processes [38,39], more and more examples have demonstrated that their properties and applications show high dependency on the sophisticated organic moieties reticulated in the frameworks [24-29,40]. For instance, by modifying the length of organic backbones, isoreticular MOFs with different pore sizes could be achieved [41-43]; by introducing chiral centers into organic ligands, MOFs for enantiomer separation and asymmetric catalysis were constructed [44,45]; by utilizing fluorinated compounds as organic precursors in the ligand synthesis, moisture-resistant and superhydrophobic MOFs were assembled [46,47]; and by taking biocompatible natural products as ligands, edible MOFs were obtained [48]. The inherent feature of incorporating decorative organic components as building blocks has facilitated MOF fabrications by ingenious pre-design and synthesis of functional organic ligands [49,50] or post-synthetic modification of the organic moieties by grafting functional groups into the pristine networks [51,52]. Therefore, a rational selection of efficient and reliable reactions to synthesize and/or modify organic ligands becomes a pivotal step to construct unique MOF architectures or composites toward targeted applications.

The click chemistry has become a group of effective and robust reactions since it was proposed in 2001 [53]. Such reactions could be carried out in non-stringent conditions with wide scopes of reactants to generate highly yielded (stereospecific) products [53,54]. Among these unique reactions, azide-alkyne 1,3-dipolar cycloaddition is usually conducted in mild conditions using diverse available substrates, highly yielding 1,4-regioisomers of 1,2,3-triazoles as sole products instead of regiorandom triazole adducts [55,56], which complies fully with the definition of the conceptual click chemistry and has been referred as the premier example of a click reaction [57]. The investigation of azide-alkyne cycloaddition could be traced back to 1960s [58], but its affirmatory breakthrough is based on the landmark event of introducing copper(I) as a catalyst into the reaction systems reported in 2002 [55,56]. In recent years, copper(I)-free clicked azide-alkyne 1,3-dipolar cycloaddition was also well developed to overcome the cytotoxic challenge of copper(I) ion, especially in biological systems [59]. Here, azide-alkyne 1,3-dipolar cycloaddition is adopted instead of the terms of copper(I)-catalyzed azide-alkyne cycloaddition, copper(I)-free azide-alkyne 1,3-dipolar

cycloaddition, or Huisgen 1,3-dipolar cycloaddition for fully describing and summarizing this type of reactions in this review. Since the toxicity of copper(I)-catalyzed azide-alkyne cycloaddition restricts its practical applications in certain situations, *e.g.*, bioconjugation, the development of copper-free click reaction would overcome this issue. So far, the azide-alkyne 1,3-dipolar cycloaddition has been broadly exploited in the fabrication and modification of various functional molecules and materials [60-62], such as small organic compounds [63,64], drugs and bio-active molecules [56,65,66], dendritic compounds [67], and organic polymers [68-72], which have been widely used in molecular recognition, heterogenous catalysis, bioconjugation, pharmaceutical industry and so on. In recent years, the click reaction of azide-alkyne 1,3-dipolar cycloaddition was also employed in the research field of porous organic polymers (POPs) and covalent-organic frameworks (COFs) [73-82]. While some POPs or COFs with crystallizing frameworks could be easily modified by the click chemistry [81,82], the POPs or COFs constructed by direct click reaction of two modular building blocks are often amorphous with low- or non-porosity and irregular pore distribution, probably due to its feature of irreversible reaction [73-80]. Since the azide-alkyne 1,3-dipolar cycloaddition is the most widely used reaction among all the click reactions, it has been often referred as the "click reaction".

**(Insert Scheme 1 herein)**

In 2007, the azide-alkyne 1,3-dipolar cycloaddition as the representative reaction of the click chemistry was introduced into the research field of MOFs by Devic and coworkers [83]. Since then, lots of MOFs have been pre-designed, constructed (Scheme 1a) or post-synthetically modified (Scheme 1b) by this user-friendly and robust reaction. Although other click reactions, such as Diels–Alder click reaction and thiol−ene click reaction, have also been employed in the MOF field, more and more successful examples have undoubtedly demonstrated that the azide-alkyne 1,3-dipolar cycloaddition is a powerful click reaction in both pre-design and post-synthetic modification of MOFs toward purposed applications. Previous reviews have focused on either prosperous MOFs [1-40] or click chemistry [59-72] separately. A very few reports have briefly covered the topic of MOFs derived from the click

reaction. For instance, some MOFs constructed by the clicked 1,2,3-triazole-containing ligands were discussed in reviews regarding (i) coordination materials constructed from triazoles and tetrazoles reported by Gameza and coworkers in 2011, and (ii) metal azolate frameworks reported by Chen *et. al.* in 2012 [24,25]. Several MOFs post-synthetically modified by the click reaction were also mentioned in some reviews [51,84,85]. However, the research progresses on MOFs based on this versatile click chemistry have still not been comprehensively summarized so far, to the best of our knowledge.

In this review, we highlight recent significant research progresses on the pre-design, construction and post-synthetic modification of MOFs by the click reaction of azide-alkyne 1,3-dipolar cycloaddition along with their attractive applications. In the section of clicked ligands and constructed MOFs, various types of organic ligands including (i) clicked carboxylate ligands, (ii) clicked triazolates, (iii) clicked carboxylate-containing triazolates, and (iv) click-extended bipyridine ligands, and related triazole-containing MOF architectures are discussed in detail. In addition to the MOF construction *via* clicked pre-design, lots of MOFs were also post-synthetically modified by the click chemistry. Thus, four sections including (i) azide-tagged MOFs modified by alkynes, (ii) alkyne-tagged MOFs modified by azides, (iii) one-pot, two-step click modification of amino-derived MOFs by alkynes, and (iv) copper-free strain-promoted click modification of MOFs are separately discussed. The versatile azide-alkyne 1,3-dipolar cycloaddition not only enriches the library of MOF structures, but also widely broadens the application of MOFs by incorporating functional groups into the frameworks during the processes of ligand pre-design and MOF post-synthetic modification. Therefore, various attractive applications of MOFs derived from the azide-alkyne 1,3-dipolar cycloaddition in (i) gas adsorption, (ii) heterogeneous catalysis, (iii) large-molecule capture and separation, (iv) drug delivery and cancer therapy, and (v) templated polymer-gel fabrications are summarized in this review.

## 2. Clicked ligands and related MOF structures

In the ligand design and syntheses, the click reaction of azide-alkyne 1,3-dipolar cycloaddition not only affords an effective combination between polytopic-symmetrical organic moieties and electron donor coordination groups to produce diverse

triazole-containing carboxylates for MOF constructions, but also leads to the generation of coordinative 1,2,3-triazole ring. Since 1,2,3-triazole ring is an electron donor group, the coordination between metal ions and the triazole ring could be formed [24,25,33]. Therefore, various types of organic ligands including clicked carboxylate ligands, clicked triazolates, clicked carboxylate-containing triazolates, and clicked pyridine ligands were successfully synthesized *via* the modular click combinations of polytopic-symmetrical acetylene-containing organic components and azide-containing components. Subsequently, diverse triazole-containing MOF architectures were constructed through the coordination of these clicked organic ligands with suitable metal ions.

**(Insert Scheme 2 herein)**

### 2.1. MOFs derived from clicked carboxylate ligands

Among several types of clicked ligands, clicked carboxylate ligands are one of the most well studied groups. Diverse clicked carboxylate ligands (Scheme 2) including tricarboxylic acids, tetracarboxylic acids, hexacarboxylic acids, and octacarboxylic acids were successfully synthesized *via* the clicked combinations of dual-, triple-, or tetrapolar-symmetrical acetylene-containing organic components with azide-containing carboxylates, such as 4-azidobenzoates and 5-azidoisophthalates. Subsequently, various MOFs with coordination-free triazole groups were constructed after the coordination between these clicked organic ligands and metal ions.

**(Insert Figure 1 herein)**

#### 2.1.1 MOFs derived from clicked tri-carboxylate ligands

Utilizing the azide-alkyne 1,3-dipolar cycloaddition as the core reaction through the conjugation between triple-symmetrical acetylene-containing 1,3,5-triethynylbenzene and the azide precursor of azidoglycine ethylester, a flexible tricarboxylic acid, {4-[3,5-bis-(1-carbonylmethyl-1*H*-[1,2,3]triazol-4-yl)-phenyl]-[1,2,3]triazol-1-yl}acetic acid ($H_3L1$ in Scheme 2), was synthesized by Devic and coworkers in 2007 [83]. After

solvothermal reaction with Td(III) ions, a triazole-containing MOF, denoted as MIL-112 (Figure 1), was then obtained as a counterexample of isoreticular chemistry [41-43]. On account of the flexibility of the clicked tritopic carboxylate linker, a $4^4$ network (Figure 1b) instead of an isotypic hexagonal $6^3$ network in prototypical MIL-103 (a MOF based on Td and benzene-tricarboxylic acid) [86] was presented in MIL-112, although infinite one-dimensional (1D) secondary building units (SBUs) similar to that in MIL-103 was also observed in MIL-112.

**(Insert Figure 2 herein)**

Replacing the azide precursor of azidoglycine ethylester by 4-azidobenzoate to react with triple-symmetrical 1,3,5-triethynylbenzene followed by the deprotection, a tricarboxylate ligand, 4,4',4''-benzene-1,3,5-tryl-tri(1*H*-1,2,3-triazol-1-yl)benzoic acid ($H_3L2$, Scheme 2), was synthesized by our group [87]. After solvothermal reaction with Zn(II) ion in DMF, block colorless crystals of a MOF, denoted as NTU-130, with a framework formula of $[Zn_6(L2)_4(H_2O)_3]_n$ were obtained. Structural analysis reveals that, in NTU-130, linear $Zn_3$ clusters [88,89] were *in-situ* generated by six distributed carboxylate groups from six different L2 ligands coordinated with three neighboring Zn(II) ions (Figure 2a). Although two-fold interpenetrated uninodal (10,3)-net with intrinsically chiral $SrSi_2$ topology in an *srs* symbol [89] was formed by the coordination of click-extended L2 and $Zn_3$ clusters, a framework with a Brunauer-Emmett-Teller (BET) surface area of 2819 $m^2\ g^{-1}$, and large pores having opening windows of 14.8 × 19.9 $Å^2$ along *a*-axis (Figure 2b), and channels with opening diameters of about 10.2 Å perpendicular to the (110) plane was successfully constructed, attributed to enough length of click-extended organic backbone of the tricarboxylate ligand.

**(Insert Figure 3 herein)**

### 2.1.2 MOFs derived from clicked planar tetracarboxylate ligands

Reacting two isophthalate compounds, *i.e.*, dimethyl 5-azidoisophthalate and dimethyl 5-ethynylisophthalate, followed by the hydrolysis, a sandwich-type tetracarboxylate ligand,

5,5’-(1H-1,2,3-triazole-1,4-diyl)di-isophthalic acid ($H_4$L3 in Scheme 2), was also synthesized by our group [90]. Colorless block-shaped crystals of a MOF, denoted as NTU-101-Zn, was then constructed under solvothermal reaction of the ligand with Zn(II) ion. Structure analysis reveals that $Zn_2$ clusters are *in situ* formed within the framework by three DMF and four carboxylates coordinated with two neighboring Zn ions, four of which are then connected by one tetracarboxylate L3 (Figure 3a) to finally give the formation of a three-dimensional (3D) framework of NTU-101-Zn. By simplifying the tetracarboxylate L3 into a 4-connected square-planar linker and four carboxylate coordinated $Zn_2$ clusters into a tetrahedral node, a topological PtS-type network could be obtained (Figure 3b).

By replacing the Zn ion by lanthanide ions (Ln(III)) and reacting with the clicked $H_4$L3, a family of isostructural MOFs with a framework formula of $[Ln(HL3)(H_2O)_4]\cdot xH_2O$ (Ln = La, Eu, Tb, and Er; $2 < x < 2.5$) and 3,6-connected rutile topology was hydrothermally synthesized by Liang and coworkers [91]. Luminescent studies show that Eu- and Tb-based MOFs present characteristic emission of Eu(III) and Tb(III), and Tb-based MOF exhibits selective luminescent sensing for Cu(II) ion in aqueous solution. The authors also found that Tb- and Er-based MOFs exhibit distinct magnetic behavior in different temperature regions.

**(Insert Figure 4 herein)**

Subsequently, other two longer tetra-carboxylate ligands, 5,5'-(benzene-1,4-diyl)di(1H-1,2,3-triazole-1,4-diyl)diisophthalic acid ($H_4$L4 in Scheme 2) and 5,5'-(benzene-1,3-diyl)di-(1H-1,2,3-triazole-1,4-diyl)diisophthalic acid ($H_4$L5 in Scheme 2), were also designed and synthesized by our group *via* the click extension of diisophthalates with two different diethynyl- benzenes, *i.e.*, 1,4-diethynylbenzene and 1,3-diethynylbenzene, respectively [92]. The three ligands $H_4$L3, $H_4$L4, and $H_4$L5 were then reacted directly with Cu(II) ions to afford blue crystals of three MOFs, denoted as NTU-111, 112, and 113, respectively. Structure analysis shows that all three MOFs possess 3D porous frameworks with the same basic framework formula of $[Cu_2(L)(H_2O)_2]_n$, in which typical unsaturated paddlewheel $Cu_2$ clusters were formed (Figures 4a,c,e) [26,93] and coordination-free clicked triazole rings as the extending spacer in the tetra-carboxylate ligands were uniformly located

(Figures 4b,d,f) [22,23]. On the other hand, topological analysis indicates that NTU-111 shows an NbO-type network with $6^4 \cdot 8^2$ topology, while NTU-112 exhibits a rare *acs* net and NTU-113 gives a PtS-type network with $4^2 \cdot 8^4$ topology. Such detailed investigation demonstrated that subtle variation of clicked extension on the model tetracarboxylate ligand, *i.e.*, di-isophthalate, could lead to a high diversity of the target frameworks

A longer tetra-carboxylate ligand, $H_4$L6 in Scheme 2, was prepared *in situ* using an unconventional approach to generate the MOF structure [94]. Verpoort and coworkers integrated the synthetic steps for the formations of organic linker and metal-organic self-assembly into one stride, and blue block crystals of a porous Cu-MOF were obtained. Structure analysis reveals that this framework has a 3,4-coordinated net with the fof topology. When they changed the metal ion from Cu(II) to Zn(II), this unconventional approach was failed to afford the Zn-MOF due to the absence of the catalytic Cu ion. While coordinating the pre-clicked ligand $H_4$L6 with Zn ion, Zn-MOF crystallized in the monoclinic chiral space group $P2_1$ was obtained.

**(Insert Figure 5 herein)**

### 2.1.3. MOFs derived from clicked tetragonal tetra-carboxylate ligands

Similar to other tetragonal tetracarboxylate ligands [95-103], a tetragonal tetracarboxylate ligand, 4,4',4",4"'-((methane-tetrayl-tetrakis (benzene-4,1-diyl)) tetrakis(1*H*-1,2,3-tri-azole-4,1-diyl)) tetra-benzoic acid ($H_4$L7 in Scheme 2), was synthesized through the click combination of 4-azidobenzoate with a tetrapolar-symmetrical acetylene-containing organic precursor, tetrakis(4-ethynylphenyl) methane by our group [104]. Interestingly, high quality blue crystals of two kinds of MOFs, denoted as NTU-140 and 141, were obtained when solvothermal reacting $H_4$L7 with Cu(II) ion in different solvents. Structure analysis shows that both MOFs share the same typical PtS-type network with a framework formula of $[Cu_2(L7)]_n$ constructed by the coordination of clicked L7 and *in situ* generated paddlewheel $Cu_2$ cluster (Figures 5a,b), similar to those reported Cu-MOFs with tetragonal tetracarboxylate ligands [95-98]. Interestingly, 2-fold interpenetration of basic networks in NTU-140 (Figure 5c) and 4-fold interpenetration in NTU-141 (Figure 5d) were

presented. As a result, porous channels with a diameter of ~20 Å in NTU-140 and close-packing with nearly no pores in NTU-141 were observed.

**(Insert Figure 6 herein)**

### 2.1.4. MOFs derived from clicked hexa-carboxylate ligands

Inspired by diverse examples of highly porous MOFs constructed by dendritic hexacarboxylate ligands with Cu(II) ions [105-120], a triazole-containing hexacarboxylate ligand, 5,5',5''-(4,4',4''-(benzene-1,3,5-triyl) tris(1*H*-1,2,3-triazole-4,1-diyl))triisophthalic acid ($H_6$L8 in Scheme 2), was prepared in our group *via* the clicked combination of 1,3,5-triethynylbenzene and pre-synthesized di-*tert*-butyl 5-azidoisophthalate followed by the deprotection [121]. After solvothermal reaction of ligand $H_6$L8 with Cu(II) ion, high quality blue crystals of a MOF, denoted as NTU-105, were obtained. As expected, structure investigation reveals that NTU-105 shares the same (3,24)-connected network as prototypical *rht*-type MOFs with coordination-free triazole groups uniformly embedded (Figure 6a), in which three types of metal-organic polyhedrons, *i.e.*, cuboctahedron (*cub*-Oh), truncated tetrahedron (*T*-Td), and truncated octahedron (*T*-Oh) with theoretical inner sphere diameters of about 12, 15, and 20 Å respectively, were synchronically constructed (Figure 6b). Nearly at the same time, the same structure but denoted as NOTT-122 and NU-125 was also reported by Schröder and Hupp, respectively [122,123]. In their reports, both $CO_2$ and $CH_4$ adsorption of the MOFs was investigated. In particular, high-pressure $CH_4$ adsorption was measured at 298 K using NU-125 in gram scale.

**(Insert Figure 7 herein)**

After that, an amine-functionalized $H_6$L8 ligand, ascribed as $H_6$L8-$NH_2$ in Scheme 2 [124], and two symmetry-reduced dendritic hexacarboxylate ligands, *i.e.*, 5,5'-(4,4'-(5-(3,5-dicarboxyphenyl-carbamoyl)-1,3-phenylene)bis(1*H*-1,2,3-triazole-4,1-diyl))diisophthalic acid (abbreviated as ABTA or $H_6$L9 in Scheme 2) [125] and 5,5'-(4,4'-(5-(3-(3,5-dicarboxyphenyl) ureido)-1,3-phenylene)bis(1*H*-1,2,3-triazol-4,1-diyl)) diisophthalic acid (abbreviated as

UBTA or $H_6$L10 in Scheme 2) [126], were also designed and synthesized by our group *via* click reactions. X-ray diffraction analyses reveal that all three constructed Cu-based MOFs (denoted as NTU-105-$NH_2$, Cu-ABTA and Cu-UBTA, respectively) possess the same prototypical *rht*-type network as shown in Figure 7.

Three other triazole-containing $H_6$L ligands, *i.e.*, 5,5',5''-((tripropargylamine-triyl)-tris (1H-1,2,3-triazole-4,1-diyl))-tri-iso-phthalic acid ($H_6$L11 in Scheme 2), 5,5',5''-(4,4',4''-((triphenylamine)-4,4',4''-triyl)-tris(1H-1,2,3-triazole-4,1-diyl))tri-iso-phthalic acid ($H_6$L12 in Scheme 2), and 5,5',5''-(4,4',4''-((1,3,5-triphenyl-benzene)-4',4'',4'''-triyl)-tris (1*H*-1,2,3-tri-azole-4,1-diyl))tri-isophthalic acid ($H_6$L13 in Scheme 2) were synthesized by Farha and coworkers *via* clicked combinations of dimethyl 5-azidoisophthalate with three triethynyl-containing precursors, tripropargylamine, tris(4-ethynylphenyl)amine, and 1,3,5-tris(4-ethynylphenyl)benzene, respectively [127]. Then, three MOFs, denoted as NU-138, 139, and 140, were constructed after reacting these ligands with Cu(II) ion (Figure 7). Structure analyses show that these MOFs have isoreticular *rht*-type network but different pore sizes. Similar to NU-125, these three MOFs also show high capability for $CH_4$ uptake.

Facilitated by the conceptual approach of reticular chemistry, three types of transparent crystals of MOFs, denoted as NTU-161, 162 and 163, were successfully assembled after reacting $H_6$L8, $H_6$L12 and $H_6$L13 with Zn(II) ion [128]. Structure analyses reveal that they are isoreticular framework of NTU-105 with the same inner sphere diameters of the *cub*-Oh polyhedron (approximately 11.0 Å), but their apertures of both *T*-Td and *T*-Oh polyhedrons expand from 13.0 and 20.0 Å in NTU-161 to 14.0 and 23.0 in NTU-162, and to 15.0 and 25.0 Å in NTU-163, respectively.

**(Insert Figure 8 herein)**

### 2.1.5. MOFs derived from clicked oct-carboxylate ligands

Similar to other reported oct-carboxylate ligands [129-136], a triazole-containing octcarboxylate ligand, 5,5',5'',5'''-((methanetetrayltetrakis-(benzene-4,1-diyl)) tetrakis(1*H*-1,2,3-triazole-4,1-diyl)) tetraisophthalic acid ($H_8$L14 in Scheme 2), was designed and synthesized *via* the click reaction followed by the deprotection [137]. Blue crystals of the

MOF, denoted as NTU-180, were successfully obtained after solvothermal reaction with Cu(II) ion. Structure analysis reveals that NTU-180 is a 3D porous network with a basic framework formula of $[Cu_4(L14)(H_2O)_4]_n$ constructed by the connection of "clicked" L14 ligands with *in-situ* generated paddlewheel $Cu_2$ clusters (Figure 8a), in which two kinds of pores in diameters of 7.9 Å and 12.6 Å were observed (Figure 8b).

**(Insert Scheme 3 herein)**

### 2.2. MOFs derived from clicked triazolate ligands

In addition to carboxylate-containing ligands, nitrogen-containing heterocyclic organic compounds, such as pyrazolates, triazoles and tetrazoles, are another large group of organic ligands for constructions of coordination materials [24,25,138-145]. The azide-alkyne 1,3-dipolar cycloaddition can easily give the generation of nitrogen-containing heterocyclic triazoles. Thus, organic ligands having coordinative triazolates were also synthesized *via* the click reaction of dual-, or triple-symmetrical acetylene-containing organic components and azide components such as trimethylsilyl azide. Taking the generated triazole group as an electron donor group, metal-organic polyhedrons (MOPs), cages, coordination polymers, and other coordinated complexes were constructed. For example, by taking 1,3-diethynylbenzene, 1,6-heptadiyne, and 1,4-diethynylbenzene as spacers in the click reaction with azide compounds, a series of triazolates were synthesized ($R_2L15$-$R_2L17$ in Scheme 3) [146,147]. After assemblies with Pd(II) ion, a group of $[Pd_2L_4](BF_4)_4$ cages were successfully obtained.

Recently, organic ligands having terminal triazolates, such as benzeneditriazolate and benzenetristriazolate, were synthesized *via* the click reaction. Subsequently, MOFs with fascinating networks were constructed through strong coordination between the clicked polytopic triazolates and metal ions.

**(Insert Figure 9 herein)**

#### 2.2.1. MOFs derived from clicked benzeneditriazolates

A ditopic triazolate ligand, 1,4-benzenedi(1*H*-1,2,3-triazole) ($H_2$L18 in Scheme 3, abbreviated as $H_2$BDTri), was designed and synthesized *via* the click reaction of pre-synthesized 1,4-diethynylbenzene with azide-containing precursor by Long and coworkers [148]. After solvothermal reactions with Cu(II) in different solvents (N,N-dimethylformamide (DMF) or N,N-diethylformamide (DEF)), two 3D flexible microporous MOFs possessing the same structure type but with different coordinated solvent molecules in a formula of Cu(BDTri)L (L = DMF or DEF) were obtained. The crystal structural transformation featuring the "breathing" behavior through single-crystal to single-crystal conversion was observed (Figure 9), similar to some MOFs having the structure feature such as MIL-53 and Co(1,4-benzenedipyrazolate) [138,149-151]. Upon the exposure of the single crystals of Cu(BDTri)(DMF) in ambient atmosphere, 1D channels along the [010] direction gradually become narrow along with the crystal color change from green to blue and finally gray. On account of strong coordination between metals and the clicked triazolates, the initial and final structures together with an intermediate state of highly stable triazolate-bridged framework were well characterized by the X-ray analyses for detailed understanding of the structural deformations associated with framework breathing (Figure 9). During the $N_2$ and $O_2$ adsorption investigations, two-step isotherm based hysteresis was also observed, further revealing the flexibility of the framework.

When replacing the organic ligand in Cu(BDTri)(DMF) by another clicked ditopic triazolate ligand, 2,3,5,6-tetrafluoro-1,4-benzeneditriazolate ($H_2$L19 in Scheme 3, abbreviated as TFBDTri$^{2-}$) [152], its fluorinated analogue, Cu(TFBDTri)(DMF), was constructed, in which the framework flexibility was once again observed during the solvent exchange by DEF and DMSO.

**(Insert Figure 10 herein)**

### 2.2.2. MOFs derived from clicked benzenetristriazolates

1,3,5-Tris(1H-1,2,3-triazol-5-yl)benzene) ($H_3$L20 in Scheme 3, abbreviated as $H_3$BTTri) was designed and synthesized *via* click reaction of pre-synthesized 1,3,5-triethynylbenzene with trimethylsilyl azide in 2009 [153]. After the coordination with Cu(II) under solvothermal

reaction, a porous MOF, denoted as CuBTTri, was successfully constructed by BTTri-bridged *in situ*-generated chloride-centered $[Cu_4Cl]^{7+}$ square. Structure analysis reveals that the MOF possesses a cubic sodalite-type framework (Figure 10). Characterization measurements indicate that it shows both remarkable chemical and thermal stability. Immersion experiments and powder X-ray diffraction (XRD) measurements show that it is highly stable in air, boiling water, methanol and even acidic media. Its framework could be well maintained until at least 270 °C. High porosity together with the remarkable stability makes the constructed CuBTTri an excellent MOF in wide applications

**(Insert Figure 11 herein)**

By replacing Cu(II) ion with Fe(II) or Co(II) ions, two structural analogous of CuBTTri, *i.e.*, Fe-BTTri and Co-BTTri, were also constructed by Long and coworkers [154,155]. Investigations of gas adsorption reveal that Fe-BTTri not only is highly selective toward CO over a variety of other gas molecules, but also exhibits readily reversible CO binding (Figure 11), rendering it a promising adsorbent for CO scavenging from gas molecules such as $H_2$, $N_2$, $CH_4$, and ethylene. The desolvated Co-BTTri exhibits a strong preference for binding $O_2$ over $N_2$, with the isosteric heat of adsorption ($Q_{st}$) value of -34(1) and -12(1) kJ/mol, respectively. The high stability, selectivity, and $O_2$ adsorption capacity of Co-BTTri make it highly useful for the air separation.

### 2.3. MOFs derived from clicked carboxylate-containing triazolate ligands

By employing the versatile click chemistry, bifunctional carboxylate-containing triazolate ligands were synthesized for MOF constructions. In 2007, a carboxylate-containing triazolate, 1-(3,5-dicarboxyphenyl)-4-phenyl-1*H*-1,2,3-triazole ($H_2$dcppt, $H_2$L21 in Scheme 3), was synthesized *via* click reactions of 3,5-dicarboxyphenyl azide with azidobenzene [156]. After the solvothermal reaction with Co(II) ion, a (3,10)-connected 2D coordination polymer was successfully constructed. 1-(3,5-Dicarboxyphenyl)-4-carboxy-1*H*-1,2,3-triazole was also synthesized *via* click reaction, but when it was reacted with Mn(II) or Co(II) ion, *in situ* hydrothermal decarboxylation happened and it was transformed into 1-(3,5-di carboxy

phenyl)-1*H*-1,2,3-triazole) ($H_3$dcpct, $H_3$L22 in Scheme 3) in the finally constructed four coordination polymers [157].

**(Insert Figure 12 herein)**

A ditopic bifunctional organic ligand, 4-(1,2,3-triazol-4-yl)-benzoate (abbreviated as tab, H23 in Scheme 3) including both 1,2,3-triazolate and carboxylate donor groups, was synthesized by Ma and coworkers [158-160]. Then, a porous MOF, denoted as MTAF-1, was constructed by the coordination between the tab ligand and *in situ* generated pentanuclear zinc cluster (Figure 12a) [159]. Gas adsorption investigations reveal that the activated MTAF-1 shows a high porosity with a Langmuir surface area of 2300 $m^2/g$, exhibiting high performance on selective uptake of $CO_2$ over $N_2$. After that, a MOF, denoted as MTAF-4, with a rare (6,9)-connected network was also constructed by the coordination of the tab ligand with *in situ* generated tetranuclear and heptanuclear zinc cluster (Figure 12b) [160]. The microporous MTAF-4 exhibits a BET surface area of ~1600 $m^2\ g^{-1}$ and a high capability for adsorbing $CO_2$, $H_2$ and $CH_4$ under high pressure.

**(Insert Figure 13 herein)**

Subsequently, a triazole-containing ligand, 5-(1*H*-1,2,3-triazol-4-yl)isophthalic acid (abbreviated as $H_3$TAIP, $H_3$L24 in Scheme 3) [161], was also synthesized *via* clicked reaction in order to replace the tetrazole moiety of 5-tetrazolylisophthalic acid in *rht*-MOF-1 [105]. A new *rht*-type MOF, denoted as *rht*-MOF-tri (tri is short for triazolate), was then constructed (Figure 13) by the assembly of the ligand with Cu(II) ion, which as expected exhibited high porosity and remarkably enhanced water/chemical stability by incorporating *in situ* generated triangular inorganic building unit [$Cu_3O(Tri)_3$]. These studies successfully demonstrate that employing bifunctional linkers incorporating both the azolate and carboxylate groups as donor units provide a promising way to construct highly stabile MOFs for various applications.

### 2.4. MOFs incorporating click-extended bipyridine

In addition to the pyrazolates, triazoles and tetrazoles, pyridine derivatives are also a large group of nitrogen-heterocyclic organic ligands in the construction of coordination complexes [162-173]. Taking click reaction as an effective approach, some pyridine derivatives, such as L25-L37 in Scheme 3, were synthesized and subsequently used for assemblies of coordination complexes. Among these clicked pyridines, polytopical 1,2,3-triazol-4-ylpyridyl ligands can strongly chelate with metal ions through the nitrogen atoms of triazole and pyridine units, and thus, these ligands have been intensively investigated for synthesizing coordination compounds. For example, helicates were constructed by coordinating metal ions with the clicked pyridine derivatives (L26-L33 in Scheme 3) [174-178] and cages were also assembled *via* the coordination between metal ions and the clicked triazole-containing pyridines (L34-L37 in Scheme 3) [179-182].

**(Insert Figure 14 herein)**

In the MOF construction, a custom-designed ligand, 4,4'-(2*H*-1,2,3- triazole-2,4- diyl)di-pyridine, was synthesized *via* click chemistry by Ma and coworkers [183]. Introducing the clicked new ligand into a prototypal pillared MOF, *i.e.*, MOF-508 [184], to replace 4,4'-bipyridine, a triazole-containing MOF, denoted as MTAF-3, was successfully constructed (Figure 14). Since the incorporated 1,2,3-triazolate moieties feature exposed nitrogen atoms, the constructed MTAF-3 exhibits a remarkable enhancement of uptake capacity as well as significantly boosted $Q_{st}$ toward $CO_2$. These interesting results well demonstrate that incorporating 1,2,3-triazole functional groups to act as relatively moderate Lewis base centers is a feasible strategy for constructing novel porous MOFs with enhanced $CO_2$ uptake performance.

## 3. MOFs modified by click reaction

In addition to the direct synthesis of MOFs through the coordination of pre-designed polytopic organic ligands with inorganic metal ions, an effective approach to achieve functional MOFs is post-synthetic modification. By incorporating functional groups into

pristine MOFs that usually cannot be achieved during the direct synthesis processes, the modified MOFs often exhibit unique physical and chemical properties that are rarely presented in the pristine MOFs. Thus, post-synthetic modification has become a powerful strategy for the rational functionalization of the readily-available MOFs. Since the post-synthetic modification was introduced into MOFs in 2007 [185], a variety of MOFs have been post-synthetically modified so far [51,52,85,186,187]. For instance, amino-derived MOFs were intensively modified by various synthons such as aldehydes, isocyanates, and acid anhydrides. As aforementioned, the azide-alkyne 1,3-dipolar cycloaddition is an efficient reaction with wide readily-available reactants, which broadens the selectivity of reaction conditions and substrates. By using post-synthetic modification approach, a lot of functional groups including alkyne and azide derivatives have been grafted into or onto MOFs for diverse applications. When classifying these click post-synthetic modifications, four main types of reactions were developed as discussed below: (a) azide-tagged MOFs click-modified by alkynes, (b) alkyne-tagged MOFs click-modified by azides, (c) one-pot, two-step click modification of amino-derived MOFs by alkynes, and (d) copper-free strain-promoted click modification.

**(Insert Figure 15 herein)**

### 3.1. Click modification of azide-tagged MOFs by alkynes

Soon after the click chemistry being introduced into the process of ligand synthesis for the MOF construction, it was also used for post-synthetic modifications of MOFs. In 2008, Sada and coworkers investigated the click modification of a MOF (an analogue of IRMOF-16) bearing the azide group on the organic linker (denoted as $N_3$-MOF-16) by five small external alkynes, *i.e.*, methyl propargylate, propargyl alcohol, 1-hexyne, propargylamine, and propiolic acid (1-5 in Figure 15) [188]. After copper(I)-catalyzed click reaction of $N_3$-MOF-16 with methyl propargylate, characterizations were carried out to check whether the host MOF was clickable or not. IR spectra reveal that the MOF was thoroughly modified, due to the complete disappearance of the feature peak of azide stretching band at 2100 $cm^{-1}$. The solution $^1H$ NMR spectrum of the decomposed product after click reaction illustrates that

the corresponding triazole derivative as the major product was formed and no starting material was detected. Powder XRD patterns indicate that the framework was still well maintained after the click reaction. Reactions with substrates 2 and 3 in Figure 15 further confirm the feasibility of the MOF modification by the effective click chemistry, although the framework decomposition was observed during the reactions with substrates 4 and 5 in Figure 15.

**(Insert Figure 16 herein)**

By following this method, Zr-based PCN-58 and PCN-59 were then click-modified by a series of acetylene-containing compounds with different functional groups, and the obtained modified MOFs were used for $CO_2$ adsorption by Zhou *et. al.* (Figure 16) [189]. After that, some highly stable MOFs were also click-modified by acetylene compounds [190-193]. For instance, azide-tagged UiO-66 (UiO-66-$N_3$) was modified by phenylacetylene [193], and the resulted MOF was used as a fluorescent probe for selective detection of mercury (II) in aqueous media. Subsequently, clicked post-synthetic modification of azide-bearing MOFs by polytopical acetylene compounds for the fabrication of polymer gels was also investigated, as discussed in section 4.5.

### 3.2. Click modification of alkyne-tagged MOFs by azides

Nearly at the same time when the azide-tagged MOFs were reported to be click-modified by alkynes, alkyne-tagged MOFs were also click-modified by azides. The surface of a MOF bearing trimethylsilyl (TMS) protected alkyne was post-synthetically modified with azides reported by Nguyen and coworkers in 2008 [194]. After solvothermal reaction of 3-[(trimethylsilyl)ethynyl]-4-[2-(4-pyridinyl)ethenyl]pyridine, 2,6-naphthalene-di- carboxylic acid, and Zn(II) ion, a two-fold interwoven MOF containing TMS-protected acetylenes was obtained. Characterizations reveal that when employing tetrabutylammonium fluoride (TBAF) as the desilylation reagent, only the MOF surface was desilylated due to large molecule size of $tBu_4N^+$ counterion and pore-size limitation of the two-fold interwoven MOF. Copper(I)-catalyzed click reaction with an azide-containing dye, ethidium bromide

monoazide, further confirm that the reaction only occurred on the crystal surface of contracted MOF, since the fluorescence from the clicked azide-containing dye was exclusively observed on the surface. Inspired by the surface-selective modification, azide-containing polyethylene glycol (PEG) was then grafted onto the surface of contracted MOF by click post-synthetic modification, changing the MOF crystal to be hydrophilic and wettable.

**(Insert Figure 17 herein)**

Subsequently, the authors synthesized an acetylene-bearing and non-catenated MOF, termed as TO-MOF, after solvothermal reaction of 1,2,4,5-tetrakis(4-carboxyphenyl)benzene (TCPB) and 3-[(trimethylsilyl)ethynyl]-4-[2-(4-pyridinyl)ethenyl]pyridine with Zn(II) ion [195]. When employing TBAF as the fluoride source for the removal of the TMS group, characterizations reveal complete desilylation in the internal MOF (Figure 17). The conclusion was further confirmed after copper(I)-catalyzed click reaction of deprotected TO-MOF with benzyl azide. Interestingly, when changing the fluoride source from TBAF to KF, selective external surface deprotection was detected due to poor solubility of KF in organic solvents (Figure 17). When click-modifying the surface deprotected TO-MOF by organic moieties, MOF composites in a core-shell fashion were achieved. In these processes, the MOF framework was determined both powder XRD and $N_2$ adsorption analyses, and the results show that the MOF crystallinity was well maintained.

**(Insert Figure 18 herein)**

Some other alkyne-tagged MOFs were also post-synthetic modified by copper(I)-catalyzed click reactions with azide-containing compounds. For example, azide groups were introduced into the network of NU-1000 by click reaction with pre-incorporated alkyne-containing compounds [196], and an alkyne-tagged Zr-based MOF, UiO-68-alkyne, was also click-modified with azidoethane, ethyl azidoacetate, and azidomethylbenzene by Wang and coworkers (Figure 18) [197,198].

**(Insert Figure 19 herein)**

### 3.3. One-pot, two-step click modification of amino-derived MOFs by alkynes

Due to the unavailability and instability of most azide linkers, a one-pot, two-step functionalization method using easier-available amino-derived MOFs was developed by Farrusseng *et. al.* for smoothly clicked post-synthetic modification of MOFs (Figure 19). Taking DMOF-$NH_2$ [Zn(bdc-$NH_2$) (DABCO)] (DABCO = 1,4-diazabicyclo(2.2.2)octane) as a starting MOF, an alternative approach involving stable, nonexplosive compounds under mild conditions instead of reacting with diazonium salts in acidic conditions was conducted [199]. The azide intermediate MOF, DMOF-$N_3$, was obtained after treating the freshly dried DMOF-$NH_2$ with tBuONO and $TMSN_3$ in THF at room temperature overnight. Subsequently, copper(I)-catalyzed clicked post-synthetic modification was carried out in the same vessel by adding excess phenylacetylene in the presence of $Cu^I(CH_3CN)_4PF_6$ for 24 h. IR spectroscopy, solution $^1H$ NMR analysis and powder XRD patterns confirm the formation of azide intermediate and final product of DMOF-fun without the loss of long-range order of crystallinity of parent DMOF-$NH_2$. The feasibility of such a method was further confirmed by the one-pot, two-step clicked-modification of MIL-68(In)-$NH_2$. Finally, a combinatorial library of 24 functionalized MOFs was obtained by the one-pot, two-step clicked-modification of five aminoterephthalate-containing MOFs, *i.e.*, DMOF-$NH_2$, MIL-68(In)-$NH_2$, CAU-1, MIL-53(Al)-$NH_2$ and MIL-101(Fe)-$NH_2$, with different alkynes [200]. Moreover, the grafting yields in these MOFs could be controlled from 10 to 100%.

**(Insert Figure 20 herein)**

Inspired by this method, the unconventional derivatization of $N_3$-decorated MOFs was successfully demonstrated using amine-analogues as initial reactants by Giambastiani and coworkers [84]. Firstly, amine-functionalized UMCM-1 and MIXMOF-5 were treated by stable and nonexplosive *t*BuONO and $TMSN_3$ to afford $N_3$-decorated MOFs, UMCM-1-$N_3$ and MIXMOF-5-$N_3$, respectively. Single organic/organometallic acetylene derivatives for homodecoration, and defined binary and ternary mixtures of reactive terminal alkynes in

variable molar fractions for heterodecoration of $N_3$-decorated MOFs demonstrate that the single step click chemistry is a versatile reaction for a facile and convenient MOF engineering (Figure 20).

**(Insert Figure 21 herein)**

### 3.4. Copper-free strain-promoted click modification of MOFs

To overcome intrinsic toxicity from conventional Cu-catalyzed azide-alkyne cycloaddition and broaden its utilization in biological field, strain-promoted Cu-free azide-alkyne cycloaddition was developed by using cycloalkyne derivatives as alkyne reagents [201], and this Cu-free method was rapidly employed in other areas [59,202-204]. The Cu-free approach was brought into MOFs by Rosi and coworkers in 2012 [205]. In their investigation, an azide-modified mesoporous MOF, denoted as $N_3$-bio-MOF-100, was selected as the scaffold MOF, on account of its large interconnected channels allowing for unimpeded diffusion of large molecules (Figure 21). Then, two cycloalkyne derivatives, *i.e.*, methyl 4-(11,12-didehydrodibenzo[b,f]-azocin-5(6H)-yl)-4-oxobutanoate (1 in Figure 21) and N-dodecanoyl-5,6-dihydro-11,12-didehydrodi-benzo[b,f]azocine (2 in Figure 21), were prepared to demonstrate the strain-promoted Cu(I)-free click-modification. After mixing the azide-bearing MOF with equivalent cycloalkyne derivatives in dichloromethane and standing the mixtures at room temperature overnight, characterizations indicate that the strain-promoted Cu-free click-modification was proceeded nearly quantitatively under ambient conditions without affecting the structural integrity of the MOF. The reaction was free of catalysts and byproducts, and even more efficient than the Cu-catalyzed counterpart.

**(Insert Figure 22 herein)**

After that, Woll *et. al.* demonstrated that strain-promoted Cu-free click reaction is more effective reaction than the Cu(I)-catalyzed click reaction in the field of membrane fabrications. Utilizing strain-promoted Cu-free click-modification, a complete conversion on surface-anchored MOF (SURMOF) thin films was detected, in which the contamination of

the product by cytotoxic $Cu^{I}$ ion was successfully avoided (Figure 22) [206,207]. Since then, the modifications of MOFs, such as UiO-66 and UiO-68, by the strain-promoted Cu-free click reaction were intensively investigated especially for utilizations in biological systems, as discussed in section 4.4.

## 4. Applications of MOFs constructed or modified by click reaction

The azide-alkyne 1,3-dipolar cycloaddition not only enriches the library of MOF structures, but also widely broadens the applications of MOFs by introducing the *in situ* generated triazole groups and incorporating functional groups into the frameworks during either the syntheses of organic ligands or the post-synthetic modifications of pristine MOFs. Thus, diverse utilizations of MOFs derived from the azide-alkyne 1,3-dipolar cycloaddition have been investigated, including $CO_2$ selective adsorption, heterogeneous catalytic reactions, large-molecule capture and separation, biological research, and porous material fabrication.

### 4.1. Porosity and $CO_2$ adsorption capability

$CO_2$ has been cited as the primary gas leading to average temperature increase of the global surface and climate changes [8,9,208-218]. As a group of effective porous materials, lots of newly developed MOFs have been employed as $CO_2$ adsorbents, aiming to reduce anthropogenic $CO_2$ emission. Theoretical and experimental investigations have revealed that the incorporation of accessible nitrogen-donor groups into MOFs could dramatically increase the framework affinity toward $CO_2$ due to the dipole-quadrupole interactions between the polarizable $CO_2$ molecule and the accessible nitrogen site [217,218]. While the MOFs constructed *via* click reaction possess nitrogen-rich triazole groups, clicked post-synthetic modification could also introduce $CO_2$-philic groups into MOFs. Thus, these MOFs derived from the click chemistry have been exploited for the $CO_2$ adsorption.

**(Insert Figure 23 herein)**

#### 4.1.1. MOFs containing accessible triazole groups for $CO_2$ adsorption

Although structural and topological analyses show that NTU-101-Zn processes a 3D porous framework, almost half of the pore channels are blocked by the coordinated DMF molecules. The removal of coordinated DMF molecules through the activation process causes the collapse of the framework [90]. As a result, NTU-101-Zn shows poor gas adsorption capacities. Surprisingly, a sharp improvement of framework stability was achieved after a process of metal ion exchange from Zn to Cu, and a remarkable increase of the framework porosity was observed after the activation of Cu exchanged NTU-101-Zn (named as NTU-101-Cu). The results of $N_2$ sorption at 77 K show that the activated NTU-101-Cu gives an overall $N_2$ uptake of 526 $cm^3 g^{-1}$ and a calculated BET surface area of 2017 $m^2 g^{-1}$, while the pristine NTU-101-Zn shows an overall $N_2$ uptake of 30 $cm^3 g^{-1}$ with a BET surface area of only 37 $m^2 g^{-1}$ (Figure 23a). The $CO_2$ adsorption capability was then carried out, and the results indicate that NTU-101-Cu presents the $CO_2$ uptake of 101 $cm^3 g^{-1}$ (16.6 wt%) at 1 atm and 273 K (Figure 23b) and the $Q_{st}$ for $CO_2$ was determined to be 25-20 kJ $mol^{-1}$. Meanwhile, NTU-101-Cu shows low $N_2$ and $CH_4$ uptake capabilities of 7 and 20 $cm^3 g^{-1}$ at 1 atm and 273 K, respectively [90]. These results clearly demonstrate that the triazole-containing NTU-101-Cu could act as an efficient adsorbent for $CO_2$ selective adsorption.

**(Insert Figure 24 herein)**

The gas adsorption measurements were also carried out on the activated NTU-111, NTU-112 and NTU-113, and the results show that all of them possess high framework stability and high porosity with overall $N_2$ uptake of 660, 829, 873 $cm^3 g^{-1}$ and calculated BET surface areas of 2450, 2992 and 3095 $m^2 g^{-1}$, respectively [92]. Gas adsorption investigations indicate an increase of the $CO_2$-uptake capability from NTU-111 to NTU-113. At 273 K and 1 atm, NTU-111, NTU-112 and NTU-113 give $CO_2$-uptake values of 124.6, 158.5 and 166.8 $cm^3 g^{-1}$ respectively, while corresponding $N_2$-uptake values are of only 10.5, 11.0 and 11.9 $cm^3 g^{-1}$. The calculations show corresponding $Q_{st}(CO_2)$ values of ~30.7, ~32.0 and ~33.2 kJ $mol^{-1}$ at low loading range of $CO_2$. All of them present high $CO_2$ selectivity and high $CO_2$-framework interactions, especially in the case of NTU-113. Therefore, a simulation was conducted to investigate the performance of NTU-113 toward post-combustion $CO_2$ capture

from a flue gas. The breakthrough times were calculated to be 13.8 for $N_2$ and 181.2 for $CO_2$ when the $CO_2/N_2$ mixture with initial molar ratio of 0.15:0.85 passes through a fixed-bed packed by NTU-113 (Figure 24). The positive result based on the theoretical simulation clearly indicates that the clicked triazole-containing MOFs are highly useful systems for the $CO_2/N_2$ separation.

**(Insert Figure 25 herein)**

As the activated NTU-105 exhibits an overall $N_2$ uptake of 861 $cm^3\ g^{-1}$ at 1 atm with a surface area of up to 3543 $m^2\ g^{-1}$, its $CO_2$ adsorption capability was also investigated [121]. Gas sorption isotherms reveal that it possesses an $CO_2$-uptake capability as high as 187 $cm^3\ g^{-1}$ (36.7 wt%) but a $N_2$ uptake capability of only 16 $cm^3\ g^{-1}$ at 1 atm and 273 K, making it one of top MOFs for $CO_2$ selective adsorption. The calculation based on isothermals reveals that it has a $Q_{st}$ value of ~35 kJ $mol^{-1}$ for $CO_2$ at low loading range. Molecular simulation studies were further utilized to investigate the remarkable $CO_2$-framework interactions (Figure 25), and the calculated radial distribution functions *g*(r) reveal that not only the open Cu sites but also all of the three N atoms in the coordination-free triazole ring provide high affinities to $CO_2$ molecule. Then, the isoreticular MOFs of NTU-105, NU-138, NU-139, NU-140 were also studied for the $CO_2$ adsorption. Gas adsorption experiments reveal that, among them, NU-140 exhibits not only gravimetric methane uptake of 0.34 g $g^{-1}$ at 65 bar and 298 K, corresponding to almost 70% of the target (0.5 g $g^{-1}$) set by the U.S. Department of Energy [127], but also rather high $CO_2$ uptake of 1.52 g $g^{-1}$ at 298 K and 30 bar and a significant $H_2$ uptake of 90 mg $g^{-1}$ at 65 bar at 77K.

**(Insert Figure 26 herein)**

After the activation, NTU-180 shows a high porosity with an overall $N_2$ uptake of 655 $cm^3\ g^{-1}$ at 1 atm and 77 K, and a BET surface area of 2436 $m^2\ g^{-1}$ [137]. It displays a $CO_2$-uptake value of 160.8 $cm^3\ g^{-1}$ at 273 K and 1 atm with a calculated $Q_{st}$ of ~32.2 kJ $mol^{-1}$ at low loading range of $CO_2$. In order to monitor its affinity to $CO_2$ molecule, *in situ* Raman spectral

measurements were then implemented to the activation NTU-180. After adsorbing $CO_2$, a new peak corresponding to $CO_2$ adsorbed in the framework clearly appears at 1377 $cm^{-1}$ instead of 1388 $cm^{-1}$ for gaseous $CO_2$ (Figure 26), which gives unambiguous evidence of the framework affinity to $CO_2$ in the clicked triazole-containing MOF.

As aforementioned, MOFs derived from the clicked carboxylate-containing triazolate ligands and click-extended bipyridines also show high performance on $CO_2$ selective-adsorption [159-161,183]. Experimental measurements of $CO_2$ adsorption, theoretical simulations, and *in situ* Raman spectral studies clearly reveal that the incorporation of coordination-free triazole-containing groups into MOFs could dramatically increase the framework affinity to $CO_2$ molecule and the MOFs derived from the click reaction are highly promising materials for $CO_2$ selective adsorption.

**(Insert Figure 27 herein)**

### 4.1.2 Amine modified triazolate-MOFs for $CO_2$ adsorption

CuBTTri itself is an effective adsorbent for $CO_2$ selective adsorption [219]. Amine derivatives were introduced into its framework to further improve the $CO_2$ selectivity on account of its remarkable chemical and thermal stability. Firstly, ethylenediamine (en) molecule was incorporated into CuBTTri by Long and coworkers [153]. The resulting en-functionalized framework (CuBTTri-en) exhibits higher uptake of $CO_2$ at very low pressures as compared with the non-grafted pristine MOF, and displays very high affinity for $CO_2$ binding with the $Q_{st}$ value of up to 90 kJ $mol^{-1}$. Subsequently, they also introduced N,N'-dimethylethylenediamine (mmen) into the robust porous CuBTTri, and the resulted mmen-CuBTTri could adsorb 2.38 mmol $CO_2$ $g^{-1}$ (9.5 wt%) with a $Q_{st}$ of up to 96 kJ $mol^{-1}$ and a high selectivity of up to 327 [220]. Although the chemisorption between amines and $CO_2$ was supported by infrared spectra, the $CO_2$ uptake was fully reversible, and the framework could be easily regenerated at 60 $^oC$ with a cycling time of just 27 min. Thus, mmen-CuBTTri is an effective adsorbent for $CO_2/N_2$ separation based on the $CO_2$ selective adsorption (Figure 27). Piperazine (pip) was also used to modify CuBTTri by D'Alessandro *et. al.* for the purpose of $CO_2$ selective adsorption [221]. The post-synthetically modified product,

pip-CuBTTri, exhibits an improved $CO_2$ uptake capability as compared with the non-grafted material, showing a $Q_{st}$ of up to 96.5 kJ $mol^{-1}$ and a selectivity factor of 130 over $N_2$. The pip-CuBTTri could also be regenerated *via* both pressure and temperature swing processes. These results clearly indicate that highly stable MOFs constructed by the coordination of clicked triazolates with metal ions could be modified by organic amines to achieve high $CO_2$ adsorption capabilities.

### 4.1.3 Click modified MOFs for $CO_2$ adsorption

Through Cu-catalyzed azide-alkyne cycloaddition, some highly stable azide-tagged MOFs such as Zr-based PCN-58 and PCN-59 were post-synthetically modified by alkynes and then utilized for $CO_2$ adsorption [189]. The results reveal that, when introducing $CO_2$-philic amine and hydroxyl groups into the MOF networks, increased performance on $CO_2$ uptake and selective adsorption was observed.

**(Insert Figure 28 herein)**

To mimic conventional amine-based aqueous absorbents in the process of $CO_2$ adsorption, $CO_2$-philic amine group and in situ generated triazole group were both introduced into a highly stable mesoporous MIL-101 by the Cu-catalyzed azide-alkyne cycloaddition (Figure 28) [190]. As compared with the pristine MIL-101, MIL-101-triazo-$NH_2$ exhibits remarkably improved $CO_2$-uptake capability of up to 128.3 $cm^3$ $g^{-1}$ (20.1 wt%) at 1 atm and 273 K, and significantly enhanced selectivity to $CO_2$ over $N_2$. All the results clearly demonstrate that both the triazole-containing MOFs derived from click reactions and MOFs modified by $CO_2$-philic groups *via* click reactions could serve as excellent adsorbents for $CO_2$ selective adsorption.

## 4.2 Heterogeneous catalytic reactions

Owning to their high surface areas, larger molecule-accessible pores, and intrinsic properties, MOFs have also been employing as a group of effective heterogeneous catalysts or catalyst supports [14-17,222]. The MOFs constructed or modified by click reaction were considered as heterogeneous catalysts for different kinds of reactions, and their applications in

$CO_2$ chemical conversion, biomimetic catalytic NO generation, asymmetric aldol reactions, transesterification reactions, and Knoevenagel condensations were well studied.

**(Insert Scheme 4 herein)**

### 4.2.1 Catalytic $CO_2$ conversion

In addition to the physical adsorption, an alternative strategy to reduce the anthropogenic $CO_2$ emission is the catalytically chemical conversion of $CO_2$ into value-added chemicals [223,224]. MOFs incorporating coordination-free triazole groups usually have a good $CO_2$-philic property, thus facilitating the heterogeneous reaction of $CO_2$ involved. Meanwhile, open Cu sites could usually be incorporated after the assembly of the clicked ligands with Cu ion. The embedded open Cu metal sites as active Lewis-acid species together with their inherent $CO_2$-philic property endow these triazole-containing MOFs highly promising catalysts for $CO_2$-involved reactions. The cycloaddition of $CO_2$ with epoxides to produce various carbonates (Scheme 4) was taken as a representative reaction for such an investigation [225-228].

**(Insert Table 1 herein)**

When taking cuboctahedral nanoparticles of NTU-105 as a catalyst with *tetra-n*-butylammonium bromide (TBAB) as a co-catalyst and small-sized epoxides as substrates, the reaction yields after reactions at room temperature under 1 atm $CO_2$ pressure for 48 h were found to be 89%, 88% and 87% for 4-ethyl-1,3-dioxolan-2-one, 4-(bromomethyl)-1,3-dioxolan-2-one, and 4-(chloromethyl)-1,3-dioxolan-2-one, respectively [229]. However, the reaction gives lower yield of only 38% for 4-phenyl-1,3-dioxolan-2-one after the same process. Due to the difference of their porosity derived from different degree of the framework interpenetration, NTU-140 and 141 exhibited an obviously different catalytic activity toward the same substrates [95]. After stirring the reactions with TBAB as the co-catalyst in tubes at room temperature under 1 atm $CO_2$ for 60 h, the yields of cyclic carbonate products catalyzed by NTU-140 are 94%, 80%, 83% and 85% for 2-methyloxirane,

2-ethyloxirane, 2-(chloromethyl)oxirane, and 2-(bromomethyl)oxirane respectively, while corresponding yields catalyzed by NTU-141 are only 49%, 33%, 35%, and 36%.

**(Insert Figure 29 herein)**

The catalytic activity of activated NTU-180 toward $CO_2$ chemical conversion was also investigated with the same type reaction [137]. After catalytic reaction under 1 atm $CO_2$ pressure at room temperature for 48 h with TBAB as the co-catalyst, the yields of cyclic carbonates catalyzed by NTU-180 are 96%, 83%, 85%, and 88% for 2-methyloxirane, 2-ethyloxirane, 2-(chloromethyl)oxirane, and 2-(bromomethyl)oxirane, respectively (Table 1). Their related turnover frequency (TOF) values are 200.0, 172.9, 177, and 183.3 $h^{-1}$ per paddlewheel $Cu_2$ cluster. In the control experiments catalyzed by HKUST-1, the yields are only 65%, 54%, 56%, and 57%, respectively. On the other hand, when larger epoxide substrates were exploited, a sharp decrease of the product yields was observed under the same catalytic process (Figure 29). They were just 8%, 6% and 5% for 1,2-epoxyoctane, 1,2-epoxydodecane, and 2-ethylhexyl glycidyl ether, respectively (Table 1). Thus, remarkably high efficiency and selectivity to small epoxides on catalytic $CO_2$ cycloaddition make the Cu-based MOFs derived from clicked ligands suitable heterogeneous catalysts for carbon fixation.

**(Insert Figure 30 herein)**

### 4.2.2 Biomimetic catalytic NO generation

Since CuBTTri has robust porosity and high stability even in media routinely used for *in vitro* and *in vivo* experiments, it has been exploited for biological application by Reynolds and coworkers (Figure 30) [230-232]. By blending CuBTTri into biomedical polyurethane matrices, a composite denoted as CuBTTri-poly was firstly fabricated for use as a biomimetic catalyst to generate bioactive agent nitric oxide (NO) as therapeutic species from endogenous sources, *S*-nitrosothiols (RSNOs). The catalytic function of CuBTTri in the composite was demonstrated by CuBTTri catalyzed RSNO substrate, *i.e.*, *S*-nitrosocysteamine (CysamNO)

[230]. The CuBTTri-poly composite displays tunable NO-release kinetics proportional to the total content of CuBTTri embedded into the composite. Its surface flux corresponding to the therapeutic range of 1-100 nM $cm^{-2}$ $min^{-1}$, which is within the physiologically relevant range, was maintained in biological fluids such as blood. In order to mimic the proprietary composition of medical grade Tygon used in extracorporeal circuits, CuBTTri was also embedded into a mixture of poly(vinyl chloride) (PVC) and dioctyl sebacate plasticizer to give the formation of a CuBTTri/polymer composite film [231]. They fund that the composite film could enhance NO-generation from the RSNO substrate, *i.e.*, *S*-nitroso-*N*-acetyl-D-penicillamine (SNAP). The cytotoxicity of CuBTTri/polymer composite film was evaluated. Cumulative copper release from the probable CuBTTri degradation during the catalytic process in both phosphate buffered saline (PBS) and cell culture media under physiological conditions for a 4-week duration was recorded to be less than 1% of theoretical copper content present in the CuBTTri/polymer composite film, and no significant toxicity was observed from *in vitro* cell studies in 3T3-J2 murine embryonic fibroblasts and primary human hepatocytes. When replacing the hydrophobic polyurethane or PVC by naturally derived polysaccharide chitosan, hydrophilic CuBTTri composite membrane was also fabricated by the same group [232], and the fabricated CuBTTri composite membrane exhibited the ability to enhance the NO generation from the most abundant small-molecule RSNO, *i.e.*, *S*-nitrosoglutathione (GSNO). All these investigations provide insight into the function and utility of CuBTTri based polymer systems in biomedical applications.

**(Insert Figure 31 herein)**

### 4.2.3 Heterogeneous asymmetric catalysis

An achiral alkyne-bearing MOF, denoted as Zn-DPYI, was pre-constructed by Duan *et. al* [233]. After clicked modification by two azide compounds with opposite chiral centers, L-N-2-azidomethylpyrrolidine (L-AMP) and D-N-2-azidomethylpyrrolidine (D-AMP), two enantiomeric Zn-MOFs with asymmetric catalytic sites were achieved (Figure 31). Taking various aromatic aldehydes as substrates and reacting with cyclohexanone catalyzed by the click modified Zn-MOFs, decent yields with fairly high enantioselectivity were detected in all

reaction systems. On the other hand, very low conversion with undetectable enantiomeric excess was obtained when taking the pristine MOF as the catalyst in the same reaction. These results indicate that introducing catalytic chiral centers into achiral MOFs by click chemistry to synthesize effective chiral catalysts could be easily achieved for heterogeneous asymmetric catalysis.

**(Insert Figure 32 herein)**

### 4.2.4 Transesterification reaction

Through the one-pot, two-step click modification, a strong organic base ($pK_b$ = ~3 for trialkylamines), diethylpropargylamine, as a catalytic center was grafted into an amino-derived MOF, and thus a mono-functionalized MOF catalyst was obtained by Farrusseng and coworkers [234]. A lipophilic group, *i.e.*, phenylacetylene, was respectively introduced into the amino-derived MOF and another mono-functionalized MOF with moderate basicity originated from the triazolyle group ($pK_b$ = ~9.4) and strong lipophilicity from the phenyl group. Meanwhile, modified by both diethylpropargylamine and phenylacetylene, a bifunctionalized MOF with an optimized balance between basicity and lipophilicity was also obtained (Figure 32). Subsequently, their catalytic activities in the transesterification reactions were investigated. The results clearly show that the bifunctionalized MOF presents the highest activity toward the transesterification of ethyldecanoate in methanol, while the modification degree affects the ethyldecanoate conversion in the case of the monofunctionalized MOFs. These interesting results indicate that effective catalysts could be achieved though ingenious click modification of host MOFs.

**(Insert Figure 33 herein)**

### 4.2.5 Knoevenagel condensation

An azide-tagged Zr-based MOF, UiO-67–$N_3$, was initially constructed by Gao and coworkers [235]. Subsequently, three alkyne compounds, *i.e.*, methyl propargylate, propargyl alcohol, and propargylamine, were introduced into the framework by copper(I)-catalyzed

click modification, leading to more stable MOFs, UiO-67–Tz–$COOCH_3$, UiO-67–Tz–OH, and UiO-67–Tz–$NH_2$, with different functional groups (Figure 33). Due to moderate basicity derived from *in situ* generated triazolyle group, all three MOFs were taken as base catalysts for the Knoevenagel condensation between carbonyl and activated methylene. Catalytic reaction of benzaldehyde ethyl and cyanoacetate was conducted in DMF. The results reveal that, in the presence of UiO-67–Tz–$NH_2$, ethyl (E)-$\alpha$-cyanocinnamate as the only product was detected and the condensation could be completely achieved within 8 hours at 40 $^oC$ or only 3 hours at 80 $^oC$, while in the present of UiO-67–Tz–$COOCH_3$ and UiO-67–Tz–OH, only a comparable conversion to that in the absence of any catalyst was observed, indicating that the grafted amino group, instead of the *in situ* generated triazole group or other component of the framework, is the crucial active site for Knoevenagel condensation reaction. Further studies also demonstrate that the UiO-67–Tz–$NH_2$ catalyst was recyclable for the reaction with malononitrile, but not for the reaction with ethyl cyanoacetate, probably because the reaction between the amino site and the ester group of ethyl cyanoacetate leads to the formation of amide. The investigations also reveal that, although the basicity of the *in situ* generated triazolyle group is not strong enough, organic base groups could be grafted into the framework for Knoevenagel condensation by click post-synthetic modification.

### 4.3 Dye-probed applications toward large organic molecules

In addition to the gas adsorption and catalytic reactions, MOFs with large pores derived from the click-extended ligands or modified by the clicked reaction were also investigated in the applications toward large organic molecules.

#### 4.3.1 Dye-probed large organic molecule capture and separation

Taking the clicked triazole group as an extending spacer, large organic ligands were successfully obtained by the click reaction of triple-symmetrical acetylene-containing organic moieties with 4-azidobenzoates or 5-azidoisophthalates. After the assembly with Zn(II) ion, transparent crystals of MOFs, *i.e.*, NTU-130, NTU-161, NTU-162, and NTU-163, with large-molecule accessible pores were achieved [87,128]. Among large organic molecules, organic dyes are a useful group of organic molecules with visible colors, which have been

widely used in environmental science and biological imaging. Colorless/light-yellow transparent property and large-molecule accessible pores of these Zn-based MOF crystals and visible color feature of dye molecules jointly facilitate the investigation of the MOF applications for large-molecule capture and separation probed by organic dyes.

**(Insert Figure 34 herein)**

As previously reported [236-238], the investigation toward large molecule adsorption and capture was carried out by immersing the activated crystals of three isoreticular MOFs, *i.e.*, NTU-161, NTU-162, and NTU-163, into the DMF solution of dyes, methylene blue (MeB, blue), rhodamine 6G (R6G, red), and brilliant blue R (BBR, blue), respectively [128]. The visible large-molecule soaking experiments clearly demonstrate that all these click-extended MOFs, especially NTU-163 with the largest pores, could be used as adsorbents for large molecule capture (Figure 34). Subsequently, their promising applications in environmental science for pollutant removal were proven by dye capture experiments after passing-through MOF packed columns, and their potentials as drug carriers in biological applications were also demonstrated by the adsorption of an anticancer drug doxorubicin (Dox). The same capability of NTU-130 was also observed [87].

**(Insert Figure 35 herein)**

Inspired by the size-dependent adsorption of these clicked-extended MOFs toward organic dyes with different molecule size, the capabilities of size-dependent separation for the mixtures of large molecules were also examined. As shown in Figure 35, after the DMF solution of dye mixtures, R6G and BBR, passing though the column packed by crystals of NTU-130, the dye with small molecule size (R6G) was undoubtedly captured by the MOF, while relatively large one (BBR) was eluted [87]. Effective separation capability of the three clicked-extended isoreticular MOFs was observed during the large molecule separation experiments probed by dye mixtures [128]. These successful experiments of large-molecule capture, uptake and separation probed by dye molecules demonstrate that extending organic

backbones of ligands *via* the versatile click reaction to increase the pore size of MOFs is an efficient approach to fabricate large porous MOFs toward large guest molecule based applications, such as catalysis, drug delivery, bioimaging, pollutant removal, and large organic molecule separation.

**(Insert Figure 36 herein)**

### 4.3.2 Dye-probed luminescence and imaging

Upon multimodal derivatization of aforementioned $N_3$-decorated MOFs, UMCM-1-$N_3$ and MIXMOF-5-$N_3$, by single organic/organometallic acetylene derivatives or defined binary and ternary mixtures [84], acetylene end-capped *tert*-thiophene derivatives were introduced into the pristine UMCM-1 and MIXMOF-5, and the obtained materials were subsequently employed as both polycyclic reagents and fluorescent probes for the monitoring of guest molecules. For the MOFs fluorescently labeled by *tert*-thiophene derivative, the studies indicate homogeneous fluorescent probe diffusion into MOF bulk materials (Figure 36).

**(Insert Figure 37 herein)**

An organic dye, alkyne-BODIPY, was successfully grafted into the pores of azide-tagged PCN-333(Sc) *via* the click reaction in 2015 [192]. In both suspension and solid-state of BODIPY-clicked PCN-333(Sc), strong fluorescence was observed (Figure 37). Interestingly, dye aggregates of alkyne-BODIPY show a red emission, while the emission of BODIPY-clicked PCN-333(Sc) in the solid state is green ($\lambda$ = 550 nm, Figure 37c), suggesting that the clicked dye in PCN-333(Sc) behaves as a monomeric dye.

**(Insert Figure 38 herein)**

### 4.4 Drug delivery and cancer therapy

Developing drug delivery systems for cancer therapy has become one of the important tasks for the scientific community, and MOFs have been showing a high potential in this area.

As click chemistry is a powerful tool for bioconjugation, lots of MOFs have been modified by click reaction for the drug delivery and cancer therapy. A nano-sized metal-organic polyhedron (MOP, one-dimensional MOF), denoted as Cu(pi), with alkyne groups covered on the surface was synthesized using 5-(prop-2-ynyloxy)iso phthalic acid ($H_2$pi) as the ligand precursor by Zhou and coworkers in 2011 [239]. Using $[Cu(CH_3CN)_4]PF_6$ instead of $CuSO_4$/sodium ascorbate as the catalyst system for clicked modification, azide-terminated PEG was successfully grafted onto the MOP surface (Figure 38), and thus water-stable colloid Cu(pi)-PEG5k was obtained. Subsequently, Cu(pi)-PEG5k was used as a carrier for drug release studies. A widely-used anticancer drug, 5-fluorouracil (5-FU), was selected as a drug model in this investigation, and the drug-loaded Cu(pi)-PEG5k, Cu(pi)-PEG5k⊃5-FU, was prepared based on the solubility difference of 5-FU between chloroform and methanol. During the drug release experiments on the Cu(pi)-PEG5k⊃5-FU system, after the initial burst release stage (2 hours), much flatter release curve up to 24 hours was observed, and around 20% of the loaded 5-FU was released. For pure 5-FU, close to 90% of the total drug was released within 7 hours. This successful demonstration of drug release from post-synthetically modified MOP opens an avenue for promising applications in the drug delivery.

**(Insert Figure 39 herein)**

MOF nanoparticle-nucleic acid conjugates were fabricated *via* the strain-promoted Cu-free click reaction by Mirkin and coworkers in 2014 (Figure 39) [240]. Firstly, nanoparticles of an azide-bearing MOF, UiO-66-$N_3$, were prepared. Utilizing the strain-promoted Cu-free click reaction between DNA appended with dibenzylcyclooctyne and the UiO-66-$N_3$ nanoparticles, the surface of the MOF nanoparticles was covalently functionalized by oligonucleotides. On account of the pore size limitation, the click post-synthetic modification only occurred on the MOF surface, and the surface coverage of DNA was quantified. Characterizations reveal that the framework structure of the MOF was preserved throughout the chemical transformation, and the click modified UiO-66-$N_3$ nanoparticles exhibit increased stability and enhanced

cellular uptake as compared to un-functionalized MOF particles with a comparable size when dispersed in aqueous NaCl.

**(Insert Figure 40 herein)**

By utilizing the strain-promoted Cu-free click reaction, nucleic acid tethers were covalently modified onto the surface of UiO-68 MOF nanoparticles, denoted as UiO-68 NMOF, by Willner *et. al.* (Figure 40) [241]. Firstly, dibenzocyclooctyne-sulfo-N-hydroxysuccinimidyl ester (DBCOsulfo-NHS ester) was conjugated to the amine-modified nucleic acid, and then the resulted DBCO-modified nucleic acid was linked with the azide group on the surface of UiO-68 MOF nanoparticles *via* strain-promoted click chemistry. After the dye/drug loading, two different stimuli-responsive DNA duplex capping/locking units were respectively hybridized with the surface-linked nucleic acid. For the pH-responsive MOF/drug system, AS1411 aptamer-modified pH-responsive MOF nanoparticles reveal selective and targeted cytotoxicity to MDA-MB-231 breast cancer cells. For the metal ion ($Mg^{2+}$ or $Pb^{2+}$ ions) responsive MOF/drug system, the metal-ion-dependent DNAzyme/substrate complexes were used as locking units, and adenosine 5'-triphosphate (ATP)/$Mg^{2+}$-triggered Dox-loaded NMOF reveals selective cytotoxicity to MDA-MB-231 cancer cells.

**(Insert Figure 41 herein)**

Under solvothermal condition by the addition of *p*-azidomethylbenzoic acid (L1), well-defined nontoxic UiO-66 nanoparticles in the size of around 100–200 nm coated with azide modulators were synthesized by Forgan and coworkers. Subsequently, the surface modification by Cu(I)-catalyzed azide-alkyne cycloaddition with amphiphilic PEG (PEG2000) was carried out to afford UiO-66-L1-PEG2000 (Figure 41) [242]. Characterizations reveal that PEG chains not only prevent the aggregation of MOF nanoparticles and further increase their solution stability, but also improve the stability of MOF nanoparticles by delaying their decomposition. When carrying out the click reaction in the presence of calcein, a calcein-loaded system (cal@UiO-66-L1-PEG2000) was obtained. The effect of the surface

modification on the drug release was tested by taking calcein as a probe, showing that the release of calcein from cal@UiO-66-L1-PEG2000 could be affected by pH. The release at pH = 7.4 was drastically decreased, while rapid cargo release at pH = 5.5 was observed, which could facilitate the drug delivery selectivity because cancerous cells are typically more acidic than healthy ones. Successful internalization of cal@UiO-66-L1-PEG2000 by HeLa cells and subsequent calcein release were further confirmed by confocal fluorescence microscopy. When replacing calcein by dichloroacetic acid (DCA), an anticancer drug that is cytotoxic only once it is internalized by cells, another drug loaded system DCA@UiO-66-L1-PEG2000 was constructed. Studies reveal significant cell death at the utilization concentrations of 0.75 mg $mL^{-1}$ and above. These results indicate that a proper click modification on the surface of MOF nanoparticles by PEG could increase their stability and cellular internalization with improved therapeutic effect.

**(Insert Figure 42 herein)**

Meanwhile, a unique framework denoted as $N_3$-UiO-66-$NH_2$ was synthesized by Xue and coworkers. The pre-synthesized $N_3$-UiO-66-$NH_2$ possesses dual tunable groups, *i.e.*, azide group and amino group. After the amidation with a carboxyl substituted zinc phthalocyanine (Pc) and click-reacted with Erlotinib (E), a dual functionalized MOF named E-UiO-66-Pc was obtained (Figure 42) [243]. The zinc phthalocyanine is an effective photosensitizer in photodynamic therapy, while Erlotinib can target the ATP bonding region in cancer cells. Thus, the dual functionalized E-UiO-66-Pc is a promising material in photodynamic therapy. The studies on the photosensitizing efficiency show an enhanced photosensitizing activity after the conjugation of zinc phthalocyanine with UiO-66. The cytotoxicity investigation reveals that the introduction of Erlotinib into the system could significantly enhance the photodynamic activity of UiO-66-Pc. Thus, by introducing two synergistic components into MOFs by click reaction, effective anticancer systems for photodynamic cancer therapy could be achieved. At the same time, some MOF-polymer hybrids were also fabricated by clicked combination of different components and subsequently utilized for biological applications

[94,244-246]. All these examples successfully demonstrate that MOFs could be applied for biological uses after suitable click modifications.

**(Insert Figure 43 herein)**

### 4.5 Template for polymer-gel fabrication

As an effective reaction for connecting two components, click modifiable MOFs, such as azide-bearing MOFs, were investigated as templates for the fabrication of functional materials. In 2013, Sada and coworkers demonstrated a success example of MOF templated polymer-gel fabrication *via* click post-synthetic modification of organic ligands pre-organized in the MOF network. Firstly, an azide-bearing MOF denoted as AzM was assembled by the coordination of azide-containing organic ligand (AzTPDC) with Zn(II) ion (Figure 43) [247]. Then, taking tetra-acetylene cross-linker (CL4) as the guest substrate, *in situ* click reaction was carried out in the presence of Cu(I) catalyst in DEF. A cross-linked MOF (CLM) was obtained after the incubation for 1 week and washing by fresh DEF repeatedly. The decomposition of CLM by the acidification with concentrated HCl in DEF gave the final generation of a non-crystalline MOF-templated polymer (MTP) gel, and the swelling behavior was observed by immersing the resulted MTP gel in various solvents. Interestingly, the shape and size of the fabricated polymer gel were highly influenced by the shape and size of the pristine MOFs. Inspired by this success, other polymer gels were obtained by click cross-linking of other azide-bearing MOFs with various polytopic acetylene compounds. Recently, anisotropic swelling gels were also obtained by the cross-linking of organic ligands pre-organized in a pillared-layer MOF (PLMOF) through the click reaction followed by the framework decomposition [248].

**(Insert Figure 44 herein)**

A polymer gel film with homogeneous thickness was fabricated through clicked cross-linking of a surface-anchored MOF by Wöll and coworkers [249]. Subsequently, hierarchically structured MOF multi-shell encapsulated magnetic core particles (magMOFs) were synthesized by layer-by-layer synthesis. After clicked cross-linking of the MOF

structure followed by the framework decomposition, nice capsules were obtained (Figure 44) [250]. The inner shell of these capsules could serve as a reservoir and the outer one could act as a membrane that enables the controlled release of loaded dye molecules. This interesting demonstration makes the click cross-linking reaction an effective approach for polymer gel fabrications.

**(Insert Figure 45 herein)**

More recently, highly antimicrobial active porphyrin polymer thin films were fabricated through click post-synthetic modification with surface anchored MOF (SURMOF) as the template by Tsotsalas and coworkers (Figure 45) [251]. Firstly, the azido-porphyrin SURMOF was prepared utilizing layer-by-layer synthesis method. Click post-synthetic modification was carried out after the SURMOF was immersed into a solution of triple-acetylene, and then the process for removing metal ions by immersing the sample in ethylenediaminetetraacetic acid (EDTA) solution was conducted to finally give the generation of porphyrin-based, water-stable, surface anchored polymeric thin films. The morphology and thickness of the fabricated polymer thin films were not significantly changed during the removal process of the metal ions in the MOF template. By probing the ability of visible-light-promoted singlet $O_2$ generation, the antimicrobial potential of the films was investigated, showing its high antibacterial activity against pathogens. All of these interesting applications once again demonstrate that MOFs could be constructed or modified by versatile azide-alkyne cycloaddition for various applications.

## 5. Conclusion and outlook

This review summarizes recent development of MOFs prepared or modified through click reactions. Taking versatile azide-alkyne 1,3-dipolar cycloaddition as a core reaction during the ligand design for the MOF construction, a unique group of polytopic carboxylate ligands were synthesized *via* the modular combinations of polytopic symmetrical acetylene-containing organic moieties and azide-containing components such as 4-azidobenzoates and 5-azidoisophthalates. Subsequently, diverse triazole-containing MOFs

were successfully prepared by the assemblies of these clicked organic ligands with suitable metal ions. In the post-synthetic modification of MOFs, lots of functional groups were successfully grafted into/onto pristine MOFs by the azide-alkyne 1,3-dipolar cycloaddition toward targeted applications. In addition to the azide-alkyne 1,3-dipolar cycloaddition, other click reactions, such as Diels–Alder click reaction and thiol−ene click reaction, have also been employed as effective reactions in the MOF construction and modification [207,252-257]. The versatile click chemistry through both ligand pre-design and post-synthetic modification not only makes the MOF preparation easy, but also broadens their applications by integrating functional groups into the MOF networks. These examples have successfully demonstrated that the click chemistry is a useful approach in the construction and post-synthetic modification of MOFs for purposed applications including molecular capture and separation, catalysis, drug delivery and bioimaging, materials engineering, and so on.

Future studies on this rapidly developing research field will be even more diverse. Assisted by computational simulations, purposely designed organic ligands suitable for click reaction will definitely boost the application scope and depth of the resulted MOFs. In particular, interfacing such MOFs with biology and medicine would broaden the research horizon. The ease of click chemistry employed for the MOF synthesis and modification also brings a high possibility for the large-scale production of MOF materials. It is expected that, by utilizing the versatile click chemistry, more and more MOFs will be constructed and post-synthetically modified toward their practical applications.

## Acknowledgements

This research is financially supported by the Singapore Academic Research Fund (No. RG11/17 and RG114/17), and the Singapore Agency for Science, Technology and Research (A*STAR) AME IRG grant (No. A1783c0007) for the financial support.

## References

[1] H. Furukawa, K. E. Cordova, M. O'Keeffe, O. M. Yaghi, Science 341 (2013) 1230444.

[2] P. Silva, S. M. F. Vilela, J. P. C. Tome, F. A. A. Paz, Chem. Soc. Rev. 44 (2015) 6774-6803.

[3] Y. Cui, B. Li, H. He, W. Zhou, B. Chen, G. Qian, Acc. Chem. Res. 49 (2016) 483-493.

[4] B. Li, M. Chrzanowski, Y. Zhang, S. Ma, Coord. Chem. Rev. 307 (2016) 106-129.

[5] H. Wang, Q.-L. Zhu, R. Zou, Q. Xu, Chem 2 (2017) 52-80.
[6] M. P. Suh, H. J. Park, T. K. Prasad, D.-W. Lim, Chem. Rev. 112 (2012) 782-835.
[7] Y. Yan, S. Yang, A. J. Blake, M. Schröder, Acc. Chem. Res. 47 (2014) 296-307.
[8] K. Adil, P. M. Bhatt, Y. Belmabkhout, S. M. T. Abtab, H. Jiang, A. H. Assen, A. Mallick, A. Cadiau, J. Aqil, M. Eddaoudi, Adv. Mater. 29 (2017) 1702953.
[9] C. A. Trickett, A. Helal, B. A. Al-Maythalony, Z. H. Yamani, K. E. Cordova, O. M. Yaghi, Nat. Rev. Chem. 2 (2017) 17045.
[10] B. Li, H.-M. Wen, W. Zhou, J. Q. Xu, B. Chen, Chem 1 (2016) 557-580.
[11] H. Wu, Q. Gong, D. H. Olson, J. Li, Chem. Rev. 112 (2012) 836-868.
[12] E. Barea, C. Montoro, J. A. R. Navarro, Chem. Soc. Rev. 43 (2014) 5419-5430.
[13] N. S. Bobbitt, M. L. Mendonca, A. J. Howarth, T. Islamoglu, J. T. Hupp, O. K. Farha, R. Q. Snurr, Chem. Soc. Rev. 46 (2017) 3357-3385.
[14] A. H. Chughtai, N. Ahmad, H. A. Younus, A. Laypkov, F. Verpoort, Chem. Soc. Rev. 44 (2015) 6804-6849.
[15] L. Zhu, X.-Q. Liu, H.-L. Jiang, L.-B. Sun, Chem. Rev. 117 (2017) 8129-8176.
[16] Q.-L. Zhu, Q. Xu, Chem. Soc. Rev. 43 (2014) 5468-5512.
[17] Q. Yang, Q. Xu, H.-L. Jiang, Chem. Soc. Rev. 46 (2017) 4774-4808.
[18] C. He, D. Liu, W. Lin, Chem. Rev. 115 (2015) 11079-11108.
[19] X. Lian, Y. Fang, E. Joseph, Q. Wang, J. Li, S. Banerjee, C. Lollar, X. Wang, H.-C. Zhou, Chem. Soc. Rev. 46 (2017) 3386-3401.
[20] V. Stavila, A. A. Talin, M. D. Allendorf, Chem. Soc. Rev. 43 (2014) 5994-6010.
[21] L. Sun, M. G. Campbell, M. Dinca, Angew. Chem. Int. Ed. 55 (2016) 3566-3579.
[22] M. O'Keeffe, O. M. Yaghi, Chem. Rev. 112 (2012) 675-702.
[23] M. Li, D. Li, M. O'Keeffe, O. M. Yaghi, Chem. Rev. 114 (2014) 1343-1370.
[24] G. Aromí, L. A. Barrios, O. Roubeau, P. Gamez, Coord. Chem. Rev. 255 (2011) 485-546.
[25] J.-P. Zhang, Y.-B. Zhang, J.-B. Lin, X.-M. Chen, Chem. Rev. 112 (2012) 1001-1033.
[26] Y. He, B. Li, M. O'Keeffe, B. Chen, Chem. Soc. Rev. 43 (2014) 5618-5656.
[27] W.-Y. Gao, M. Chrzanowski, S. Ma, Chem. Soc. Rev. 43 (2014) 5841-5866.
[28] M. Zhang, Z.-Y. Gu, M. Bosch, Z. Perry, H.-C. Zhou, Coord. Chem. Rev. 293–294 (2015) 327-356.
[29] H. Zhang, R. Zou, Y. Zhao, Coord. Chem. Rev. 292 (2015) 74-90.
[30] T. Devic, C. Serre, Chem. Soc. Rev. 43 (2014) 6097-6115.
[31] V. Guillerm, D. Kim, J. F. Eubank, R. Luebke, X. Liu, K. Adil, M. S. Lah, M. Eddaoudi, Chem. Soc. Rev. 43 (2014) 6141-6172.
[32] A. Schoedela, M. J. Zaworotko, Chem. Sci. 5 (2014) 1269-1282.
[33] W.-X. Zhang, P.-Q. Liao, R.-B. Lin, Y.-S. Wei, M.-H. Zeng, X.-M. Chen, Chem. Rev. 293-294 (2015) 263-278.
[34] A. Schoedel, M. Li, D. Li, M. O'Keeffe, O. M. Yaghi, Chem. Rev. 116 (2016) 12466-12535.
[35] Y. Bai, Y. Dou, L.-H. Xie, W. Rutledge, J.-R. Li, H.-C. Zhou, Chem. Soc. Rev. 45 (2016) 2327-2367.
[36] H. Assi, G. Mouchaham, N. Steunou, T. Devic, C. Serre, Chem. Soc. Rev. 46 (2017) 3431-3452.
[37] J. Zhu, P.-Z. Li, W. Guo, Y. Zhao, R. Zou, Chem. Rev. 359 (2018) 80–101.
[38] Z. Zhang, M. J. Zaworotko, Chem. Soc. Rev. 43 (2014) 5444-5455.
[39] M. Bosch, S. Yuan, W. Rutledge, H.-C. Zhou, Acc. Chem. Res. 50 (2017) 857−865.
[40] T.-H. Chen, I. Popov, W. Kaveevivitchai, O. Š. Miljanić, Chem. Mater. 26 (2014) 4322-4325.
[41] M. Eddaoudi, J. Kim, N. Rosi, D. Vodak, J. Wachter, M. O'Keeffe, O. M. Yaghi, Science 295 (2002) 469-472.
[42] L. Ma, J. M. Falkowski, C. Abney, W. Lin, Nat. Chem. 2 (2010) 838-846.

[43] H. Deng, S. Grunder, K. E. Cordova, C. Valente, H. Furukawa, M. Hmadeh, F. Gándara, A. C. Whalley, Z. Liu, S. Asahina, H. Kazumori, M. O'Keeffe, O. Terasaki, J. F. Stoddart, O. M. Yaghi, Science 336 (2012) 1018-1023.

[44] Z.-G. Gu, C. Zhan, J. Zhang, X. Bu, Chem. Soc. Rev. 45 (2016) 3122-3144.

[45] L. Ma, C. Abney, W. Lin. Chem. Soc. Rev. 38 (2009) 1248-1256.

[46] C. Yang, U. Kaipa, Q. Z. Mather, X. Wang, V. Nesterov, A. F. Venero, M. A. Omary, J. Am. Chem. Soc. 133 (2011) 18094-18097.

[47] T.-H. Chen, I. Popov, O. Zenasni, O. Daugulis, O. S. Miljanic, Chem. Commun. 49 (2013) 6846-6848.

[48] R. A. Smaldone, R. S. Forgan, H. Furukawa, J. J. Gassensmith, A. M. Z. Slawin, O. M. Yaghi, J. F. Stoddart, Angew. Chem. Int. Ed. 49 (2010) 8630-8634.

[49] D. Zhao, D. J. Timmons, D. Yuan, H.-C. Zhou, Acc. Chem. Res. 44 (2011) 123–133.

[50] W. Lu, Z. Wei, Z.-Y. Gu, T.-F. Liu, J. Park, J. Park, J. Tian, M. Zhang, Q. Zhang, T. Gentle, M. Bosch, H.-C. Zhou, Chem. Soc. Rev. 43 (2014) 5561-5593.

[51] Z. Wang, S. M. Cohen, Chem. Soc. Rev. 38 (2009) 1315–1329.

[52] S. M. Cohen, J. Am. Chem. Soc. 139 (2017) 2855−2863.

[53] H. C. Kolb, M. G. Finn, K. B. Sharpless, Angew. Chem. Int. Ed. 40 (2001) 2004-2021.

[54] C. Wang, D. Ikhlef, S. Kahlal, J.-Y. Saillard, D. Astruca, Coord. Chem. Rev. 316 (2016) 1-20.

[55] V. V. Rostovtsev, L. G. Green, V. V. Fokin, K. B. Sharpless, Angew. Chem. Int. Ed. 41 (2002) 2596-2599.

[56] C. W. Tornøe, C. Christensen, M. Meldal, J. Org. Chem. 67 (2002) 3057-3064.

[57] H. C. Kolb, B. K. Sharpless, Drug Discov. Today 8 (2003) 1128-1137.

[58] R. Huisgen, Proc. Chem. Soc. 0 (1961) 357-396.

[59] X. Hou, C. Ke, J. F. Stoddart, Chem. Soc. Rev. 45 (2016) 3766-3780.

[60] J.-F. Lutz, Angew. Chem. Int. Ed. 46 (2007) 1018-1025.

[61] J. E. Moses, A. D. Moorhouse. Chem. Soc. Rev. 36 (2007) 1249-1262.

[62] K. Kacprzak, I. Skiera, M. Piasecka, Z. Paryzek, Chem. Rev. 116 (2016) 5689-5743.

[63] F. Alonso, Y. Moglie, G. Radivoy, Acc. Chem. Res. 48 (2015) 2516−2528.

[64] V. K. Tiwari, B. B. Mishra, K. B. Mishra, N. Mishra, A. S. Singh, X. Chen, Chem. Rev. 116 (2016) 3086-3240.

[65] P. Thirumurugan, D. Matosiuk, K. Jozwiak, Chem. Rev. 113 (2013) 4905-4979.

[66] H. Y. Yoon, H. Koo, K. Kim, I. C. Kwon, Biomaterials 132 (2017) 28-36.

[67] L. Liang, D. Astruc, Coord. Chem. Rev. 255 (2011) 2933–2945.

[68] D. Fournier, R. Hoogenboom. U. S. Schubert, Chem. Soc. Rev. 36 (2007) 1369-1380.

[69] R. K. Iha, K. L. Wooley, A. M. Nystrom, D. J. Burke, M. J. Kade, C. J. Hawker, Chem. Rev. 109 (2009) 5620-5686.

[70] P. L. Golas. K. Matyjaszewski, Chem. Soc. Rev. 39 (2010) 1338-1354.

[71] A. Qin, J. W. Y. Lam, B. Z. Tang, Chem. Soc. Rev. 39 (2010) 2522-2544.

[72] D. Döhler, P. Michael, W. H. Binder, Acc. Chem. Res. 50 (2017) 2610-2620.

[73] J. R. Holst, E. Stockel, D. J. Adams, A. I. Cooper, Macromolecules 43 (2010) 8531-8538.

[74] P. Pandey, O. K. Farha, A. M. Spokoyny, C. A. Mirkin, M. G. Kanatzidis, J. T. Hupp, S. T. A Nguyen, J. Mater. Chem. 21 (2011) 1700-1703.

[75] L.-H. Xie, M. P. Suh, Chem. Eur. J. 19 (2013) 11590–11597.

[76] P. Lindemann, M. Tsotsalas, S. Shishatskiy, V. Abetz, P. Krolla-Sidenstein, C. Azucena, L. Monnereau, A. Beyer, A. Gölzhäuser, V. Mugnaini, H. Gliemann, S. Bräse, C. Wöll, Chem. Mater. 26 (2014) 7189-7193.

[77] L. Li, H. Zhao, J. Wang, R. Wang, ACS Nano 8 (2014) 5352-5364.

[78] H. Zhong, C. Liu, H. Zhou, Y. Wang, R. Wang, Chem. Eur. J. 22 (2016) 12533-12541.

[79] H. Zhong, C. Liu, Y. Wang, R. Wang, M. Hong, Chem. Sci. 7 (2016) 2188-2194.

[80] X. Ren, S. Kong, Q. Shu, M. Shu, Chin. J. Chem. 34 (2016) 373-380.

[81] A. Nnagai, Z. Guo, X. Feng, S. Jin, X. Chen, X. Ding, D. Jiang, Nat. Commun. 2 (2011) 536.

[82] H. Xu, J. Gao, D. Jiang, Nat. Chem. 7 (2015) 905-912.

[83] T. Devic, O. David, M. Valls, J. Marrot, F. Couty, G. Ferey, J. Am. Chem. Soc. 129 (2007) 12614-12615.

[84] G. Tuci, A. Rossin, X. Xu, M. Ranocchiari, J. A. van Bokhoven, L.Luconi, I. Manet, M. Melucci, G. Giambastiani, Chem. Mater. 25 (2013) 2297-2308.

[85] B. Gui, X. Meng, H.; Xu, C. Wang, Chin. J. Chem. 34 (2016) 186-190.

[86] T. Devic, C. Serre, N. Audebrand, J. Marrot, G. Ferey, J. Am. Chem. Soc. 127 (2005) 12788-12789.

[87] P.-Z. Li, J. Su, J. Liang, J. Liu, Y. Zhang, H. Chen, Y. Zhao, Chem. Commun. 53 (2017) 3434-3437.

[88] H. Li, C. E. Davis, T. L. Groy, D. G. Kelley, O. M. Yaghi, J. Am. Chem. Soc. 120 (1998) 2186-2187.

[89] T.-H. Chen, I. Popov, Y.-C. Chuang, Y.-S. Chen, O. S. Miljanic, Chem. Commun. 51 (2015) 6340-6342.

[90] X.-J. Wang, P.-Z. Li, L. Liu, Q. Zhang, P. Borah, J. D. Wong, X. X. Chan, G. Rakesh, Y. Li, Y. Zhao, Chem. Commun. 48 (2012) 10286-10288.

[91] L. Sun, Y. Li, Z. Liang, J. Yu, R. Xu, Dalton Trans. 41 (2012) 12790-12796.

[92] P.-Z. Li, X.-J. Wang, K. Zhang, A. Nalaparaju, R. Zou, R. Zou, J. Jiang, Y. Zhao, Chem. Commun. 50 (2014) 4683-4685.

[93] S. S.-Y. Chui, S. M.-F. Lo, J. P. H. Charmant, A. G. Orpen, I. D. A Williams, Science 283 (1999) 1148-1150.

[94] N. Ahmad, H. A. Younus, A. H. Chughtai, K. V. Hecke, M. Danish, G. Zhang, F. Verpoort, Sci. Rep. 7 (2017) 832.

[95] B. Chen, M. Eddaoudi, T. M. Reineke, J. W. Kampf, M. O'Keeffe, O. M. Yaghi, J. Am. Chem. Soc. 122 (2000) 11559-11560.

[96] L. Ma, A. Jin, Z. Xie, W. Lin, Angew. Chem. Int. Ed. 48 (2009) 9905-9908.

[97] D. Liu, Z. Xie, L. Ma, W. Lin, Inorg. Chem. 49 (2010) 9107-9109.

[98] L.-L. Liang, J. Zhang, S.-B. Ren, G.-W. Ge, Y.-Z. Li, H.-B. Du, X.-Z. You, CrystEngComm 12 (2010) 2008-2010.

[99] Z. Guo, R. Cao, X. Wang, H. Li, W. Yuan, G. Wang, H. Wu, J. Li, J. Am. Chem. Soc.131 (2009) 6894-6895.

[100] L. Wen, P. Cheng, W. Lin, Chem. Sci. 3 (2012) 2288-2292.

[101] M. Zhang, Y.-P. Chen, H.-C. Zhou, CrystEngComm 15 (2013) 9544-9552.

[102] M. Zhang, Y.-P. Chen, M. Bosch, T. Gentle III, K. Wang, D. Feng, Z. U. Wang, H.-C. Zhou, Angew. Chem. Int. Ed. 53 (2014) 815-818.

[103] H. Furukawa, F. Gándara, Y.-B. Zhang, J. Jiang, W. L. Queen, M. R. Hudson, O. M. Yaghi, J. Am. Chem. Soc. 136 (2014) 4369-4381.

[104] P.-Z. Li, X.-J. Wang, J. Liu, J. Liang, J. Y. J. Chen, Y. Zhao, CrystEngComm 19 (2017) 4157-4161.

[105] F. Nouar, J. F. Eubank, T. Bousquet, L. Wojtas, M. J. Zaworotko, M. Eddaoudi, J. Am. Chem. Soc. 130 (2008) 1833-1835.

[106] J. F. Eubank, F. Nouar, R. Luebke, A. J. Cairns, L. Wojtas, M. Alkordi, T. Bousquet, M. R. Hight, J. Eckert, J. P. Embs, P. A. Georgiev, M. Eddaoudi, Angew. Chem. Int. Ed. 51 (2012) 10099–10103.

[107] D. Zhao, D. Yuan, D. Sun, H.-C. Zhou, J. Am. Chem. Soc. 131 (2009) 9186-9188.

[108] Y. Yan, X. Lin, S. Yang, A. J. Blake, A. Dailly, N. R. Champness, P. Hubberstey, M. Schröder, Chem. Commun. (2009) 1025-1027.

[109] D. Yuan, D. Zhao, D. Sun, H.-C. Zhou, Angew. Chem. Int. Ed. 49 (2010) 5357-5361.

[110] Y. Yan, I. Telepeni, S. Yang, X. Lin, W. Kockelmann, A. Dailly, A. J. Blake, W. Lewis, G. S. Walker, D. R. Allan, S. A. Barnett, N. R. Champness, M. Schröder, J. Am. Chem. Soc. 132 (2010) 4092-4094.

[111] O. K. Farha, A. Ö. Yazaydın, I. Eryazici, C. D. Malliakas, B. G. Hauser, M. G. Kanatzidis, S. T. Nguyen, R. Q. Snurr, J. T. Hupp, Nat. Chem. 2 (2010) 944-948.

[112] B. Zheng, J. Bai, J. Duan, L. Wojtas, M. J. Zaworotko, J. Am. Chem. Soc. 133 (2011) 748-751.

[113] Z. Guo, H. Wu, G. Srinivas, Y. Zhou, S. Xiang, Z. Chen, Y. Yang, W. Zhou, M. O'Keeffe, B. Chen, Angew. Chem. Int. Ed. 50 (2011) 3178 –3181.

[114] Y. Yan, S. Yang, A. J. Blake, W. Lewis, E. Poirier, S. A. Barnett, N. R. Champness, M. Schröder, Chem. Commun. 47 (2011) 9995-9997.

[115] D. Yuan, D. Zhao, H.-C. Zhou, Inorg. Chem. 50 (2011) 10528-10530.

[116] B. Li, Z. Zhang, Y. Li, K.Yao, Y. Zhu, Z. Deng, F. Yang, X. Zhou, G. Li, H. Wu, N. Nijem, Y. J. Chabal, Z. Lai, Y. Han, Z. Shi, S. Feng, J. Li, Angew. Chem. Int. Ed. 51 (2012) 1412-1415.

[117] O. K. Farha, C. E. Wilmer, I. Eryazici, B. G. Hauser, P. A. Parilla, K. O'Neill, A. A. Sarjeant, S. T. Nguyen, R. Q. Snurr, J. T. Hupp, J. Am. Chem. Soc. 134 (2012) 9860-9863.

[118] O. K. Farha, I. Eryazici, N. C. Jeong, B. G. Hauser, C. E. Wilmer, A. A. Sarjeant, R. Q. Snurr, S. T. Nguyen, J. T. Hupp, J. Am. Chem. Soc. 134 (2012) 15016-15021.

[119] R. Luebke, J. F. Eubank, A. J. Cairns, Y. Belmabkhout, L. Wojtas, M. Eddaoudi, Chem. Commun. 48 (2012) 1455-1457.

[120] B. Zheng, Z. Yang, J. Bai, Y. Li, S. Li, Chem. Commun. 48 (2012) 7025-7027.

[121] X.-J. Wang, P.-Z. Li, Y. Chen, Q. Zhang, H. Zhang, X. X. Chan, R. Ganguly, Y. Li, J. Jiang, Y. Zhao, Sci. Rep. 3 (2013) 1149.

[122] Y. Yan, M. Suyetin, E. Bichoutskaia, A. J. Blake, D. R. Allan, S. A. Barnett, M. Schröder, Chem. Sci. 4 (2013) 1731-1736.

[123] C. E. Wilmer, O. K. Farha, T. Yildirim, I. Eryazici, V. Krungleviciute, A. A. Sarjeant, R. Q. Snurr, J. T. Hupp, Energy Environ. Sci. 6 (2013) 1158–1163.

[124] X.-J. Wang, J. Li, P.-Z. Li, L.-B. Xing, H. Lu, H. Wu, Y. Shi, R. Zou, Y. Zhao, Inorg. Chem. Commun. 46 (2014) 13-16.

[125] J. Li, P.-Z. Li, Q.-Y. Li, Y. Cao, H. Lu, H. Wu, F. Li, Y. Shi, X.-J. Wang, Y. Zhao, RSC Adv. 4 (2014) 53975-53980.

[126] X.-J. Wang, J. Li, Q.-Y. Li, P.-Z. Li, H. Lu, Q. Lao, R. Ni, Y. Shi, Y. Zhao, CrystEngComm 17 (2015) 4632-4636..

[127] G. Barin, V. Krungleviciute, D. A. Gomez-Gualdron, A. A. Sarjeant, R. Q. Snurr, J. T. Hupp, T. Yildirim, O. K. Farha, Chem. Mater. 26 (2014) 1912−1917.

[128] P.-Z. Li, X.-J. Wang, S. Y. Tan, C. Y. Ang, H.-Z. Chen, J. Liu, R.-Q. Zou, Y. Zhao, Angew. Chem. Int. Ed. 54 (2015) 12748-12752.

[129] C. Tan, S. Yang, N. R. Champness, X. Lin, A. J. Blake, W. Lewis, M. Schroder, Chem. Commun. 47 (2011) 4487-4489.

[130] D. Liu, H. Wu, S. Wang, Z. Xie, J. Li, W. Lin, Chem. Sci. 3 (2012) 3032-3037.

[131] Y.-S. Xue, Y. He, S.-B. Ren, Y. Yue, L. Zhou, Y.-Z. Li, H.-B. Du, X.-Z. You, B. Chen, J. Mater. Chem. 22 (2012) 10195-10199.

[132] J. F. Eubank, H. Mouttaki, A. J. Cairns, Y. Belmabkhout, L. Wojtas, R. Luebke, M. Alkordi, M. Eddaoudi, J. Am. Chem. Soc. 133 (2011) 14204-14207.

[133] W. Lu, D. Yuan, T. A. Makal, J.-R. Li, H.-C. Zhou, Angew. Chem. Int. Ed. 51 (2012) 1580-1584.

[134] Y. He, Z. Zhang, S. Xiang, H. Wu, F. R. Fronczek, W. Zhou, R. Krishna, M. OKeeffe, B. Chen, Chem. Eur. J. 18 (2012) 1901-1904.

[135] X.-L. Yang, M.-H. Xie, C. Zou, Y. He, B. Chen, M. O'Keeffe, C.-D. Wu, J. Am. Chem. Soc. 134 (2012) 10638-10645.

[136] N. B. Shustova, A. F. Cozzolino, M. Dincă, J. Am. Chem. Soc. 134 (2012) 19596-19599.

[137] P.-Z. Li, X.-J. Wang, J. Liu, J. S. Lim, R. Zou, Y. Zhao, J. Am. Chem. Soc. 138 (2016) 2142-2145.

[138] F. Salles, G. Maurin, C. Serre, P. L. Llewellyn, C. Knofel, H. J. Choi, Y. Filinchuk, L. Oliviero, A.Vimont, J. R. Long, G. Ferey, J. Am. Chem. Soc. 132 (2010) 13782-13788.

[139] K. Wang, X.-L. Lv, D. Feng, J. Li, S. Chen, J. Sun, L. Song, Y. Xie, J.-R. Li, H.-C. Zhou, J. Am. Chem. Soc. 138 (2016) 914-919.

[140] X.-L. Lv, K. Wang, B. Wang, J. Su, X. Zou, Y. Xie, J.-R. Li, H.-C. Zhou, J. Am. Chem. Soc. 139 (2017) 211−217.

[141] K. Sumida, D. Stück, L. Mino, J.-D. Chai, E. D. Bloch, O. Zavorotynska, L. J. Murray, M. Dincă, S. Chavan, S. Bordiga, M. Head-Gordon, J. R. Long, J. Am. Chem. Soc. 135 (2013) 1083−1091.

[142] Q. Lin, T. Wu, S.-T. Zheng, X. Bu, P. Feng, J. Am. Chem. Soc. 134 (2012) 784−787..

[143] L. Wang, D. W. Agnew, X. Yu, J. S. Figueroa, S. M. Cohen, Angew. Chem. Int. Ed. 57 (2018) 511–515.

[144] S.-Q. Bai, D. J. Young, T. S. A. Hor, Chem. Asian J. 6 (2011) 292-304.

[145] R. A. S. Vasdev, D. Preston, J. D. Crowley, Dalton Trans. 46 (2017) 2402-2414.

[146] J. D. Crowley, E. L. Gavey, Dalton Trans. 39 (2010) 4035-4037.

[147] S. Ø. Scott, E. L. Gavey, S. J. Lind, K. C. Gordon, J. D. Crowley, Dalton Trans. 40 (2011) 12117-12124.

[148] A. Demessence, J. R. Long, Chem. Eur. J. 16 (2010) 5902-5908..

[149] C. Serre, F. Millange, C. Thouvenot, M. Nogues, G. Marsolier, D. Louer, G. Ferey, J. Am. Chem. Soc. 124 (2002) 13519-13526.

[150] G. Ferey, C. Serre, Chem. Soc. Rev. 38 (2009) 1380-1399.

[151] L. R. Parent, C. H. Pham, J. P. Patterson, M. S. Denny, Jr., S. M. Cohen, N. C. Gianneschi, F. Paesani, J. Am. Chem. Soc. 139 (2017) 13973−13976.

[152] K. Sumida, M. L. Foo, S. Horike, J. R. Long, Eur. J. Inorg. Chem. (2010) 3739-3744.

[153] A. Demessence, D. M. D'Alessandro, M. L. Foo, J. R. Long, J. Am. Chem. Soc. 131 (2009) 8784-8786.

[154] D. A. Reed, D. J. Xiao, M. I. Gonzalez, L. E. Darago, Z. R. Herm, F. Grandjean, J. R. Long, J. Am. Chem. Soc. 138 (2016) 5594-5602.

[155] D. J. Xiao, M. I. Gonzalez, L. E. Darago, K. D. Vogiatzis, E. Haldoupis, L. Gagliardi, J. R. Long, J. Am. Chem. Soc. 138 (2016) 7161-7170.

[156] W.-Q. Zou, M.-S. Wang, Y. Li, A.-Q. Wu, F.-K. Zheng, Q.-Y. Chen, G.-C. Guo, J.-S. Huang, Inorg. Chem. 46 (2007) 6852-6854.

[157] Y. Li, W.-Q. Zou, M.-F. Wu, J.-D. Lin, F.-K. Zheng, Z.-F. Liu, S.-H. Wang, G.-C. Guo, J.-S. Huang, CrystEngComm 13 (2011) 3868-3877.

[158] W.-Y. Gao, S. Ma, Inorg. Chem. 34 (2014) 125–141.

[159] W.-Y. Gao, W. Yan, R. Cai, L. Meng, A. Salas, X.-S. Wang, L. Wojtas, X. Shi, S. Ma, Inorg. Chem. 51 (2012) 4423-4425.

[160] W.-Y. Gao, R. Cai, L. Meng, L. Wojtas, W. Zhou, T. Yildirim, X. Shi, S. Ma, Chem. Commun. 49 (2013) 10516-10518.

[161] W.-Y. Gao, R. Cai, T. Pham, K. A. Forrest, A. Hogan, P. Nugent, K. Williams, L. Wojtas, R. Luebke, L. J. Weseliński, M. J. Zaworotko, B. Space, Y.-S. Chen, M. Eddaoudi, X. Shi, S. Ma, Chem. Mater. 27 (2015) 2144-2151.

[162] J. A. Kitchen, S. Brooker, Coord. Chem. Rev. 252 (2008) 2072-2092.

[163] M. Han, D. M. Engelhard, G. H. Clever, Chem. Soc. Rev. 43 (2014) 1848-1860.

[164] A. Schmidt, A. Casini, F. E. Kühn, Coord. Chem. Rev. 275 (2014) 19-36.

[165] J. P. Byrne, J. A. Kitchen, T. Gunnlaugsson, Chem. Soc. Rev. 43 (2014) 5302-5325.

[166] H.Vardhan, M. Yusubov, F. Verpoort, Coord. Chem. Rev. 306 (2016) 171-194.

[167] H. L. C. Feltham, A. S. Barltrop, S. Brooker, Coord. Chem. Rev. 344 (2017) 26-53.

[168] S.-Q. Bai, L. Jiang, B. Sun, D. J. Young, T. S. A. Hor, CrystEngComm 17 (2015) 3305-3311.

[169] S.-Q. Bai, D. Kai, K. L. Ke, M. Lin, L. Jiang, Y. Jiang, D. J. Young, X. J. Loh, X. Li, T. S. A. Hor, ChemPlusChem 80 (2015) 1235-1240.

[170] J. E. M. Lewis, C. J. McAdam, M. G. Gardiner, J. D. Crowley, Chem. Commun. 49 (2013) 3398-3400.

[171] J. E. M. Lewis, A. B. S. Elliott, C. J. McAdam, K. C. Gordon, J. D. Crowley, Chem. Sci. 5 (2014) 1833-1843.

[172] S. M. McNeill, D. Preston, J. E. M. Lewis, A. Robert, K. Knerr-Rupp, D. O. Graham, J. R. Wright, G. I. Giles, J. D. Crowley, Dalton Trans. 44 (2015) 11129-11136.

[173] A. B. S. Elliott, J. E. M. Lewis, H. van der Salm, C. J. McAdam, J. D. Crowley, K. C. Gordon, Inorg. Chem. 55 (2016) 3440-3447.

[174] J. D. Crowley, P. H. Bandeen, Dalton Trans. 39 (2010) 612-623.

[175] K. A. Stevenson, C. F. C. Melan, O. Fleischel, R. Wang, A. Petitjean, Cryst. Growth Des. 12 (2012) 5169-5173.

[176] N. Wu, C. F. C. Melan, K. A. Stevenson, O. Fleischel, H. Guo, F. Habib, R. J. Holmberg, M. Murugesu, N. J. Mosey, H. Nierengartene, A. Petitjean, Dalton Trans. 44 (2015) 14991-15005.

[177] B. Akhuli, L. Cera, B. Jana, S. Saha, C. A. Schalley, P. Ghosh, Inorg. Chem. 54 (2015) 4231-4242.

[178] S. V. Kumar, W. K. C. Lo, H. J. L. Brooks, J. D. Crowley, Inorg. Chim. Acta 425 (2015) 1-6.

[179] P. R. Symmers, M. J. Burke, D. P. August, P. I. T. Thomson, G. S. Nichol, M. R. Warren, C. J. Campbell, P. J. Lusby, Chem. Sci. 6 (2015) 756-760.

[180] M. J. Burke, G. S. Nichol, P. J. Lusby, J. Am. Chem. Soc. 138 (2016) 9308-9315.

[181] P. Ballester, M. Claudel, S. Durot, L. Kocher, L. Schoepff, V. Heitz, Chem. Eur. J. 21 (2015) 15339-15348.

[182] W. Brenner, T. K. Ronson, J. R. Nitschke, J. Am. Chem. Soc. 139 (2017) 75-78.

[183] W.-Y. Gao, W. Yan, R. Cai, K. Williams, A. Salas, L. Wojtas, X. Shi, S. Ma, Chem. Commun. 48 (2012) 8898–8900.

[184] B. Chen, C. Liang, J. Yang, D. S. Contreras, Y. L. Clancy, E. B. Lobkovsky, O. M. Yaghi, S. Dai, Angew. Chem., Int. Ed. 45 (2006) 1390-1393.

[185] Z. Wang, S. M. Cohen, J. Am. Chem. Soc. 129 (2007) 12368-12369.

[186] K. K. Tanabe, S. M. Cohen, Chem. Soc. Rev. 40 (2011) 498-519.

[187] S. M. Cohen, Chem. Rev. 112 (2012) 970–1000.

[188] Y. Goto, H. Sato, S. Shinkai, K. Sada, J. Am. Chem. Soc. 130 (2008) 14354-14355.

[189] H.-L. Jiang, D. Feng, T.-F. Liu, J.-R. Li, H.-C. Zhou, J. Am. Chem. Soc. 134 (2012) 14690-14693.

[190] P.-Z. Li, X.-J. Wang, R. H. D. Tan, Q. Zhang, R. Zou, Y. Zhao, RSC Adv. 3 (2013) 15566-15570.

[191] L. Li, W. Ma, S. Shen, H. Huang, Y. Bai, H. Liu, ACS Appl. Mater. Interfaces 8 (2016) 31032-31041.

[192] J. Park, D. Feng, H.-C. Zhou, J. Am. Chem. Soc. 137 (2015) 1663-1672.

[193] X. Zhang, T. Xia, K. Jiang, Y. Cui, Y. Yang, G. Qian, J. Solid State Chem. 253 (2017) 277-281.

[194] T. Gadzikwa, G. Lu, C. L. Stern, S. R. Wilson, J. T. Hupp, S. T. Nguyen, Chem. Commun. (2008) 5493-5495.

[195] T. Gadzikwa, O. K. Farha, C. D. Malliakas, M. G. Kanatzidis, J. T. Hupp, S. T. Nguyen, J. Am. Chem. Soc. 131 (2009) 13613-13615.

[196] P. Deria, W. Bury, J. T. Hupp, O. K. Farha, Chem. Commun. 50 (2014) 1965-1968.

[197] B. Li, B. Gui, G. Hu, D. Yuan, C. Wang, Inorg. Chem. 54 (2015) 5139-5141.

[198] Y. Zhang, B. Gui, R. Chen, G. Hu, Y. Meng, D. Yuan, M. Zeller, C. Wang, Inorg. Chem. 57 (2018) 2288−2295.

[199] M. Savonnet, D. Bazer-Bachi, N. Bats, J. Perez-Pellitero, E. Jeanneau, V. Lecocq, C. Pinel, D. Farrusseng, J. Am. Chem. Soc. 132 (2010) 4518-4519.

[200] M. Savonnet, E. Kockrick, A. Camarata, D. Bazer-Bachi, N. Bats, V. Lecocq, C. Pinela, D. Farrusseng, New J. Chem. 35 (2011) 1892-1897.

[201] J. M. Baskin, J. A. Prescher, S. T. Laughlin, N. J. Agard, P. V. Chang, I. A. Miller, A. Lo, J. A. Codelli, C. R. Bertozzi, Proc. Natl. Acad. Sci. U.S.A. 104 (2007) 16793-16797.

[202] R. Chakrabarty, P. J. Stang, J. Am. Chem. Soc. 134 (2012) 14738-14741.

[203] D. A. Roberts, B. S. Pilgrim, J. D. Cooper, T. K. Ronson, S. Zarra, J. R. Nitschke, J. Am. Chem. Soc. 137 (2015) 10068-10071.

[204] F. C. Pigge, Curr. Org. Chem. 20 (2016) 1902-1922.

[205] C. Liu, T. Li, N. L. Rosi, J. Am. Chem. Soc. 134 (2012) 18886-18888.

[206] Z. Wang, J. Liu, H. K. Arslan, S. Grosjean, T. Hagendorn, H. Gliemann, S. Bräse, C. Wöll, Langmuir 29 (2013) 15958-15964.

[207] Z. Wang, J. Liu, S. Grosjean, D. Wagner, W. Guo, Z. Gu, L. Heinke, H. Gliemann, S. Bräse, C. Wöll, ChemNanoMat 1 (2015) 338-345.

[208] Y.-S Bae, R. Q. Snurr, Angew. Chem. Int. Ed. 50 (2011) 11586–11596.

[209] J.-R. Li, Y. Ma, M. C. McCarthy, J. Sculley, J. Yu, H.-K. Jeong, P. B. Balbuena, H.-C. Zhou, Coord. Chem. Rev. 255 (2011) 1791–1823.

[210] K. Sumida, D. L. Rogow, J. A. Mason, T. M. McDonald, E. D. Bloch, Z. R. Herm, T.-H. Bae, J. R. Long, Chem. Rev. 112 (2012) 724–781.

[211] J. Liu, P. K. Thallapally, B. P. McGrail, D. R. Brown, J. Liu, Chem. Soc. Rev. 41 (2012) 2308–2322.

[212] Z. Zhang, Y. Zhao, Q. Gong, Z. Li, J. Li, Chem. Commun. 49 (2013) 653-661.

[213] Z. Zhang, Z.-Z. Yao, S. Xiang, B. Chen, Energy Environ. Sci. 7 (2014) 2868–2899.

[214] Y. Zeng, R. Zou, Y. Zhao, Adv. Mater. 28 (2016) 2855–2873.

[215] H. He, J. A. Perman, G. Zhu, S. Ma, Small 12 (2016) 6309–6324.

[216] C. Noiriel, D. Daval, Chem. Res. 50 (2017) 759−768.

[217] P.-Z. Li, Y. Zhao, Chem. Asian J. 8 (2013) 1680–1691.

[218] R. Boulmene, M. Prakash, M. Hochlaf, Phys. Chem. Chem. Phys. 18 (2016) 29709-29720.

[219] Z. R. Herm, J. A. Swisher, B. Smit, R. Krishna, J. R. Long, J. Am. Chem. Soc. 133 (2011) 5664-5667.

[220] T. M. McDonald, D. M. D'Alessandro, R. Krishna, J. R. Long, Chem. Sci. 2 (2011) 2022-2028.

[221] A. Das, M. Choucair, P. D. Southon, J. A. Mason, M. Zhao, C. J. Kepert, A. T. Harris, D. M. D'Alessandro, Microporous Mesoporous Mater. 174 (2013) 74-80.

[222] J. Liang, Z. Liang, R. Zou, Y. L. Zhao, Adv. Mater. 29 (2017) 1701139.

[223] D. Yu, S. P. Teong, Y. Zhang. Coord. Chem. Rev. 293–294 (2015) 279–291.

[224] G. Fang, X. Bi, Chem. Soc. Rev. 44 (2015) 8124-8173.

[225] W.-Y. Gao, Y. Chen, Y. Niu, K. Williams, L. Cash, P. J. Perez, L. Wojtas, J. Cai, Y.-S. Chen, S. Ma, Angew. Chem. Int. Ed. 53 (2014) 2615-2619.

[226] J. Zheng, M. Wu, F. Jiang, W. Su, M. Hong, Chem. Sci. 6 (2015) 3466-3470.

[227] R. Zou, P.-Z. Li, Y.-F. Zeng, J. Liu, R. Zhao, H. Duan, Z. Luo, J.-G. Wang, R. Zou, Y. Zhao, Small 12 (2016) 2334–2343.

[228] P.-Z. Li, X.-J. Wang, J. Liu; H. S. Phang, Y. Li, Y. Zhao, Chem. Mater. 29 (2017) 9256−9261.

[229] X. Han, X.-J. Wang, P.-Z. Li, R. Zou, M. Li, Y. Zhao, CrystEngComm 17 (2015) 8596-8601.

[230] J. L. Harding, J. M. Metz, M. M. Reynolds, Adv. Funct. Mater. 24 (2014) 7503-7509.

[231] M. J. Neufeld, B. R. Ware, A. Lutzke, S. R. Khetani, M. M. Reynolds, ACS Appl. Mater. Interfaces 8 (2016) 19343-19352.

[232] M. J. Neufeld, A. Lutzke, J. B. Tapia, M. M. Reynolds, ACS Appl. Mater. Interfaces 9 (2017) 5139-5148.

[233] W. Zhu, C. He, P. Wu, X. Wu, C. Duan, Dalton Trans. 41 (2012) 3072-3077.

[234] M. Savonnet, A. Camarata, J. Canivet, D. Bazer-Bachi, N. Bats, V. Lecocq, C. Pinela, D. Farrusseng, Dalton Trans. 41 (2012) 3945-3948.

[235] X.-C. Yi, F.-G. Xi, Y. Qi, E.-Q. Gao, RSC Adv. 5 (2015) 893-900.

[236] S. Han, Y. Wei, C. Valente, I. Lagzi, J. J. Gassensmith, A. Coskun, J. F. Stoddart, B. A. Grzybowski, J. Am. Chem. Soc. 132 (2010) 16358-16361.

[237] Y.-Q. Lan , H.-L. Jiang , S.-L. Li, Q. Xu, Adv. Mater. 23 (2011) 5015-5020.

[238] Q. Zhang, J. Yu, J. Cai, R. Song, Y. Cui, Y. Yang, B. Chen, G. Qian, Chem. Commun. 50 (2014) 14455-14458.

[239] D. Zhao, S. Tan, D. Yuan, W. Lu, Y. H. Rezenom, H. Jiang, L.-Q. Wang, H.-C. Zhou, Adv. Mater. 23 (2011) 90-93.

[240] W. Morris, W. E. Briley, E. Auyeung, M. D. Cabezas, C. A. Mirkin, J. Am. Chem. Soc. 136 (2014) 7261-7264.

[241] W.-H. Chen, X. Yu, A. Cecconello, Y. S. Sohn, R. Nechushtaib, I. Willner, Chem. Sci. 8 (2017) 5769–5780.

[242] I. A. Lazaro, S. Haddad, S. Sacca, C. Orellana-Tavra, D. Fairen-Jimenez, R. S. Forgan, Chem 2 (2017) 561-578.

[243] F. Nian, Y. Huang, M. Song, J.-J. Chen, J. J. Xue, J. Mater. Chem. B 5 (2017) 6227-6232.

[244] M. Ito, T. Ishiwata, S. Anan, K. Kokado, D. Inoue, A. M. R. Kabir, A. Kakugo, K. Sada, ChemistrySelect 1 (2016) 5358-5362.

[245] M. J. MacLeod, J. A. Johnson, Polym. Chem. 8 (2017) 4488-4493.

[246] S. Wuttke, M. Lismont, A. Escudero, B. Rungtaweevoranit, W. J. Parak. Biomaterials 123 (2017) 172-183.

[247] T. Ishiwata, Y. Furukawa, K. Sugikawa, K. Kokado, K. Sada, J. Am. Chem. Soc. 135 (2013) 5427-5432.

[248] T. Ishiwata, K. Kokado, K. Sada, Angew. Chem. Int. Ed. 56 (2017) 2608-2612.

[249] M. Tsotsalas, J. Liu, B. Tettmann, S. Grosjean, A. Shahnas, Z. Wang, C. Azucena, M. Addicoat, T. Heine, J. Lahann, J. Overhage, S. Bräse, H. Gliemann, C. Wöll, J. Am. Chem. Soc. 136 (2014) 8-11.

[250] S. Schmitt, M. Silvestre, M. Tsotsalas, A.-L. Winkler, A. Shahnas, S. Grosjean, F. Laye, H. Gliemann, J. Lahann, S. Bräse, M. Franzreb, C. Wöll, ACS Nano 9 (2015) 4219-4226.

[251] W. Zhou, S. Begum, Z. Wang, P. Krolla, D. Wagner, S. Bräse, C. Wöll, M. Tsotsalas, ACS Appl. Mater. Interfaces 10 (2018) 1528–1533.

[252] C. Chen, C. A. Allen, S. M. Cohen, Inorg. Chem. 50 (2011) 10534-10536.

[253] S. Nayab, V. Trouillet, H. Gliemann, S. Hurrle, P. G. Weidler, S. R. Tariq, A. S. Goldmann, C. Barner-Kowollik, B. Yameen, Chem. Commun. 53 (2017) 11461-11464.

[254] A. Aykaç, M. Noiray, M. Malanga, V. Agostoni, J. M. Casas-Solvas, É. Fenyvesi, R. Gref, A. Vargas-Berenguel, Biochim. Biophys. Acta 1861 (2017) 1606–1616.

[255] V. Mugnaini, M. Tsotsalas, F. Bebensee, S. Grosjean, A. Shahnas, S. Brase, J. Lahann, M. Buck, C. Wöll, Chem. Commun. 50 (2014) 11129-11131.

[256] S. Schmitt, J. Hümmer, S. Kraus, A. Welle, S. Grosjean, M. Hanke-Roos, A. Rosenhahn, S. Bräse, C. Wöll, C. Lee-Thedieck, M. Tsotsalas, Adv. Funct. Mater. 26 (2016) 8455-8462.

[257] S. Schmitt, S. Diring, P. G. Weidler, S. Begum, S. Heißler, S. Kitagawa, C. Wöll, S. Furukawa, M. Tsotsalas, Chem. Mater. 29 (2017) 5982−5989.

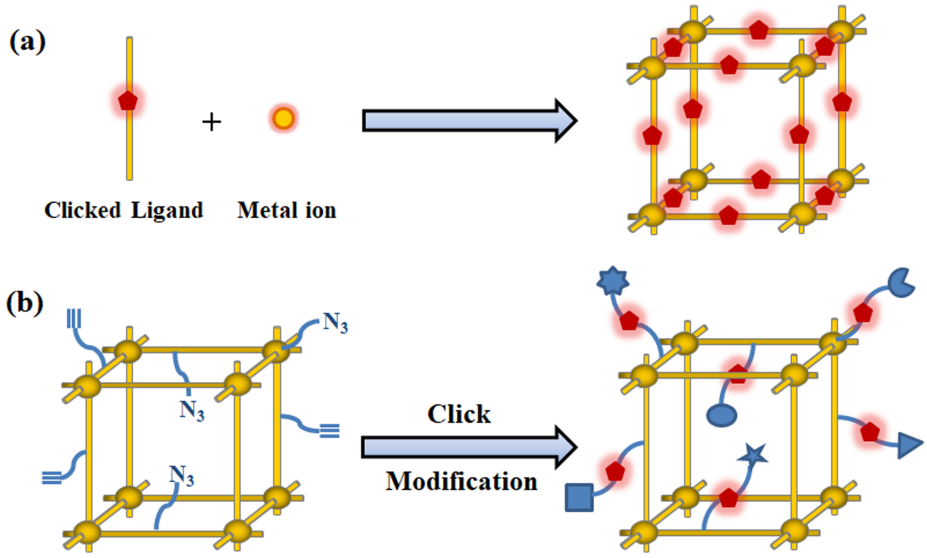


**Scheme 1.** Illustrations of MOFs (a) derived from the pre-designed clicked ligands and metal ions, and (b) modified by clicked post-synthetic modification.

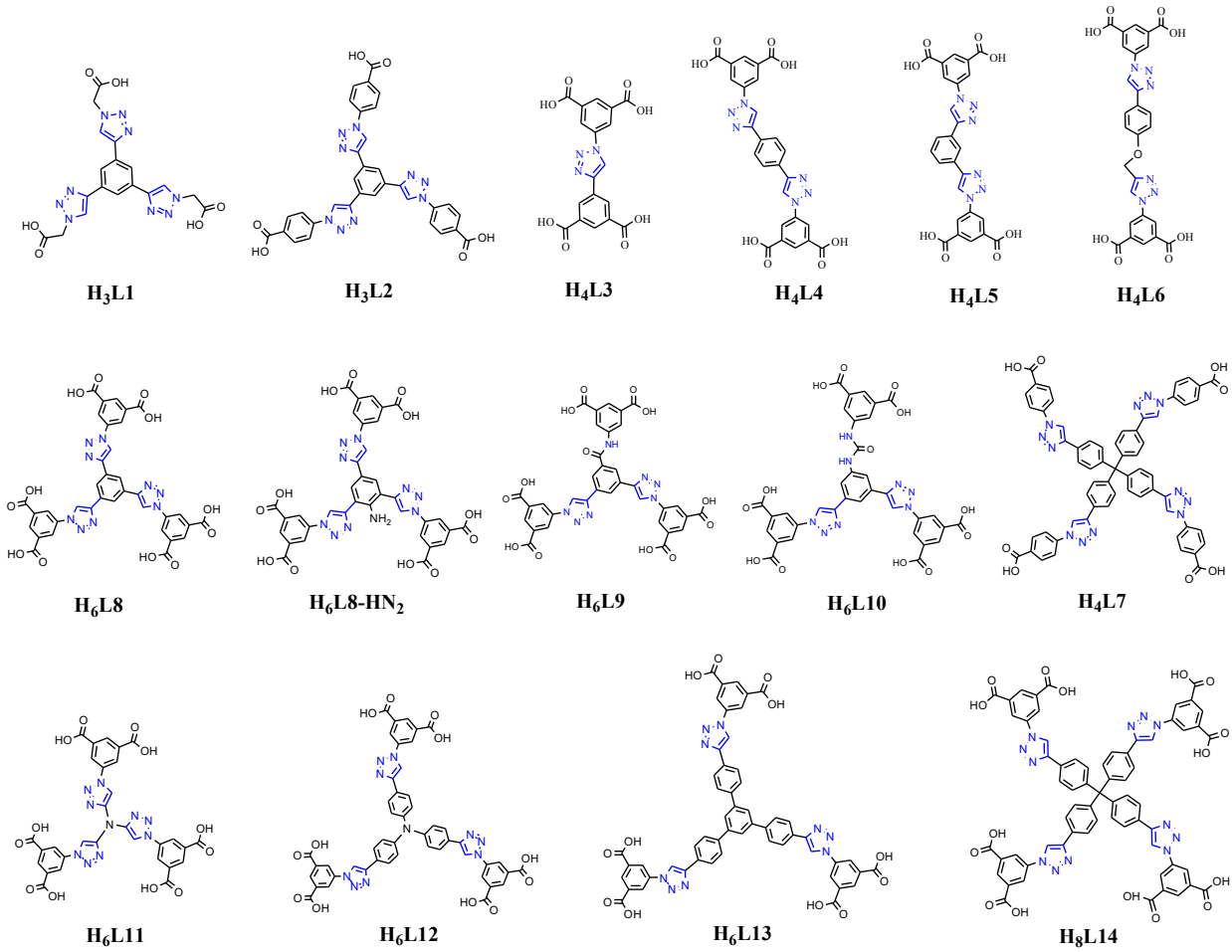


**Scheme 2. Commonly used clicked polytopic-carboxylate ligands in MOF constructions.**

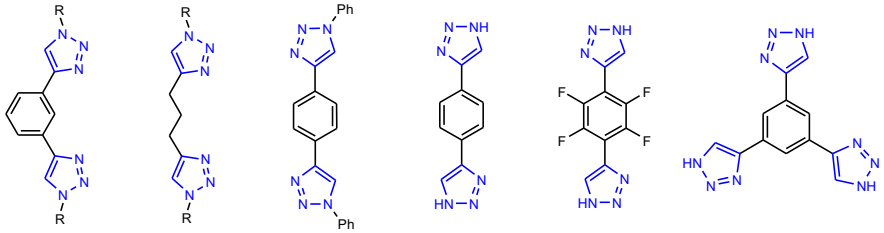

$R_2L15$ $R_2L16$ $R_2L17$ $H_2L18$ $H_2L19$ $H_3L20$

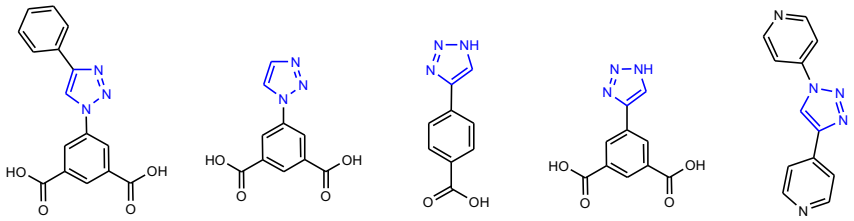

$H_2L21$ $H_2L22$ $H_2L23$ $H_3L24$ L25

L26 L27 (n = 1), L28 (n = 3)

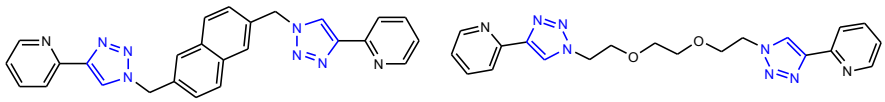

L29 L30

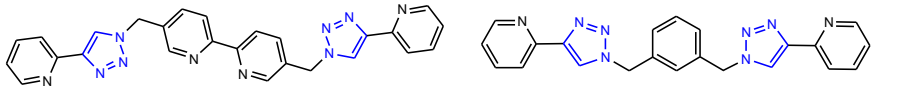

L31 L32

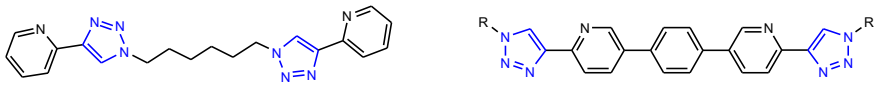

L33 L34 (R = adamantane), L35 ( R = PEG)

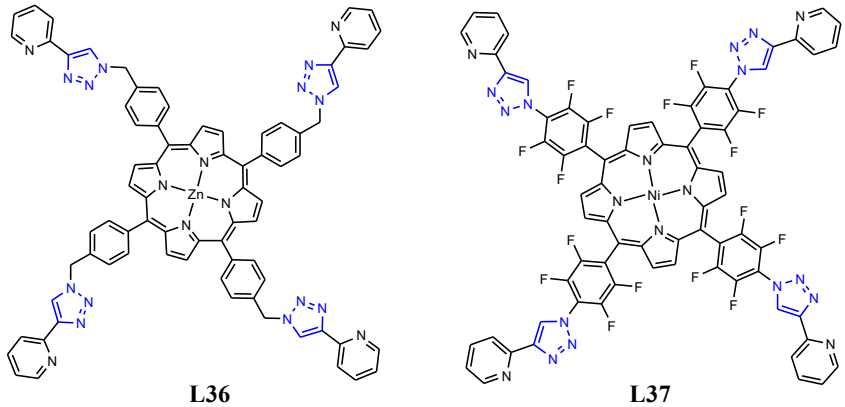

L36 L37

**Scheme 3**. Clicked polytopic triazolates (L15-L20), carboxylate-containing triazolates (L21-L24), and pyridines (L25-L35). PEG = polyethylene glycol.

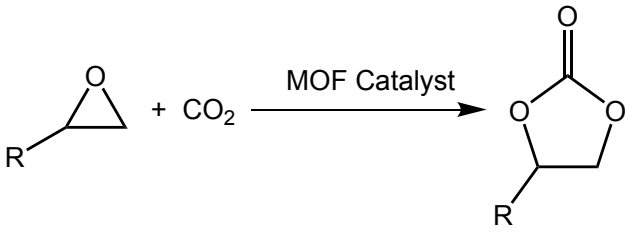


**Scheme 4**. MOF-based catalytic cycloaddition of $CO_2$ with epoxides to generate various carbonates.

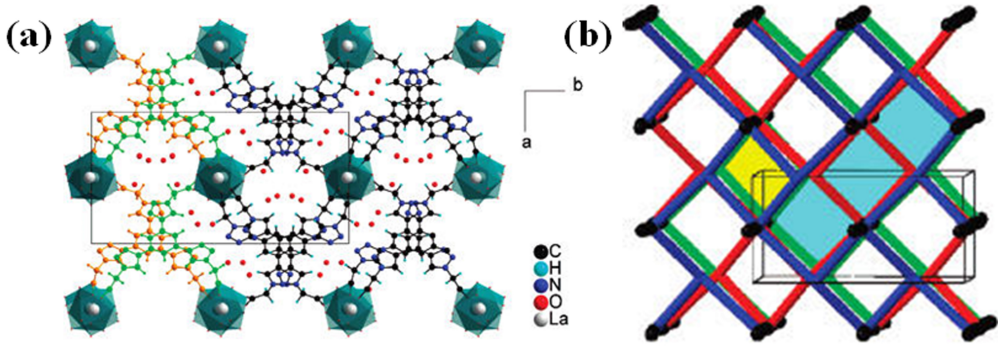


**Figure 1.** (a) Porous framework of MIL-112 and (b) its topological $4^4$ network. Adapted with permission from Ref. [83]. Copyright 2007, American Chemical Society.

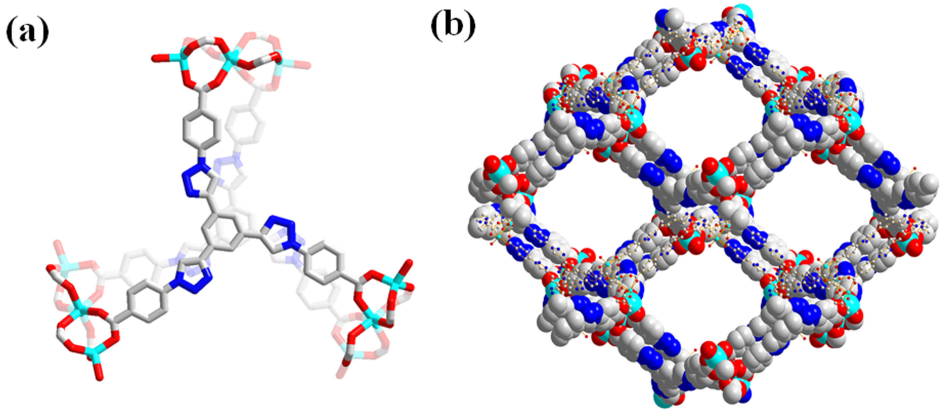


**Figure 2.** (a) L2 connected three $Zn_3$ units and (b) 1D porous channels along *c*-axis in NTU-130. Adapted with permission from Ref. [87]. Copyright 2017, Royal Society of Chemistry.

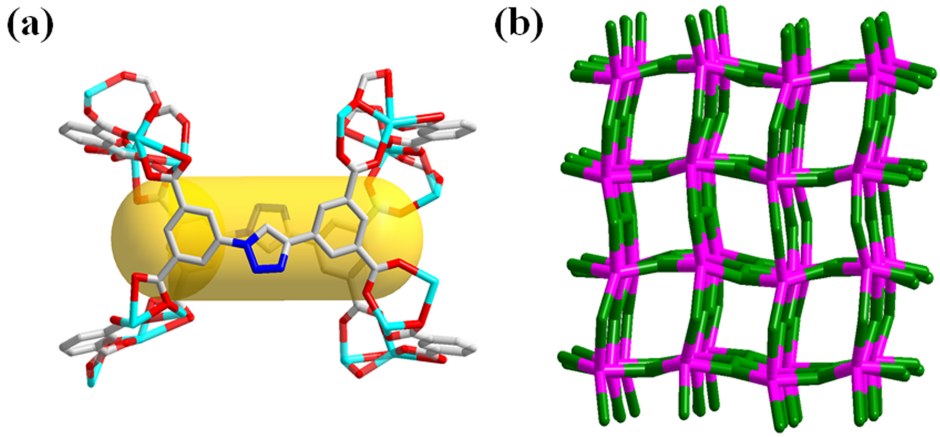


**Figure 3.** (a) Wire-and-stick representation of L3 linked four $Zn_2$ clusters in NTU-101-Zn, and (b) simplified PtS-type network of NTU-101-Zn. Adapted with permission from Ref. [90]. Copyright 2012, Royal Society of Chemistry.

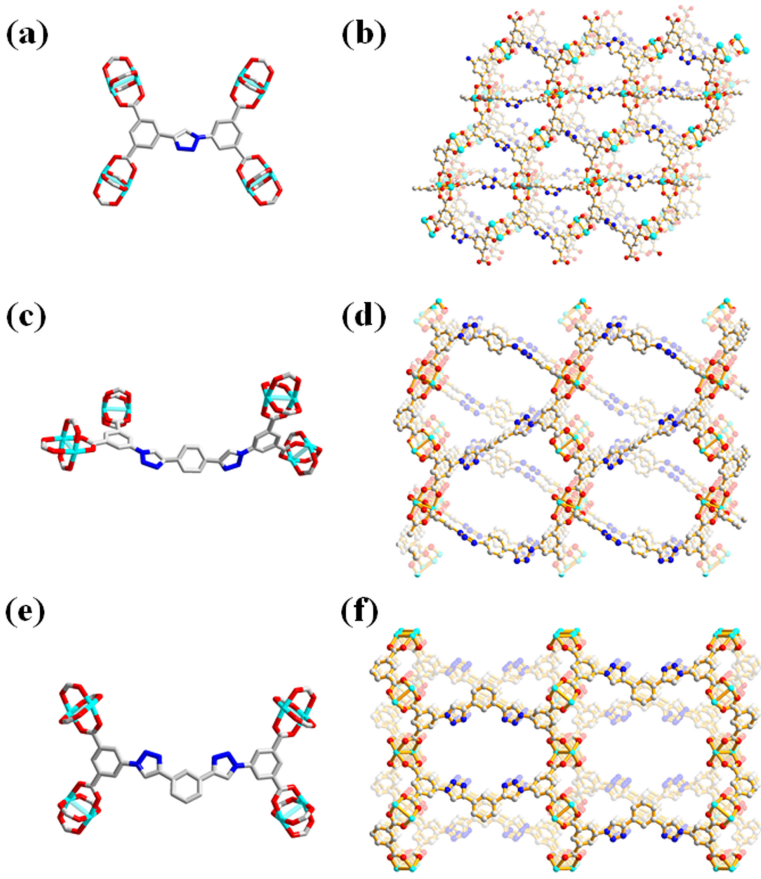


**Figure 4.** Wire-and-stick representation of L3, L4, or L5 linked four paddlewheel $Cu_2$ clusters and porous frameworks of corresponding MOFs. (a,b) NTU-111, (c,d) NTU-112, and (e,f) NTU-113. Coordinated water molecules and hydrogen atoms are omitted for the clarity. Adapted with permission from Ref. [92]. Copyright 2014, Royal Society of Chemistry.

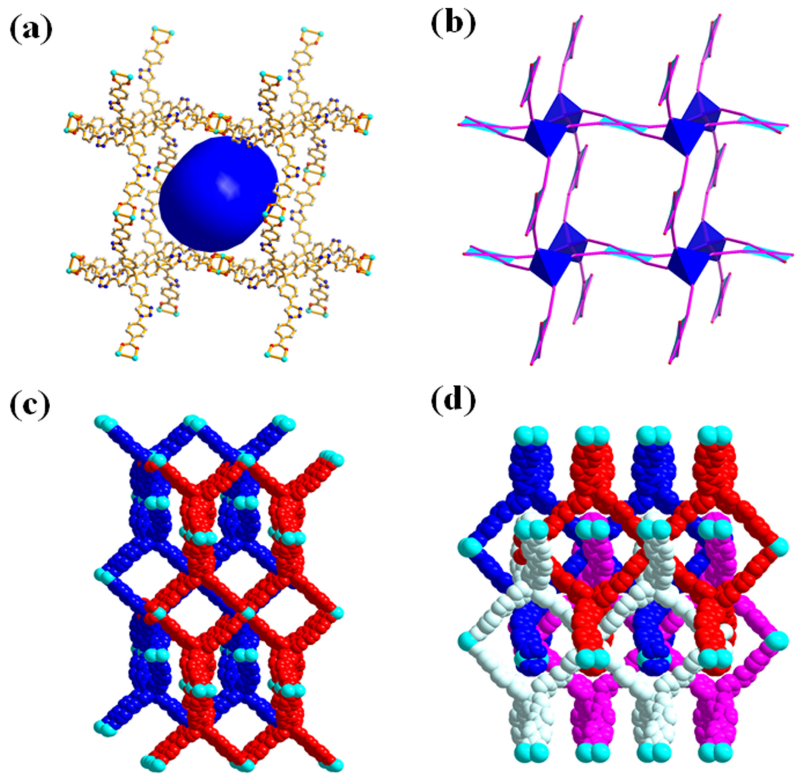


**Figure 5.** (a) Coordination of L7 ligands with paddlewheel $Cu_2$ units in the framework, (b) simplified PtS-type basic network in two MOFs, and (c,d) perspective view of 2-fold (for NTU-140) and 4-fold (for NTU-141) interpenetrations of basic networks in the two MOFs. Adapted with permission from Ref. [104]. Copyright 2014, Royal Society of Chemistry.

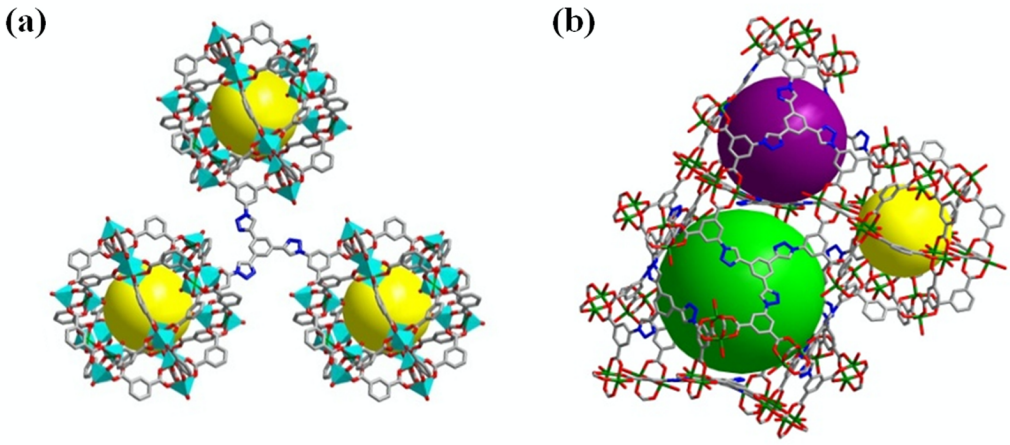


**Figure 6.** (a) Constructed (3,24)-connected *rht*-type framework of NTU-105, and (b) three types of polyhedrons in NTU-105. Adapted with permission from Ref. [121]. Copyright 2013, Springer Nature Limited.

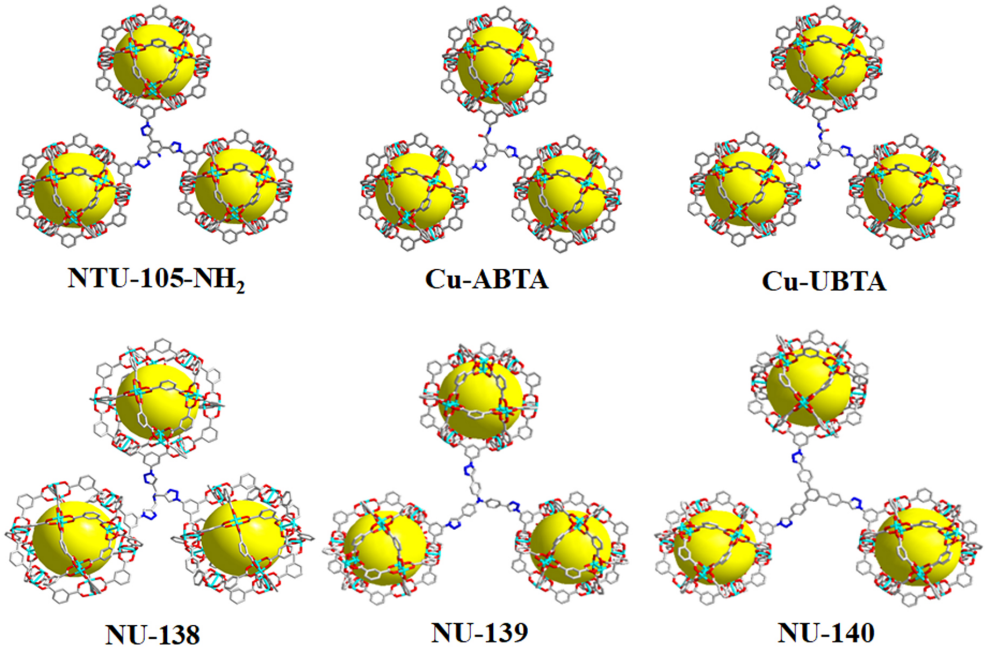


**Figure 7.** (a) Triazole-containing (3,24)-connected frameworks of NTU-105-$NH_2$ [124], Cu-ABTA [125], Cu-UBTA [126], NU-138, NU-139, and NU-140 [127]. These structures are drawn based on their crystal data.

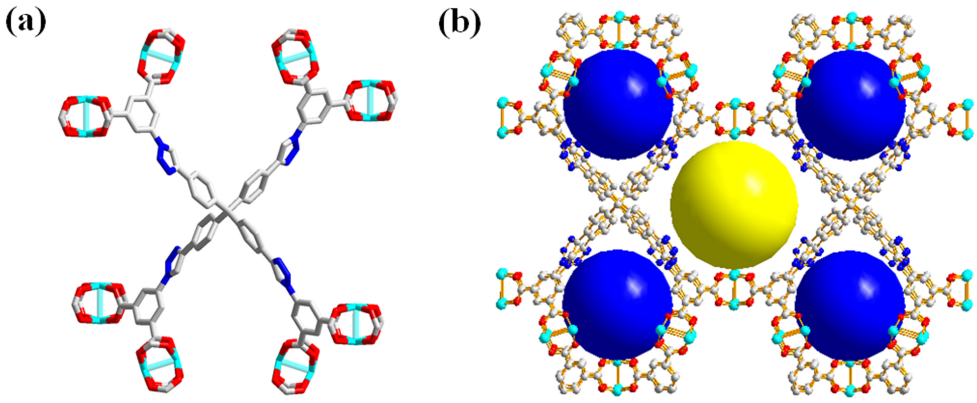


**Figure 8.** (a) Clicked oct-carboxylate linked four pairs of paddlewheel $Cu_2$ units, and (b) perspective view of the framework of NTU-180 with two kinds of cages (yellow and blue balls). Adapted with permission from Ref. [137]. Copyright 2016, American Chemical Society.

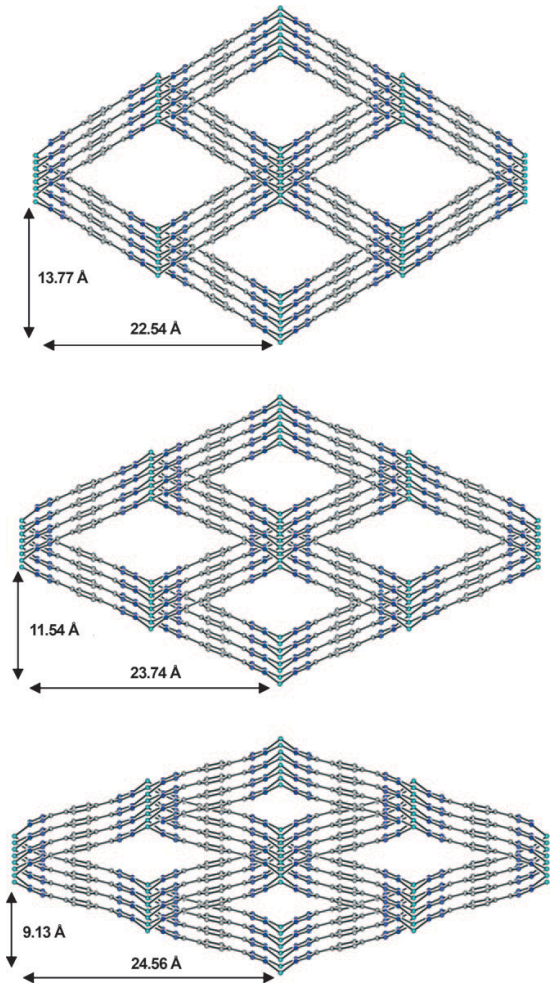


**Figure 9.** Framework transformations of Cu(BDTri) showing the "breathing" behavior through single-crystal to single-crystal conversions. Adapted with permission from Ref. [148]. Copyright 2010, WILEY-VCH Verlag GmbH & Co. KGaA, Weinheim.

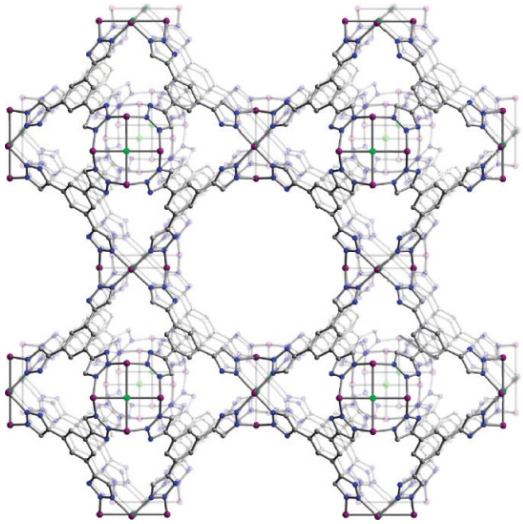

**Figure 10.** Sodalite-type framework of CuBTTri. Adapted with permission from Ref. [153]. Copyright 2009, American Chemical Society.

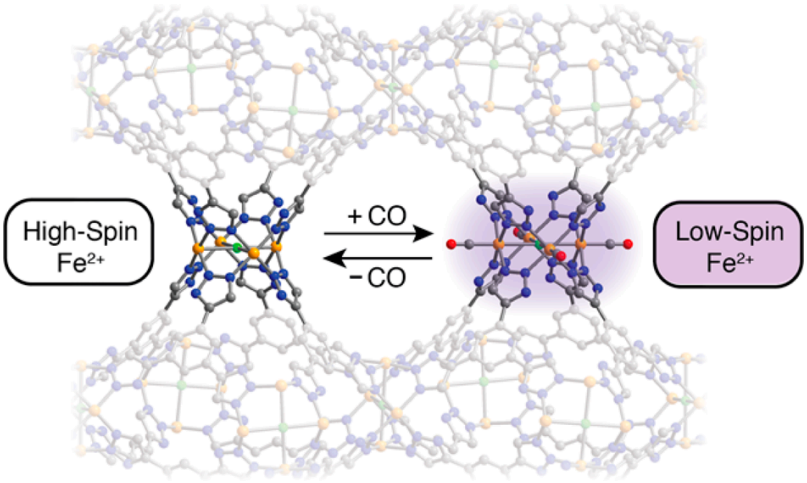


**Figure 11.** Framework of Fe-BTTri showing reversible CO adsorption by unsaturated Fe(II) site and the spin-state exchange of Fe(II) during the adsorption and desorption of CO molecule. Adapted with permission from Ref. [154]. Copyright 2016, American Chemical Society.

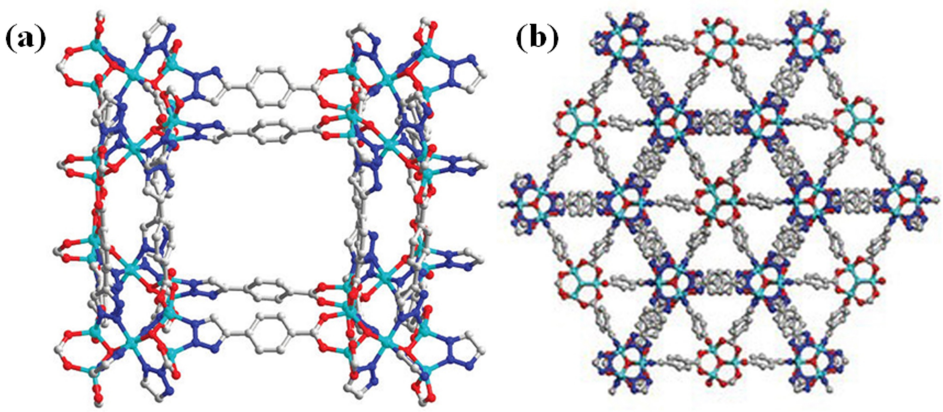


**Figure 12.** Framework structures of (a) MTAF-1 and (b) MTAF-4. Adapted with permission from Ref. [160]. Copyright 2013, Royal Society of Chemistry.

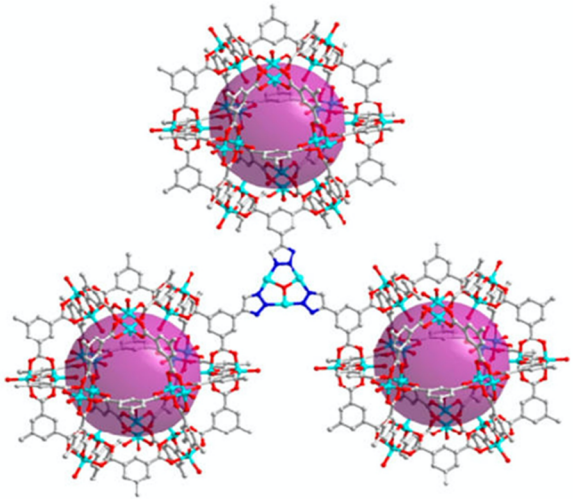

**Figure 13.** $C_3$ symmetric building moiety of *rht*-MOF-tri. Adapted with permission from Ref. [161]. Copyright 2015, American Chemical Society.

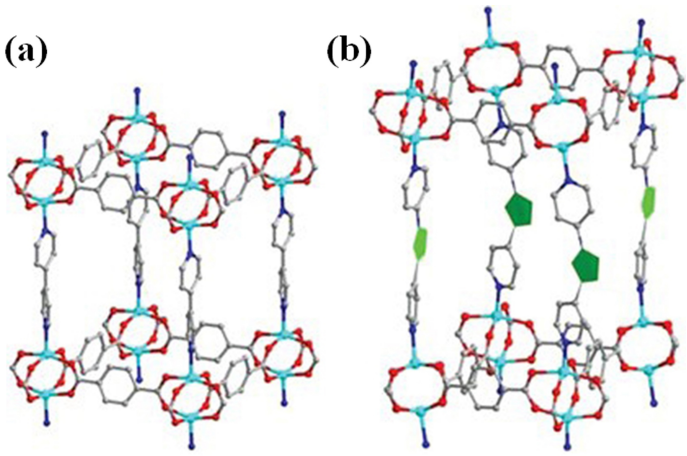


**Figure 14.** Building units of (a) MOF-508 [184] and (b) MTAF-3. Adapted with permission from Ref. [183]. Copyright 2012, Royal Society of Chemistry.

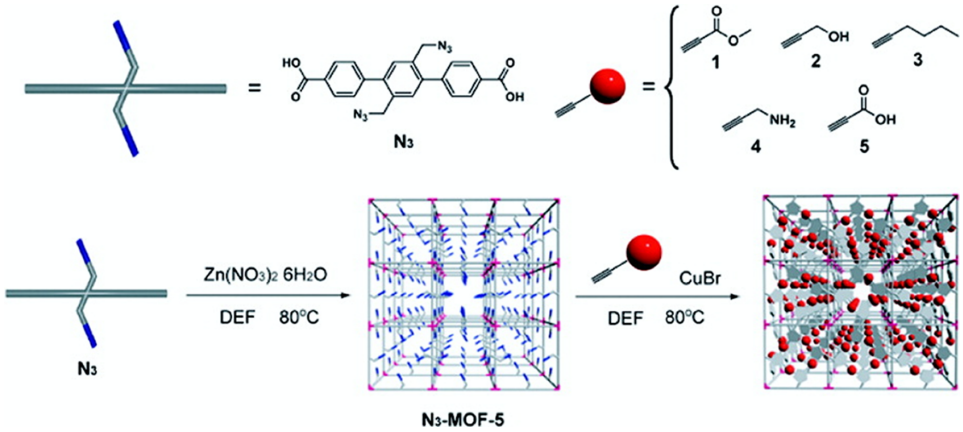


**Figure 15.** Schematic illustration of a MOF bearing the azide group ($N_3$) for the click post-modification by alkyne substrates (1-5). Adapted with permission from Ref. [188]. Copyright 2008, American Chemical Society.

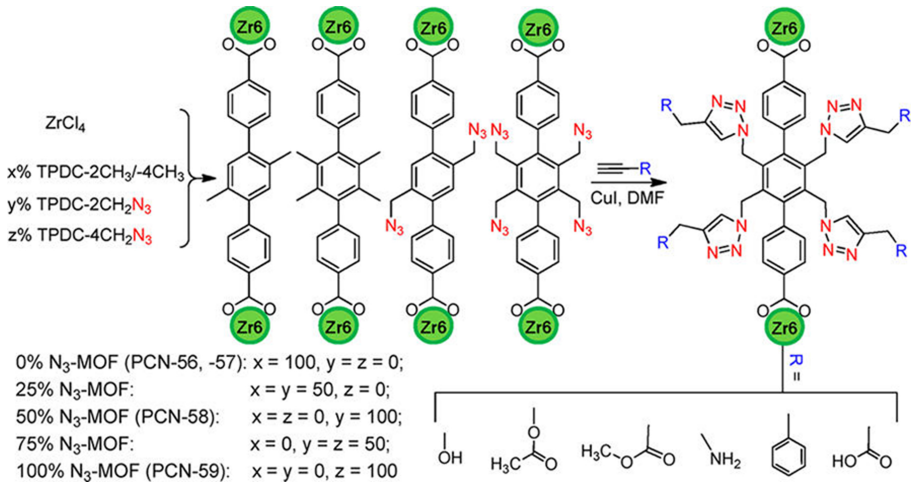


**Figure 16.** Schematic illustration of Zr-based PCN-58 and PCN-59 "click"-modified by a series of acetylene compounds containing various functional groups. Adapted with permission from Ref. [189]. Copyright 2012, American Chemical Society.

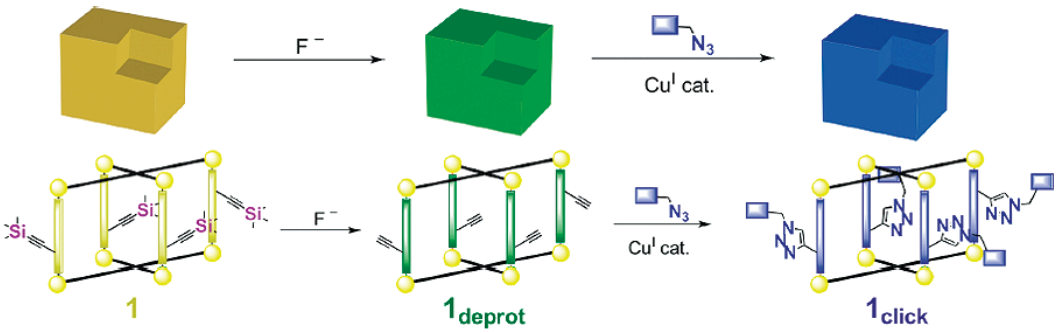


**Figure 17.** Schematic illustration of the click post-modification of a MOF through functionalizing internal and external surfaces by different azides. Adapted with permission from Ref. [195]. Copyright 2009, American Chemical Society.

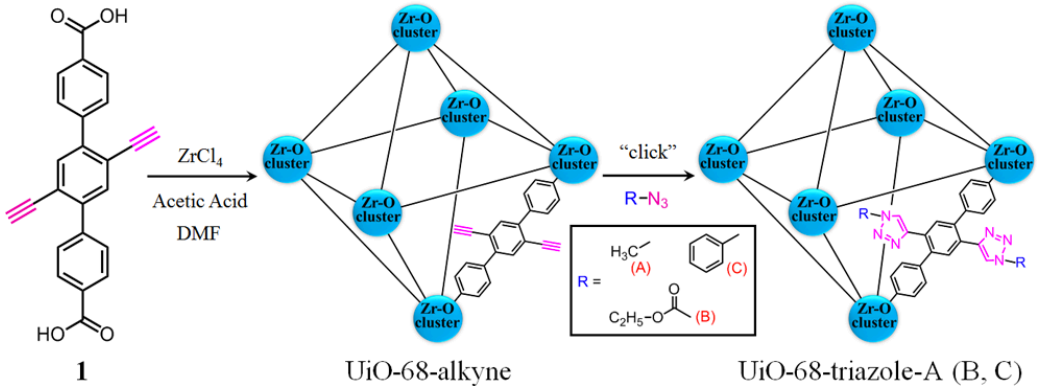


**Figure 18.** Schematic illustration for the click post-modification of an alkyne-tagged UiO-68 (UiO-68-alkyne). Adapted with permission from Ref. [197]. Copyright 2015, American Chemical Society.

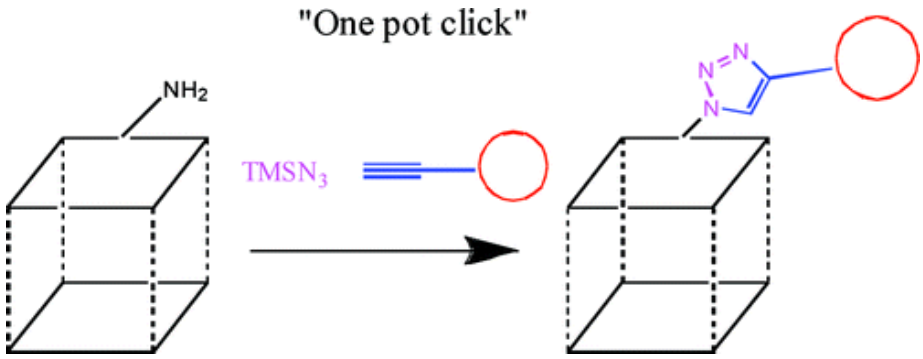


**Figure 19.** One-pot, two-step functionalization of an amine-containing MOF, DMOF-$NH_2$. Reproduced with permission. Adapted with permission from Ref. [199]. Copyright 2010, American Chemical Society.

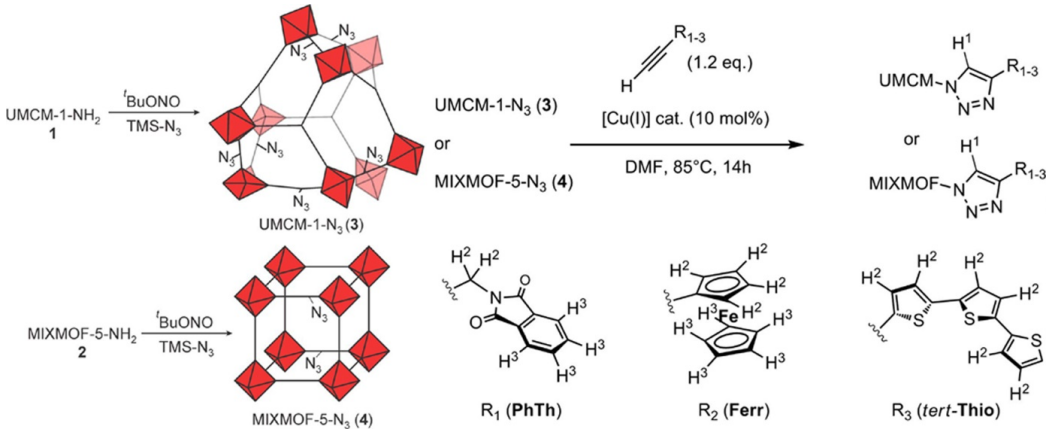


**Figure 20.** Two-step clicked post modification of amine-functionalized UMCM-1 and MIXMOF-5. Adapted with permission from Ref. [84]. Copyright 2013, American Chemical Society.

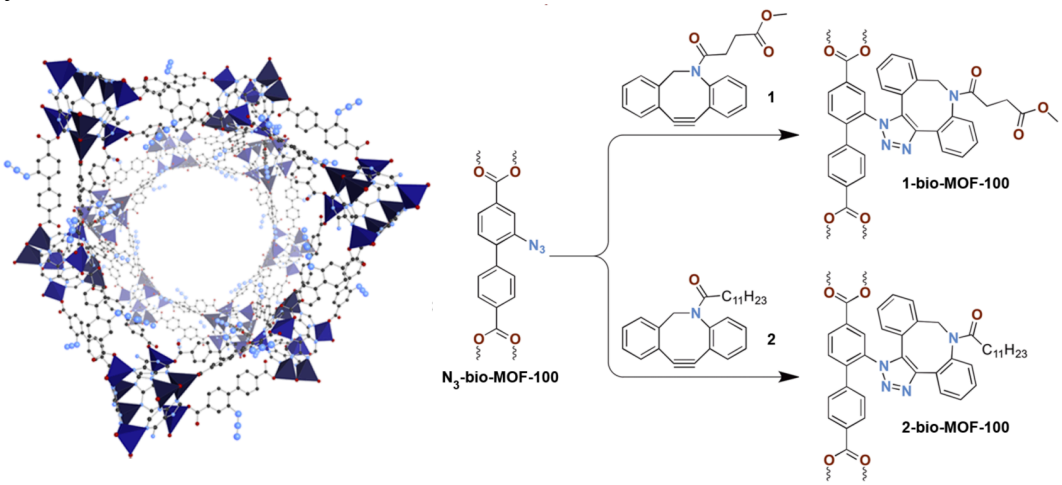


**Figure 21.** Crystal structure of azide-decorated $N_3$-bio-MOF-100, and schematic illustration for the strain-promoted click modification of $N_3$-bio-MOF-100 with 4-(11,12-didehydrodi benzo[*b*,*f*]-azocin-5(6*H*)-yl)-4-oxobutanoate (1) and N-dodecanoyl-5,6- dihydro-11,12-di dehydrodibenzo[*b*,*f*]azocine (2) to afford 1-bio-MOF-100 and 2-bio-MOF-100, respectively. Adapted with permission from Ref. [205]. Copyright 2012, American Chemical Society.

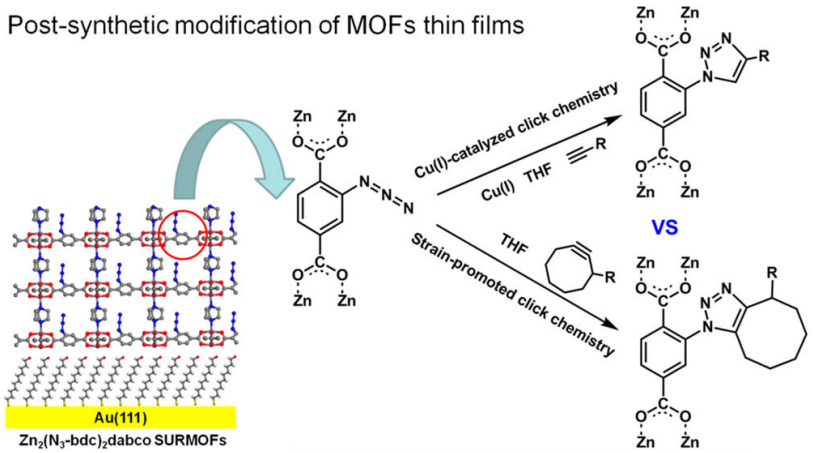


**Figure 22.** Illustration of an azide-decorated MOF thin film post-synthetic modified by copper(I)-catalyzed and copper-free strain-promoted click reaction. Adapted with permission from Ref. [209]. Copyright 2013, American Chemical Society.

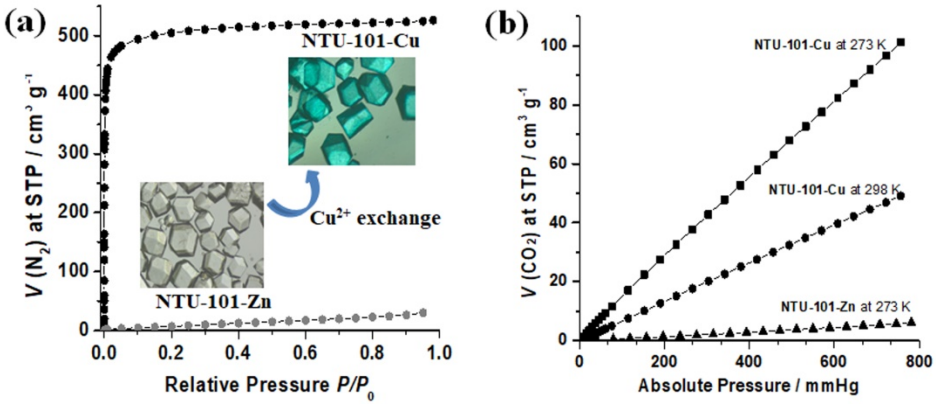


**Figure 23.** (a) $N_2$ sorption isotherms of activated NTU-101-Zn and NTU-101-Cu at 77 K, and (b) gas sorption isotherms of activated NTU-101-Cu for $CO_2$ at 273 and 298 K, and $N_2$ at 273 K. Adapted with permission from Ref. [90]. Copyright 2012, Royal Society of Chemistry.

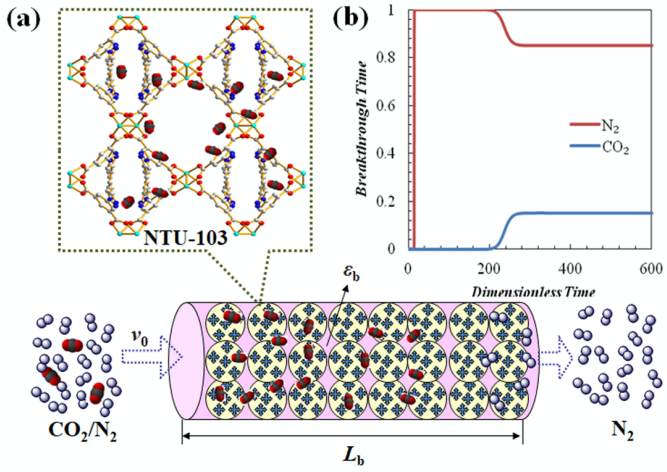


**Figure 24.** (a) Illustration of an NTU-113 packed fixed-bed, and (b) simulated breakthrough curves for $CO_2/N_2$ mixture passing through the fixed-bed. The inlet $CO_2/N_2$ ratio is 0.15/0.85 at 273 K and 100 kPa. Adapted with permission from Ref. [92]. Copyright 2014, Royal Society of Chemistry.

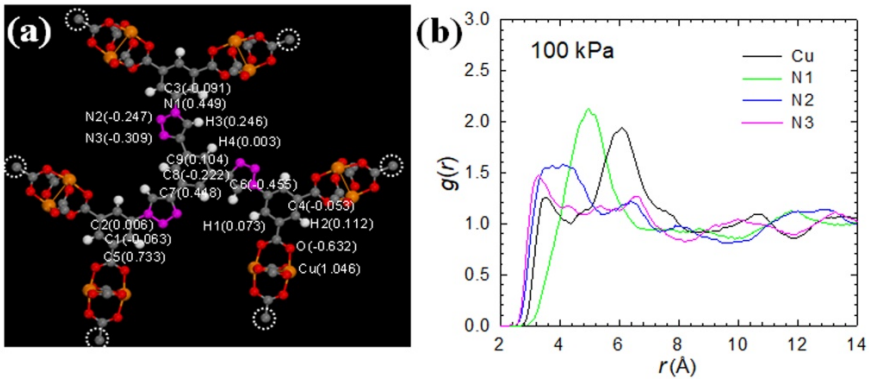


**Figure 25.** (a) Atomic charges in a fragmental cluster of NTU-105. Color code: Cu, orange; O, red; N, pink; C, grey; H, white. (b) Radial distribution functions of $CO_2$ around Cu, N1, N2 and N3 atoms at 100 kPa. Adapted with permission from Ref. [121]. Copyright 2013, Springer Nature Limited.

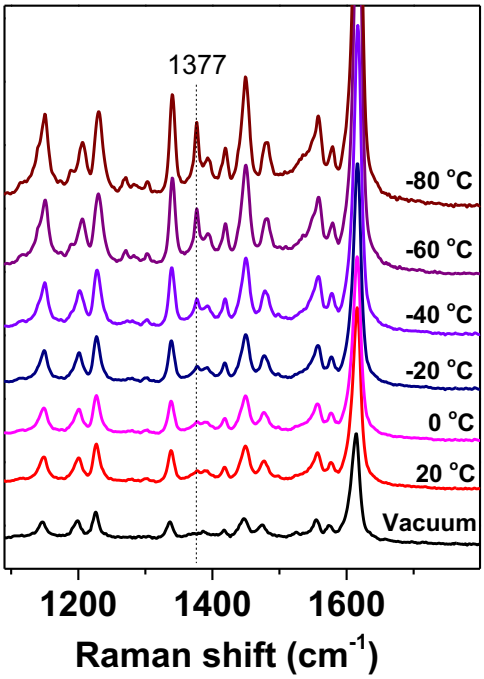


**Figure 26.** Temperature dependent Raman spectra of NTU-180 (Vacuum) and $CO_2$-adsorbed NTU-180 (20 to –80 °C) showing obvious spectroscopic changes before and after the $CO_2$ adsorption. Adapted with permission from Ref. [137]. Copyright 2016, American Chemical Society.

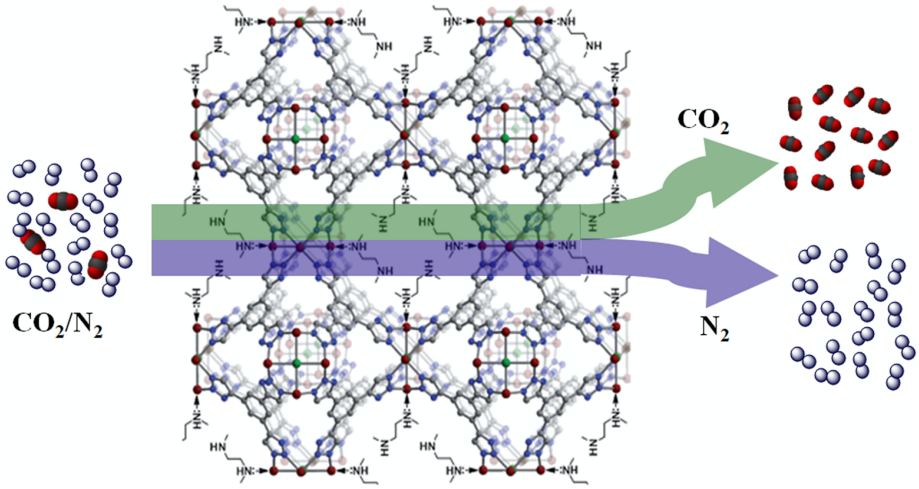


**Figure 27.** Illustration of amine functionalized CuBTTri (mmen-CuBTTri) and its excellent selectivity for $CO_2$ capture. Adapted with permission from Ref. [220]. Copyright 2011, Royal Society of Chemistry.

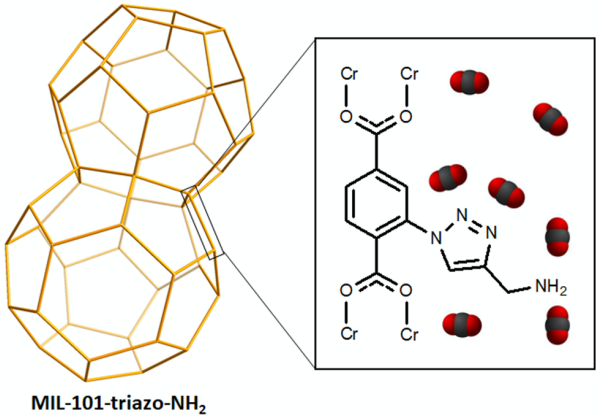


**Figure 28.** Illustration of clicked adsorbent, MIL-101-triazo-$NH_2$, for selective $CO_2$ capture. Adapted with permission from Ref. [190]. Copyright 2013, Royal Society of Chemistry.

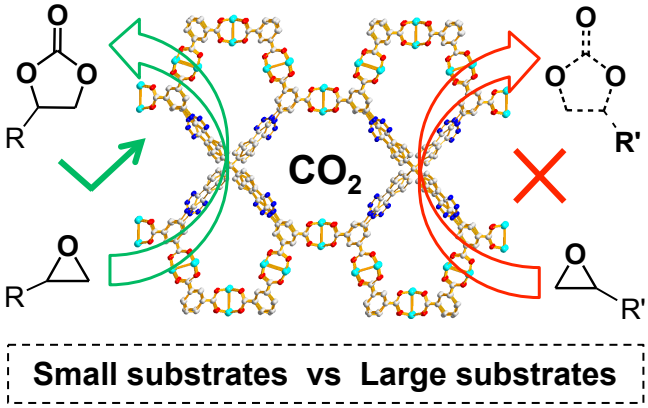


**Figure 29.** Illustration of cyclic carbonates produced from the catalytic cycloaddition of $CO_2$ with epoxides using NTU-180 as a catalyst, and the effect of substrate-size on the reactions. Adapted with permission from Ref. [137]. Copyright 2016, American Chemical Society.

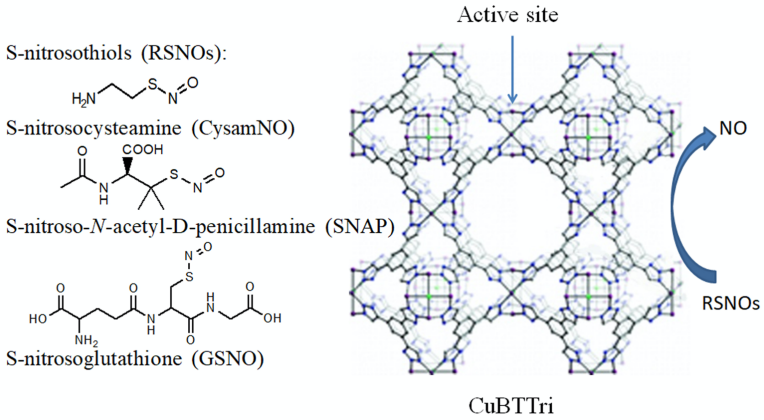


**Figure 30.** Illustration of the NO generation from bioavailable substrates, *S*-nitrosothiols, catalyzed by CuBTTri. Adapted with permission from Ref. [230]. Copyright 2014, WILEY-VCH Verlag GmbH & Co. KGaA, Weinheim.

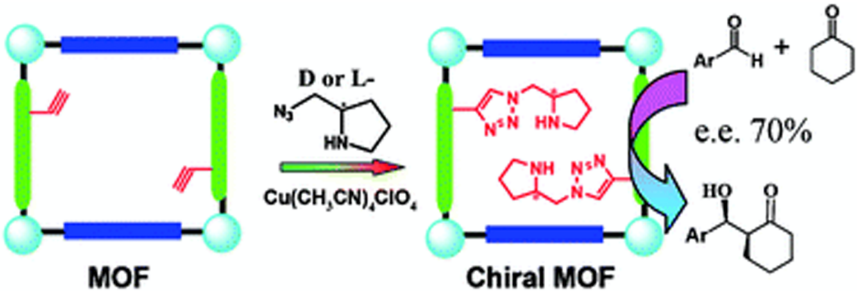


**Figure 31.** Illustration of alkyne-bearing MOF click-modified by chiral azide (*L*- and *D*-2-azidomethylpyrrolidine) for their application of asymmetric aldol reactions. Adapted with permission from Ref. [233]. Copyright 2012, Royal Society of Chemistry.

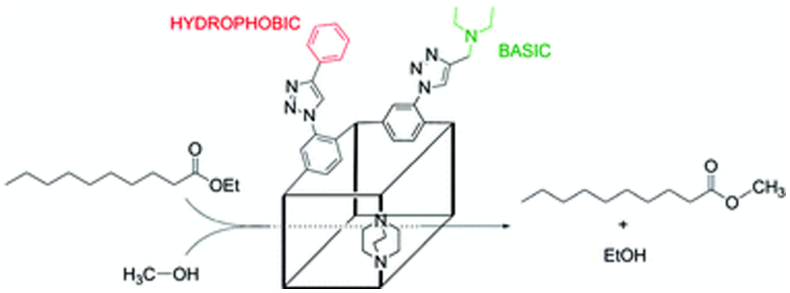


**Figure 32.** Illustration of click-modified bifunctional MOF catalyst and its applications in catalytic transesterification of ethyldecanoate in methanol. Adapted with permission from Ref. [234]. Copyright 2012, Royal Society of Chemistry.

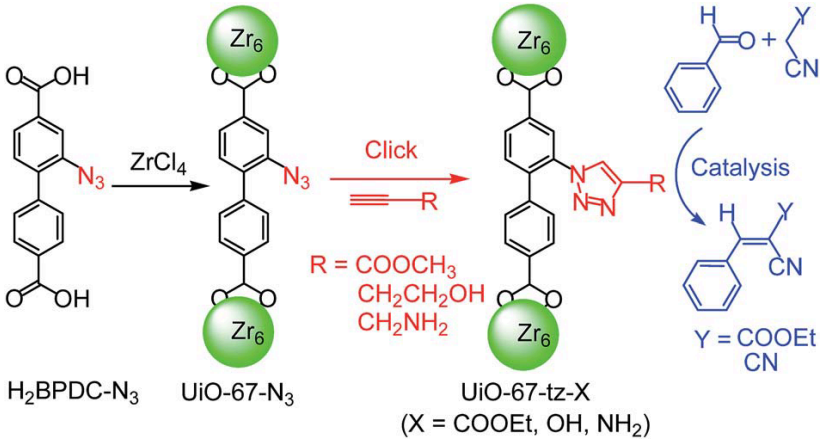


**Figure 33.** Illustration for the synthesis and click-modification of UiO-67–$N_3$ in Knoevenagel condensation reactions. Adapted with permission from Ref. [235]. Copyright 2015, Royal Society of Chemistry.

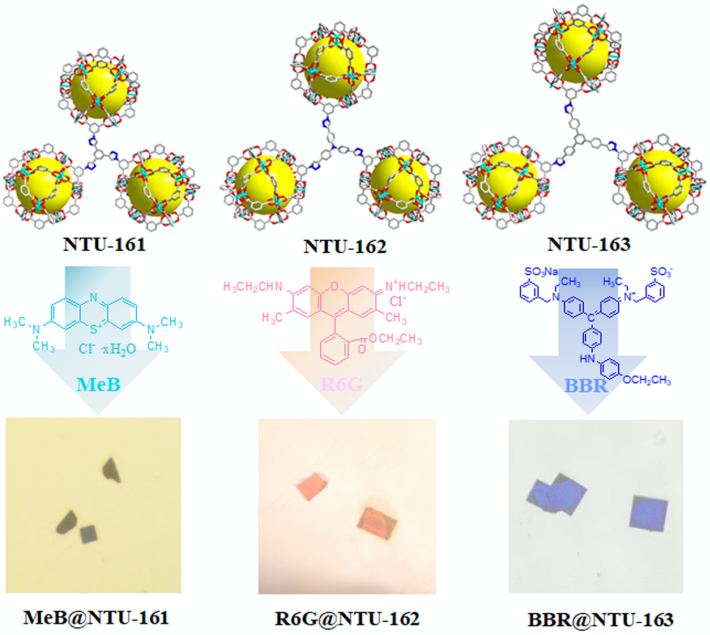


**Figure 34.** Crystal colors of organic dye-adsorbed clicked isoreticular MOFs, *i.e.*, NTU-161, NTU-162, and NTU-163. MeB: Methylene Blue; R6G: Rhodamine 6G; BBR: Brilliant Blue R. Adapted with permission from Ref. [128]. Copyright 2015, WILEY-VCH Verlag GmbH & Co. KGaA, Weinheim.

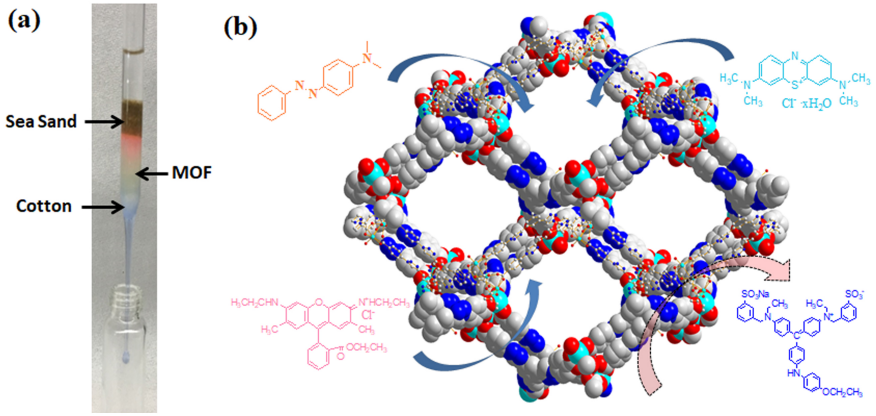


**Figure 35.** (a) Column packed by the crystals of NTU-130 for the separation of dye mixture (R6G/BBR), and (b) illustration of large molecule separation based on size-selective adsorption probed by dye molecules. Adapted with permission from Ref. [87]. Copyright 2017, Royal Society of Chemistry.

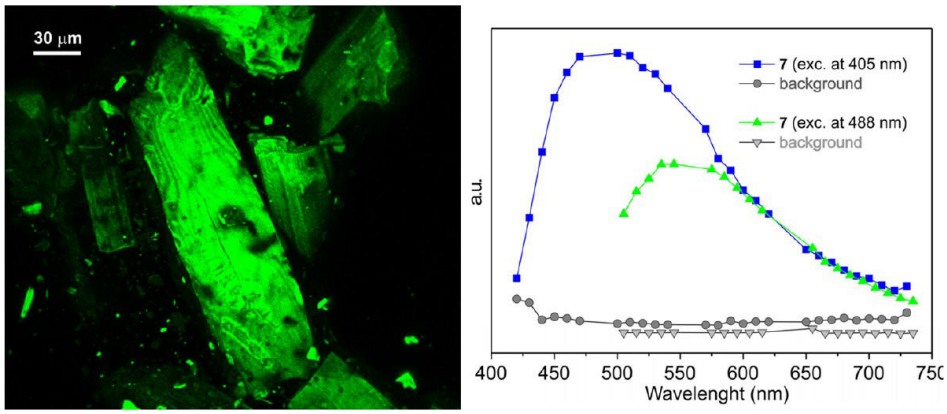


**Figure 36.** Left: Maximum intensity projection (MIP) obtained for crystals of *tert*-thiophene derivative modified UMCM-1 upon excitation at 405 nm. Right: Fluorescence spectra of *tert*-thiophene derivative modified UMCM-1 (7) under the excitation at 405 and 488 nm. Adapted with permission from Ref. [84]. Copyright 2013, American Chemical Society.

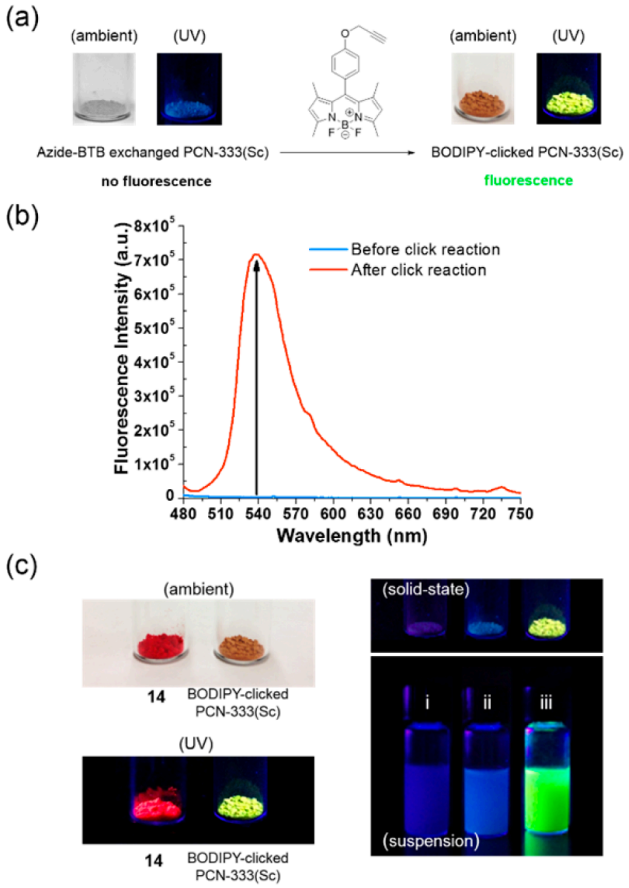


**Figure 37.** (a) Photographs of PCN-333(Sc) and BODIPY fluorophore clicked PCN-333(Sc) under ambient condition and UV light irradiation. (b) Solid-state fluorescence emission spectra of azide-tagged PCN-333(Sc) and BODIPY clicked PCN-333(Sc). $\lambda_{ex}$ = 450 nm. (c) Comparison of solid state alkyne-BODIPY (14) and BODIPY-clicked PCN-333(Sc) under ambient condition and UV light irradiation. Photographs of (i) pristine PCN-333(Sc), (ii) azide-tagged PCN-333(Sc), and (iii) BODIPY-clicked PCN-333(Sc) in both solid-state and suspension. Adapted with permission from Ref. [192]. Copyright 2015, American Chemical Society.

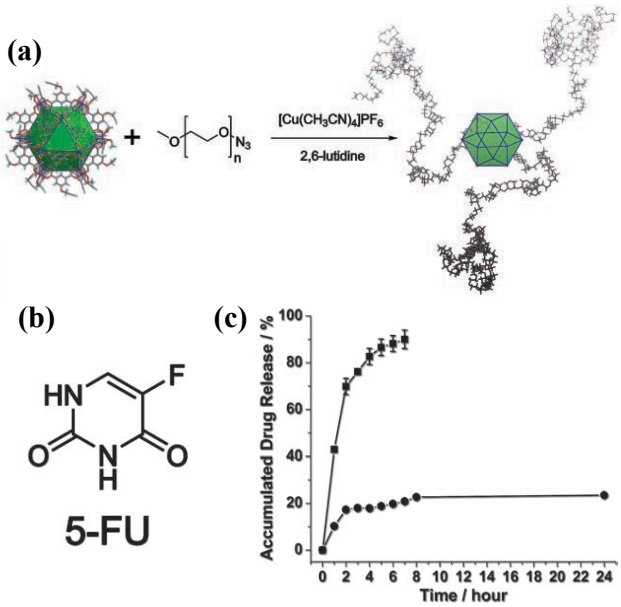


**Figure 38.** (a) Click reaction for the formation of Cu(pi)-PEG5k, (b) chemical structure of 5-fluorouracil (5-FU), and (c) the release of 5-FU from control (square) and Cu(pi)-PEG5k (circle). Adapted with permission from Ref. [239]. Copyright 2010, WILEY-VCH Verlag GmbH & Co. KGaA, Weinheim.

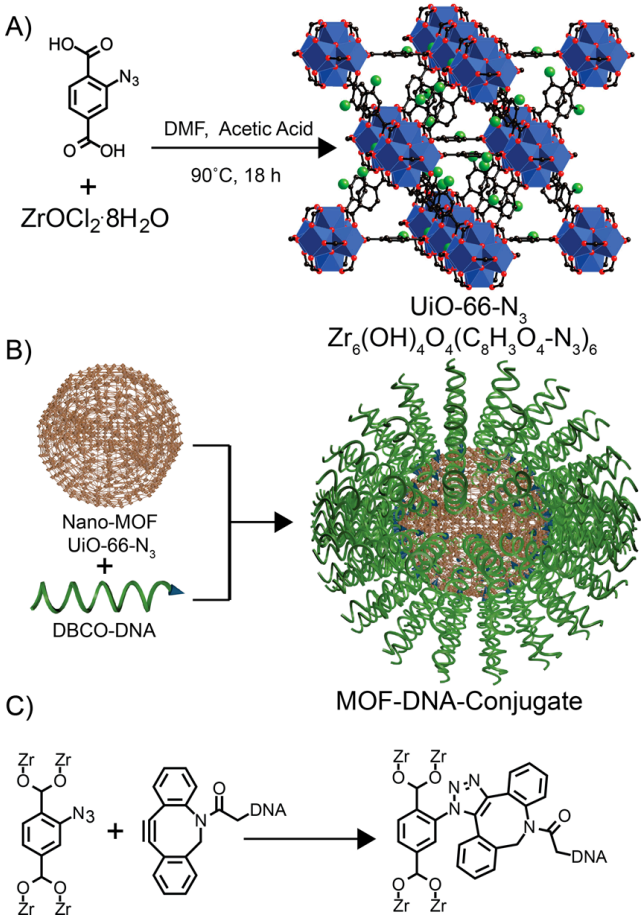


**Figure 39.** (a) Synthesis of UiO-66-$N_3$ nanoparticles, (b) DNA functionalization of UiO-66-$N_3$ nanoparticles, where DNA was functionalized with DBCO, and (c) strain promoted click reaction between a MOF strut and DNA. Adapted with permission from Ref. [240]. Copyright 2014, American Chemical Society.

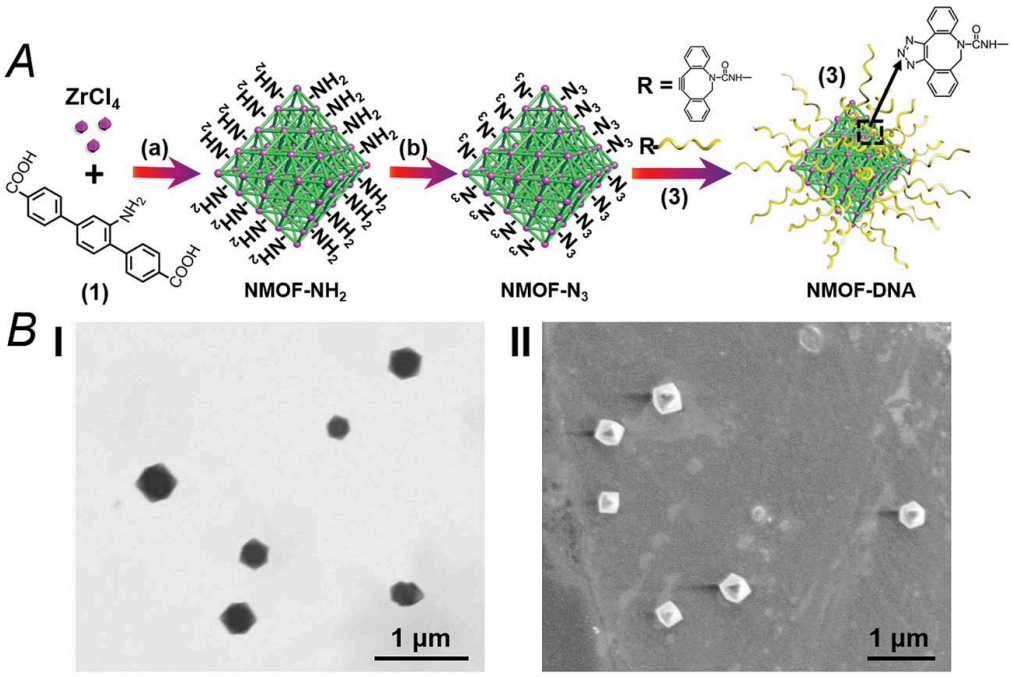


**Figure 40.** (a) Illustration of the synthesis and strain-promoted click modification of UiO-68 NMOF nanoparticles by nucleic acid. (b) TEM image (I) and SEM image (II) of the UiO-68 NMOF nanoparticles. Adapted with permission from Ref. [241]. Copyright 2017, Royal Society of Chemistry.

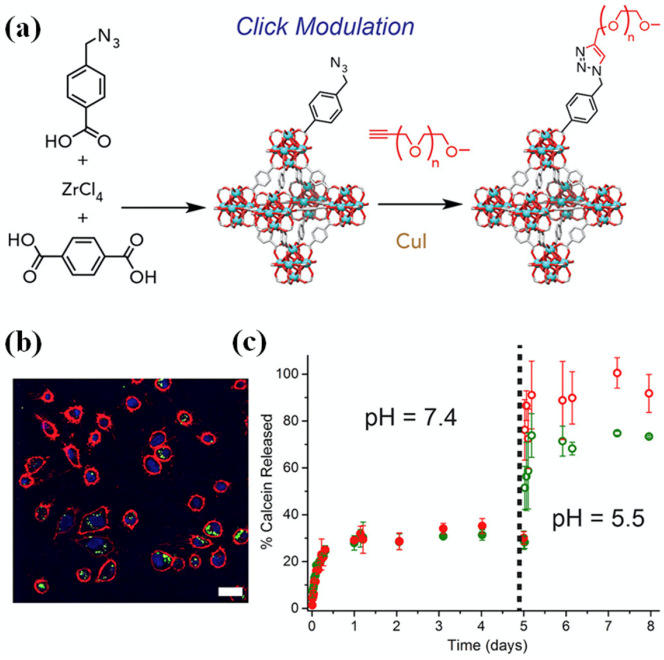


**Figure 41.** (a) Click modulation of UiO-66 by PEG, (b) confocal microscopy image of HeLa cells incubated with calcein loaded UiO-66-L1-PEG2000, and (c) pH-responsive release of calcein from the PEGylated MOF. Adapted with permission from Ref [242]. Copyright 2017, Elsevier B.V.

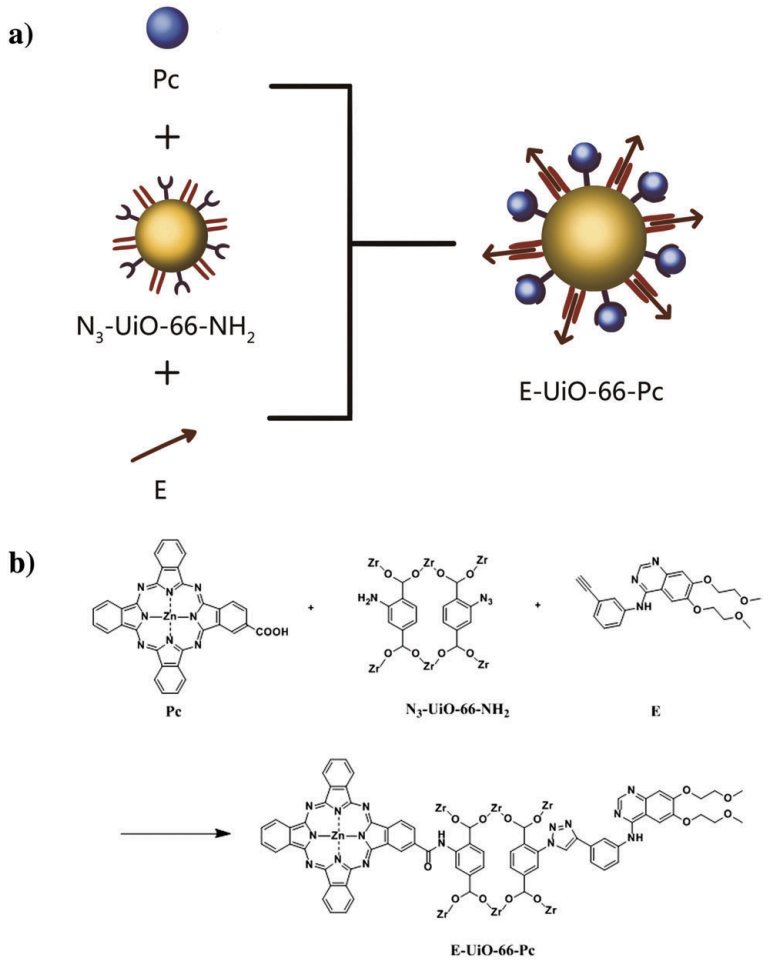


**Figure 42** (a) Schematic synthesis of $N_3$-UiO-66-$NH_2$ and E-UiO-66-Pc, and (b) synthesis of E-UiO-66-Pc *via* covalent post-synthetic modification of $N_3$-UiO-66-$NH_2$. Adapted with permission from Ref. [243]. Copyright 2017, Royal Society of Chemistry.

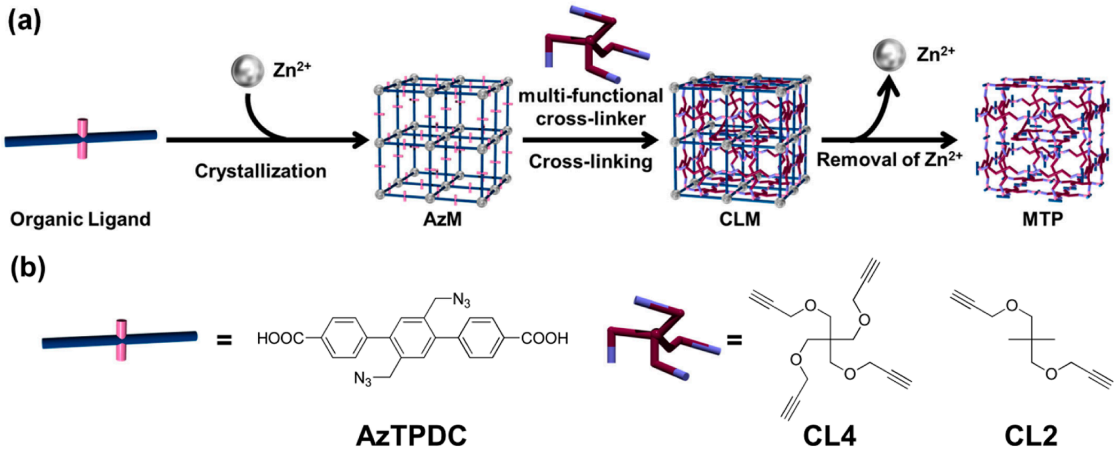


**Figure 43.** (a) Schematic illustration for the cross-linking of organic linkers in azide-bearing MOF (AzM) and subsequent decomposition to obtain MOF-templated polymer (MTP) gel. (b) Molecular structures of the organic ligand (AzTPDC) and alkyne-containing cross-linkers (CL4 and CL2). Adapted with permission from Ref. [247]. Copyright 2013, American Chemical Society.

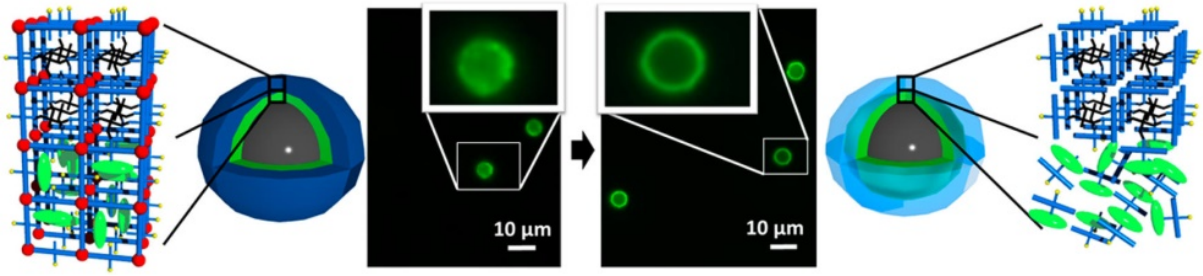


**Figure 44.** Illustration of MOF multi-shell encapsulated magnetic core particles (magMOFs, left) and the finally obtained capsules with magnetic core and converted multi-shells (right). Adapted with permission from Ref. [250]. Copyright 2015, American Chemical Society.

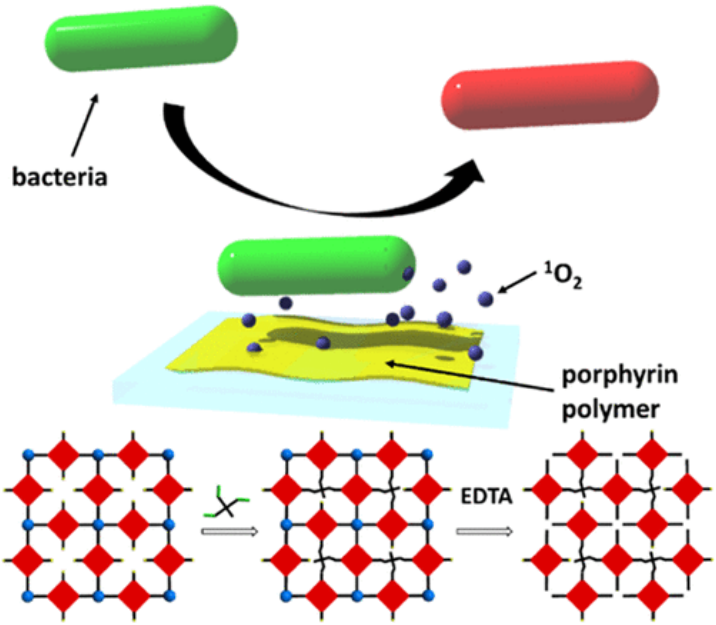


**Figure 45.** Illustration of highly antimicrobial active MOF-templated porphyrin polymer thin film fabricated by click post-modification of a surface anchored MOF. Adapted with permission from Ref. [251]. Copyright 2018, American Chemical Society.

**Table 1.** Yields of various cyclic carbonates produced from NTU-180 catalyzed $CO_2$ cycloaddition with small/big sized epoxides. Adapted with permission from Ref. [115]. Copyright 2016, American Chemical Society.

| Entry | Epoxides | Products | Yields |
|---|---|---|---|
| Small substrates | | | |
| 1 |  |  | 96 |
| 2 |  |  | 83 |
| 3 | 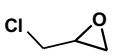 |  | 85 |
| 4 | 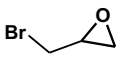 |  | 88 |
| Large substrates | | | |
| 5 | 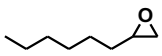 | 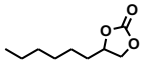 | 8 |
| 6 | 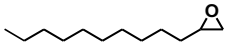 | 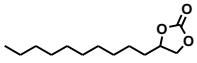 | 6 |
| 7 | 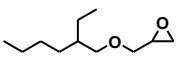 | 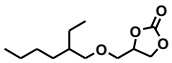 | 5 |

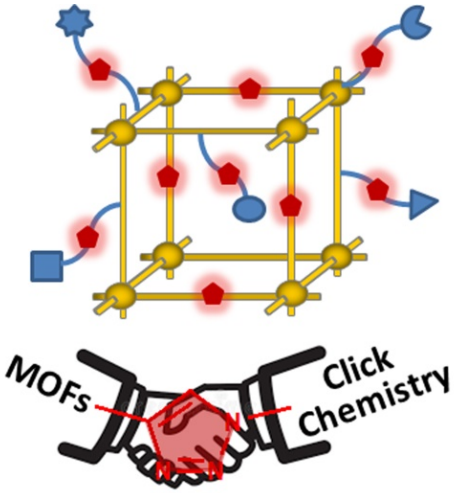


**Table of Contents**